

REGULATION OF PLANT GROWTH AND DEFENSE BY THE HORMONE JASMONATE

By

Leah Y.D. Johnson

A DISSERTATION

Submitted to
Michigan State University
in partial fulfillment of the requirements
for the degree of

Cell and Molecular Biology – Doctor of Philosophy
Molecular Plant Sciences – Dual Major

2022

ABSTRACT

From early lineages to angiosperms, plants have evolved mechanisms to protect themselves against biotic and abiotic challenges. Plant hormones are the primary regulators of growth and defense responses, and elucidation of the hormone signaling networks has provided insight into the molecular mechanisms that protect the plant. The hormone jasmonate (JA) is critical for defenses against herbivores and necrotrophic pathogens and is involved in developmental regulation such as senescence and reproduction. In the core JA signaling pathway, JAZ repressors bind to and inhibit the MYC transcription factors (TFs). Upon a stressor such as insect attack, the F-box protein, COI1, forms a JA-isoleucine (JA-Ile) co-receptor with the JAZ repressors. This association results in ubiquitin-degradation of JAZ, thereby relieving repression on the MYCs. While constitutive JA signaling mutants such as the *jaz* decuple mutant, *jazD*, displays robust resistance to insects and necrotrophic pathogens, these elevated defenses come at the cost of growth and reproduction. Although the molecular mechanisms are well-characterized for JA responses, a remaining question in the field of plant hormone signaling is how response specificity is achieved by a limited set of components. In the case of JA signaling, this question has been difficult to address because of the large size of the JAZ gene family and lack of obvious phenotypes in single *jaz* mutants. Additionally, the molecular mechanisms underlying growth and defense tradeoffs are not fully elucidated. Lastly, JA has long been associated with regulation of senescence. However, a lack of senescence phenotypes in JA biosynthetic or signaling mutants suggests that JA is not critical for natural, age-dependent senescence. Most studies of JA-induced senescence have been performed under dark conditions with high concentrations of exogenous JA, which has hindered insight into the physiological relevance of this phenomenon and its connection

to defense and metabolism. Further advances in these areas may inform biotechnological applications to tune the growth and defense balance as a means to increase crop yields.

In this dissertation, I examined the subfunctionalization of *JAZ* paralogs in *Arabidopsis thaliana* using a novel screen combining forward and reverse genetics. Among ten *JAZ* paralogs tested, I identified four members that function to repress tryptophan biosynthesis and defense responses to necrotrophic pathogens. The JA-responsive transcription factor MYC3 was also identified as a major positive regulator of these responses. I also performed genetic suppressor screens to identify molecular components that contribute to JA-regulated growth-defense balance and senescence. These studies identified six mutations in *COII* and six mutations in *MYC2*. I also used soil-grown *jazD* plants as a novel system to understand the process of JA-mediated leaf senescence. Characterization of senescing *jazD* plants over a 72-hour time course shows that the JA signaling pathway controls chloroplast metabolism and photosynthesis during the growth-to-defense transition. This collective work provides new insights into mechanisms of response specificity in the JA signaling pathway. It additionally contributes to an understanding of regulatory factors required for senescence and the growth-defense balance.

ACKNOWLEDGEMENTS

This dissertation would not have been possible without the help of a great community around me. I would foremost like to thank Dr. Gregg Howe for the opportunity to join his lab and his support and mentorship throughout my time as a graduate student. Thank you to Drs. Cornelius Barry, Jianping Hu, Lee Kroos, and Beronda Montgomery for serving on my committee and providing feedback on the directions of my projects. I would also like to thank the past and present Howe lab members, including Nate Havko, Yani Chen, George Kapali, Michael Das, Brian St. Aubin, Koichi Sugimoto, Changxian Yang, Jian Yao, Leidy Vanegas, Huijia Gong, Sam Heiler, and Julia Tu, for their contributions and feedback, and for making the lab a fun place to be for five years. In particular, thank you to Ian Major and Qiang Guo for helping me start my projects and their continued collaborations throughout. Thank you to Dr. Margaret Petroff, Alaina Burghardt, and Heather Sharick and the CMB and MPS programs for ensuring I was on top of my degree requirements, and Jim Klug and Cody Keilen for ensuring my plants had a good home. Thank you to Drs. Tony Schillmiller, Lijun Chen, and Casey Johnny for their assistance in the many mass spec experiments in this dissertation, and Alicia Withrow for her expertise in transmission electron microscopy. Thank you to Dr. Robert Last and Dr. Jyothi Kumar for their leadership of the Plant Biotechnology for Health and Sustainability program, and the opportunities for growth this program gave me. I greatly appreciate Bruce Caldwell, Dr. Jane Fife, and Dr. Becky Williams-Wagner for providing the opportunity to work at 3Bar Biologics and learn about the startup world for a summer, and the team at 3Bar for making my internship experience unforgettable. Thank you to the many labs in the Plant Research Laboratories community for their support and collaborations. I would like to acknowledge Dr. Xinyu Fu of the Walker lab, and Dr. Anastasiya Lavell and Ron Cook of the

Benning lab for teaching me new techniques and answering my many questions. Last, but not least, thank you to my friends and family for their love and support and making East Lansing feel like home.

TABLE OF CONTENTS

LIST OF TABLES	viii
LIST OF FIGURES	ix
CHAPTER 1: INTRODUCTION	1
JASMONATE SIGNALING AND FUNCTION	2
MOLECULAR MECHANISMS AND REGULATION OF JA SIGNALING	3
PHYSIOLOGICAL FUNCTION OF JAZ	7
ROLE OF JASMONATE IN THE CONTROL OF GROWTH-DEFENSE BALANCE	10
MOLECULAR MECHANISMS OF JA-INDUCED SENESCENCE	12
PHYSIOLOGICAL RELEVANCE OF JA-REGULATED SENESCENCE	15
JA AS A LINK BETWEEN METABOLISM AND CHLOROPLAST SIGNALING	19
THESIS RATIONALE AND OVERVIEW	21
REFERENCES	23
CHAPTER 2: SUBFUNCTIONALIZATION OF JAZ REPRESSORS IN PLANT IMMUNITY AND METABOLISM	32
ABSTRACT	33
INTRODUCTION	34
MATERIALS AND METHODS	38
RESULTS	42
DISCUSSION	56
REFERENCES	61
APPENDIX	66
CHAPTER 3: GENETIC SUPPRESSOR SCREENS IDENTIFY REGULATORS OF THE JASMONATE SIGNALING PATHWAY IN ARABIDOPSIS	75
ABSTRACT	76
INTRODUCTION	77
MATERIALS AND METHODS	80
RESULTS	84
DISCUSSION	97
REFERENCES	102
APPENDIX	106
CHAPTER 4: JASMONATE PROMOTES TURNOVER OF PHOTOSYNTHETIC COMPLEXES DURING THE GROWTH-TO-DEFENSE TRANSITION	107
ABSTRACT	108
INTRODUCTION	110
MATERIALS AND METHODS	113
RESULTS	118
DISCUSSION	139
REFERENCES	143
APPENDIX	148

CHAPTER 5: SYNTHESIS.....	152
SUMMARY AND FUTURE DIRECTIONS.....	153
CHAPTER 2	153
CHAPTER 3	155
CHAPTER 4	156
REFERENCES	158

LIST OF TABLES

Table A2.1 Oligonucleotide primers used for genotyping <i>JAZ</i> loci.	67
Table A2.2 Primers used for gene expression analysis by quantitative PCR (qPCR).....	68
Table A2.3 Segregation frequency of <i>jaz</i> mutations in an F ₂ population derived from a cross between wild type and the <i>jaz</i> decuple mutant (<i>jazD</i>).	70
Table 3.1 Summary of suppressor mutants described in this study.....	89
Table A3.1 Primers used for Sanger sequencing of suppressor mutants.....	106
Table 4.1 Gene ontologies of differentially expressed genes in <i>jazD</i> after coronatine treatment.	124
Table 4.2 Numbers of differentially expressed transcription factors in <i>jazD</i> after coronatine treatment.	128
Table A4.1 Differential expression of jasmonic acid biosynthesis genes after coronatine treatment.	148
Table A4.2 Differential expression of TCA cycle genes in <i>jazD</i> after coronatine treatment.	150

LIST OF FIGURES

Figure 1.1 Schematic of jasmonate signaling pathway and important processes regulated by JA.	3
Figure 1.2 Growth-defense tradeoffs in <i>jaz</i> mutants.....	9
Figure 1.3 Plastid-to-nuclear signaling scheme for JA-mediated nutrient mobilization in response to stress.....	18
Figure 1.4 Chloroplast-derived metabolites regulated by JA.	20
Figure 2.1 Regulation of tryptophan biosynthesis by the jasmonate signaling pathway.....	43
Figure 2.2 Loss of MYC3 and MYC4 results in hypersensitivity to root growth inhibition by 5-methyl tryptophan (5-MT) in Arabidopsis seedlings.	45
Figure 2.3 Genes encoding MYC TFs are required for resistance of the <i>jaz</i> decuple mutant (<i>jazD</i>) to 5-methyl tryptophan (5-MT).	47
Figure 2.4 Overexpression of dominant MYC3 and MYC4 variants confer increased resistance to growth inhibition by 5-methyl tryptophan (5-MT).	48
Figure 2.5 Identification of <i>jaz</i> mutations associated with resistance to 5-methyl tryptophan (5-MT).....	50
Figure 2.6 <i>j1256</i> mutant plants exhibit a moderate reduction in leaf growth.	52
Figure 2.7 Constitutive accumulation of select defense compounds in the <i>j1256</i> mutant.....	53
Figure 2.8 The jasmonate-ethylene branch of immunity is selectively activated in <i>j1256</i> plants.	55
Figure A2.1 PCR-based genotyping of ten <i>jaz</i> mutations segregating in the <i>jazD</i> x Col-0 F ₂ population.	66
Figure A2.2 Root lengths of Arabidopsis seedlings grown on media supplemented with 5-methyl tryptophan (5-MT) or 5-MT and methyl jasmonate (MeJA).....	69
Figure A2.3 Photographs of representative F ₂ seedlings exhibiting resistance to 5-methyl-tryptophan (5-MT).	69
Figure A2.4 Phylogenetic tree and genome location of members of the Arabidopsis JAZ family.	71
Figure A2.5 Secondary peak detected for the hydroxycinnamic acid amides.....	72
Figure A2.6 Levels of various glucosinolate derivatives in untreated leaves of 26-day-old wild-type (WT), <i>jaz</i> quintuple (<i>jazQ</i>), <i>jaz</i> decuple (<i>jazD</i>), and <i>jaz1/2/5/6</i> (<i>j1256</i>) plants.....	73
Figure 3.1 Workflow for identification of two classes of <i>jazD</i> suppressor mutants.....	85

Figure 3.2 Suppressor mutants <i>sjd10</i> and <i>sjd78</i> have an intermediate level of growth and defense relative to WT and <i>jazD</i>	87
Figure 3.3 Molecular genetic analysis of <i>sjd10</i> and <i>sjd78</i>	91
Figure 3.4 Coronatine (COR) resistance correlates with the growth phenotype of suppressor mutant <i>sjd78</i>	92
Figure 3.5 Identification of coronatine-resistant <i>sch</i> suppressor mutants.....	94
Figure 3.6 <i>sjd</i> and <i>sch</i> suppressor lines have reduced sensitivity to methyl jasmonate (MeJA)-induced root growth inhibition.....	94
Figure 3.7 Complementation testing of <i>sch</i> mutants.	95
Figure 3.8 <i>sjd</i> and <i>sch</i> suppressor mutants contain mutations in either the <i>COII</i> or <i>MYC2</i> gene.	97
Figure 4.1 MYC2 is a major regulator of coronatine-induced de-greening in <i>jazD</i>	119
Figure 4.2 Time course of leaf de-greening in response to coronatine treatment.....	120
Figure 4.3 Time course of coronatine-induced changes in gene expression in <i>jazD</i>	122
Figure 4.4 Coronatine treatment decreases the accumulation of plastid-localized lipids in <i>jazD</i>	129
Figure 4.5 Coronatine promotes jasmonate inactivation in <i>jazD</i>	131
Figure 4.6 Coronatine treatment decreases the accumulation of photosynthetic proteins in <i>jazD</i>	133
Figure 4.7 Coronatine treatment alters the free amino acid levels in <i>jazD</i>	134
Figure 4.8 Fumarate and succinate levels increase in the Arabidopsis <i>jaz</i> decuple mutant, <i>jazD</i>	136
Figure 4.9 Coronatine treatment alters chloroplast but not mitochondrion morphology in <i>jazD</i>	138
Figure A4.1 Coronatine-induced changes in amino acid levels in WT and <i>jazD</i>	149

CHAPTER 1: INTRODUCTION

Leah Y.D. Johnson, Ian T. Major, and Gregg A. Howe

Author contributions: LYDJ and GAH conceptualized and wrote the manuscript. ITM generated figure 1.4.

JASMONATE SIGNALING AND FUNCTION

In response to diverse cues, plants orchestrate complex signaling processes to optimize fitness. Stress responses are often in conflict with growth, and this so-called growth-defense tradeoff can negatively impact overall growth and reproduction (Guo et al. 2018). Hormone signaling networks coordinate growth and defense transcriptional programs and understanding how these pathways intersect is of agronomic interest due to the impacts on yield (Huot et al. 2014). For example, the hormone jasmonate (JA) regulates the production of defense compounds after a stress such as insect herbivory as well as inhibits growth (Zhang and Turner 2008; Schweizer et al. 2013; Attaran et al. 2014; Guo et al. 2022).

JA is derived from plastid-localized lipids such as monogalactosyldiacylglycerol, which provides the 18:3 fatty acid precursor for α -linolenic acid (Ishiguro et al. 2001; Hyun et al. 2008). α -linolenic acid is converted to OPDA in the chloroplast, then exported from the chloroplast to the peroxisome where OPDA undergoes beta-oxidation to form JA (Bell et al. 1995; Laudert et al. 1996; Stintzi and Browse 2000; Ziegler et al. 2000; Cruz Castillo et al. 2004; Koo et al. 2006; Schilmiller et al. 2007; Chauvin et al. 2013; Guan et al. 2019). JA is conjugated to isoleucine through JAR1 amidotransferase activity and can then be transported to the nucleus (Staswick and Tiryaki 2004; Li et al. 2017). Upon perceiving a stressor such as wounding, JA-Ile is rapidly synthesized from pools of JA to activate the signaling pathway (Glauser et al. 2009; Koo et al. 2009). JA signaling is well-characterized for its role in defense against insect herbivory and defense against necrotrophic pathogens (Fernández-Calvo et al. 2011; Zhu et al. 2011; Guo et al. 2018; Liu et al. 2021). It is also involved in the regulation of senescence, reproductive development, and abiotic stressors such as cold tolerance (Ueda and Kato 1980; Xie et al. 1998; He et al. 2002; Song et al. 2011; Hu et al. 2013; Hu et al. 2021).

Jasmonate signaling is complex and cross-talk with other pathways complicates understanding of regulatory mechanisms. In this chapter, I review the current knowledge of molecular mechanisms of JA signaling and attenuation mechanisms. I also examine the physiological function of JAZ and the mechanisms and functional relevance of JA-induced senescence. I additionally examine growth and defense regulation by JA and how shifts in metabolism contribute to the growth-defense balance. Lastly, I introduce an overview of this dissertation and the main questions I sought to address.

MOLECULAR MECHANISMS AND REGULATION OF JA SIGNALING

Jasmonate signaling is primarily executed by the MYC transcription factors, which are repressed by the JAZ proteins under unstressed conditions (Dombrecht et al. 2007; Fernández-Calvo et al. 2011) (Fig 1.1).

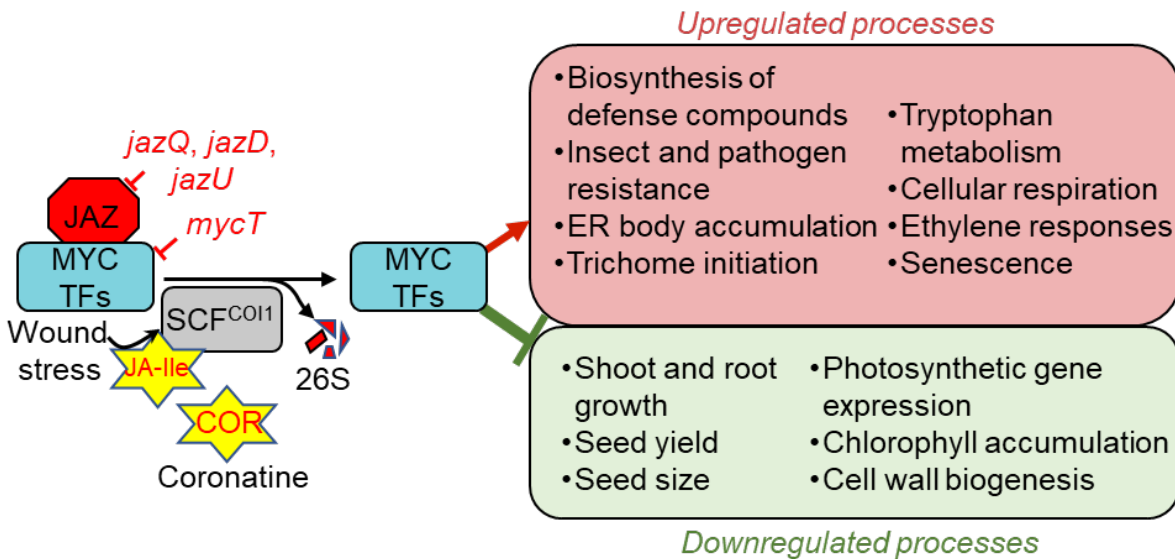


Figure 1.1 Schematic of jasmonate signaling pathway and important processes regulated by JA.

In unstressed conditions, JASMONATE ZIM DOMAIN (JAZ) proteins bind and inhibit MYC transcription factors (TFs). Upon a stressor such as wounding, JA-Ile is rapidly synthesized and promotes COI1-JAZ interactions to target the JAZ for degradation and relieve MYC repression. Coronatine (COR) is a JA agonist that can activate JA signaling. MYC TFs promote defense-

Figure 1.1 (cont'd)

related processes and repress growth-related processes. Endoplasmic reticulum (ER) body formation is associated with wounding and sequestration of defense-related proteins.

External stressors such as herbivory trigger rapid de novo synthesis of JA, which allows the F-box protein COI1 to form a co-receptor with JAZs to ubiquitinate them for degradation by the 26S proteasome (Chini et al. 2007; Thines et al. 2007; Koo et al. 2009). The degradation of JAZ proteins frees the inhibition on the MYCs to activate downstream transcriptional programs. Degradation of the JAZ proteins allows for the MYCs to interact with the Mediator complex subunit, MED25, to recruit transcriptional machinery and alter chromatin status (Kidd et al. 2009; Chen et al. 2012; An et al. 2017; Wang et al. 2019). The MYC transcription factors are members of the beta-helix-loop-helix (bHLH) family (Toledo-Ortiz et al. 2003). There are five MYC paralogs in Arabidopsis, MYC1, MYC2, MYC3, MYC4, and MYC5, but functions within the JA signaling pathway have only been ascribed to MYC2 through MYC5 (Fernández-Calvo et al. 2011; Song et al. 2017). To coordinate JA responses, MYCs exert regulatory control over a transcription factor network as well as directly regulate response genes (Zander et al. 2020). The MYCs are often described as redundant but elucidation of these non-overlapping roles will provide key insight into how response specificity is achieved by the JA signaling components. Due to the strong negative effects on growth and reproduction, defense programs must be selectively activated. Jasmonate signaling has a suite of negative regulators to attenuate signaling once activated, as well as repress responses when signals are not detected. Jasmonate signaling is repressed primarily through the direct binding of the JAZ proteins to the MYC transcription factors to prevent MYC interaction with the MEDIATOR complex (Zhang et al. 2015). JAZ proteins are able to interact with corepressors such as TOPLESS (TPL), either directly or through adaptor proteins such as NINJA (NOVEL INTERACTOR OF JAZ) and ECAP (EAR-MOTIF CONTAINING ADAPTOR PROTEIN) (Pauwels et al. 2010; Li et al. 2020). While

NINJA-TPL interactions with JA signaling are well established, the ECAP protein is a novel adaptor protein which regulates anthocyanin biosynthesis through recruitment of TOPLESS RELATED 2 (Li et al. 2020). Mutants of *ecap2* have fewer filled siliques than wild-type plants, although it is not clear if this infertility phenotype is a result of seed filling or anther deficiencies. This suggests, however, a possible role for the recruitment of general co-repressors in mediating JA signaling for proper development during reproduction.

TPL-mediated repression is thought to partially act through recruitment of histone deacetylases like HDA19, which typically act as repressive chromatin modifiers (Long et al. 2006). Interestingly, histone deacetylases such as HDA6 have conflicting roles in aiding repression or activation of JA responses (Wu et al. 2008; Zhu et al. 2011). *HDA6* mutants have lowered expression of JA-activated genes such as *VSP2*, suggesting HDA6 activity promotes the expression of these genes (Wu et al. 2008). *HDA6* mutants also show increased expression of *ERF1*, suggesting HDA6 activity represses the expression of other sets of genes (Zhu et al. 2011). JAZs additionally interact with the polycomb repressive complex to alter histone methylation, further inhibiting MYC activity at the chromatin level (Li et al. 2021). Loss of polycomb complex proteins partially restored the pollen-driven infertility of the *coil* mutant, indicating that regulation of JA signaling by chromatin modifications is a component of reproductive development. Further study into how these histone modifications are altered under various conditions is needed to clarify the role of altering chromatin accessibility for JA responses and may provide insight into how response specificity may be maintained at the chromatin level.

In addition to protein-protein interactions and histone modifiers, JA signaling is attenuated by its own transcriptional programs. JAZ proteins are rapidly synthesized after the

induction of JA signaling, including stable JAZ proteins that resist turnover through lower or abolished binding affinity with COI1 (Chung and Howe 2009; Shyu et al. 2012; Moreno et al. 2013). To balance the desensitization by alternatively spliced JAZ transcripts, MED25 can interact with the PRE-mRNA-PROCESSING-PROTEIN (PRP) splicing factors, PRP39a and PRP40a, to regulate JA alternatively spliced isoforms (Wu et al. 2020). While desensitization of JA responses by stable JAZs is important to limit MYC activity, the regulation of splicing suggests a mechanism for the basal MYC regulation to be reset to allow for rapid induction of signaling upon encountering a new stressor. JA oxidases are also rapidly transcribed to limit the pool of JA which can be converted to JA-Ile, and JA-Ile may be modified to turn over the pools of the dominant bioactive signaling molecule through the action of CYP450s (Koo et al. 2014; Caarls et al. 2017). JA-inducible IAA amidohydrolases (IAHs) may decrease the availability of JA-Ile while increasing the availability of deconjugated IAA to balance JA versus auxin signaling (Zhang et al. 2016). The crosstalk between auxin and JA suggests that proper development can be regulated in part by altering pools of the signaling molecules, as overexpression of the IAH *ILL6* leads to *coi1*-like fertility defects.

The related bHLH JASMONATE-ASSOCIATED MYC-LIKE (JAM) transcription factors are upregulated in a MYC-dependent manner and competitively inhibit MYC DNA binding (Nakata et al. 2013; Sasaki-Sekimoto et al. 2013). Loss of the JAMs accelerates JA-induced senescence in detached leaves, suggesting an important role for the attenuation of JA signaling to inhibit senescence (Qi et al. 2015). MYC protein stability can also be regulated by the CUL^{BPM} E3 ligase to decrease the pool of MYC transcription factors (Chico et al. 2020). Disruption of these attenuation mechanisms can have negative developmental effects but many of these phenotypes are relatively mild, supporting the idea that MYC activity is carefully

moderated at many levels to provide an optimal stress response without severely impacting fitness.

PHYSIOLOGICAL FUNCTION OF JAZ

The JAZ repressors are part of the TIFY family of proteins, and there are thirteen members in Arabidopsis (Bai et al. 2011; Howe et al. 2018). These thirteen proteins divide into five clades- Group I consists of JAZ1, JAZ2, JAZ5, and JAZ6, Group II consists of JAZ11 and JAZ12, Group III contains the JAZ10 isoforms, Group IV contains JAZ7, JAZ8, and JAZ13, and Group V contains JAZ3, JAZ4, and JAZ9 (Howe et al. 2018). All thirteen JAZ proteins contain a Jas domain that interacts with the MYCs and COI1 in a conformation-dependent manner, but Group IV JAZs contain a divergent sequence, and isoforms of JAZ10 contain partial or full Jas truncations due to alternative splicing (Chung and Howe 2009; Moreno et al. 2013; Thireault et al. 2015; Howe et al. 2018). Group I and Group III JAZs have a Cryptic MYC-Interacting Domain (CMID) that secondarily interacts with the MYCs (Moreno et al. 2013; Howe et al. 2018). JAZ5, JAZ6, and Group IV JAZs contain the Ethylene-responsive element-binding factor-associated Amphiphilic Repression (EAR) motif that can directly interact with TOPLESS to recruit co-repressors (Kagale et al. 2010; Shyu et al. 2012; Thireault et al. 2015). Interactions with TPL are also driven by the EAR-motif containing NINJA, which interacts with JAZ through the TIFY motif of the ZIM domain (Pauwels et al. 2010). JAZ proteins also can form homo- and heteromers through the ZIM domain although these interactions are not well-defined *in planta* (Chini et al. 2009).

The JAZ proteins are thought to be functionally redundant due to a lack of the broader defense phenotypes in single *jaz* mutants, although there are studies that describe some specific JAZ functions. For instance, JAZ2 regulates stomatal closure to promote resistance against

bacterial invasion, several JAZ members, JAZ4, JAZ7, and JAZ8, are associated with senescence regulation, and JAZ6 is involved in responses to circadian-driven changes in resistance to *Botrytis cinerea* (Ingle et al. 2015; Jiang et al. 2014; Yu et al. 2016; Gimenez-Ibanez et al. 2017). Despite these studies, the broader defense phenotypes regulated by JA are only seen in higher order JAZ mutants. Several higher order mutants show that depletion of JAZ proteins through multiple *jaz* mutations can elevate JA responses in both unstressed conditions and under biotic attack (Campos et al. 2016; Guo et al. 2018; Liu et al. 2021) (Fig 1.1). The amount of JAZ depletion correlates with the magnitude of the JA responses. The *jazQ* mutant lacking *jaz1/3/4/9/10* displays increased resistance to insect challenge from *Trichoplusia ni* larvae but is slightly more susceptible to infection by the necrotrophic fungus, *Botrytis cinerea* (Campos et al. 2016; Guo et al. 2018). In comparison to *jazQ*, the *jazD* mutant lacking *jaz1/2/3/4/5/6/7/9/10/13* displays stronger resistance to insect larvae, resistance to necrotrophic fungal challenge, and more severe fitness penalties such as decreased seed yield and seed mass (Guo et al. 2018) (Fig 1.2). In addition to increased resistance to biotic challenges, the *jazD* mutant, but not *jazQ*, undergoes senescence when treated with the JA agonist, coronatine (Guo et al. 2018). This may suggest that JA signaling attenuation by the JAZ is a critical component of balancing senescence cues. These studies indicate that the broader JA phenotypes are regulated in an additive manner, but do not address whether the differences between *jazQ* and *jazD* are additive or whether specific JAZs regulate responses. A phylogenetics-based design of *jaz* mutations shows that the Group IV/V mutant, *jaz3/4/7/9*, is more resistant to insect challenge by *Spodoptera exigua* and regulates flowering time, while the Group I mutant, *jaz1/2/5/6*, is more resistant to *B. cinerea* (Liu et al. 2021). Interestingly, in *Marchantia polymorpha*, mutation of the single *MpJAZ* gene results in similar JA phenotypes as the decuple *jaz* Arabidopsis mutant, such as decreased development

and fertility and altered expression of specialized metabolism and photosynthesis genes (Monte et al. 2019). These studies indicate that expansion and subfunctionalization of the JAZ family contributes to the regulation of JA responses.

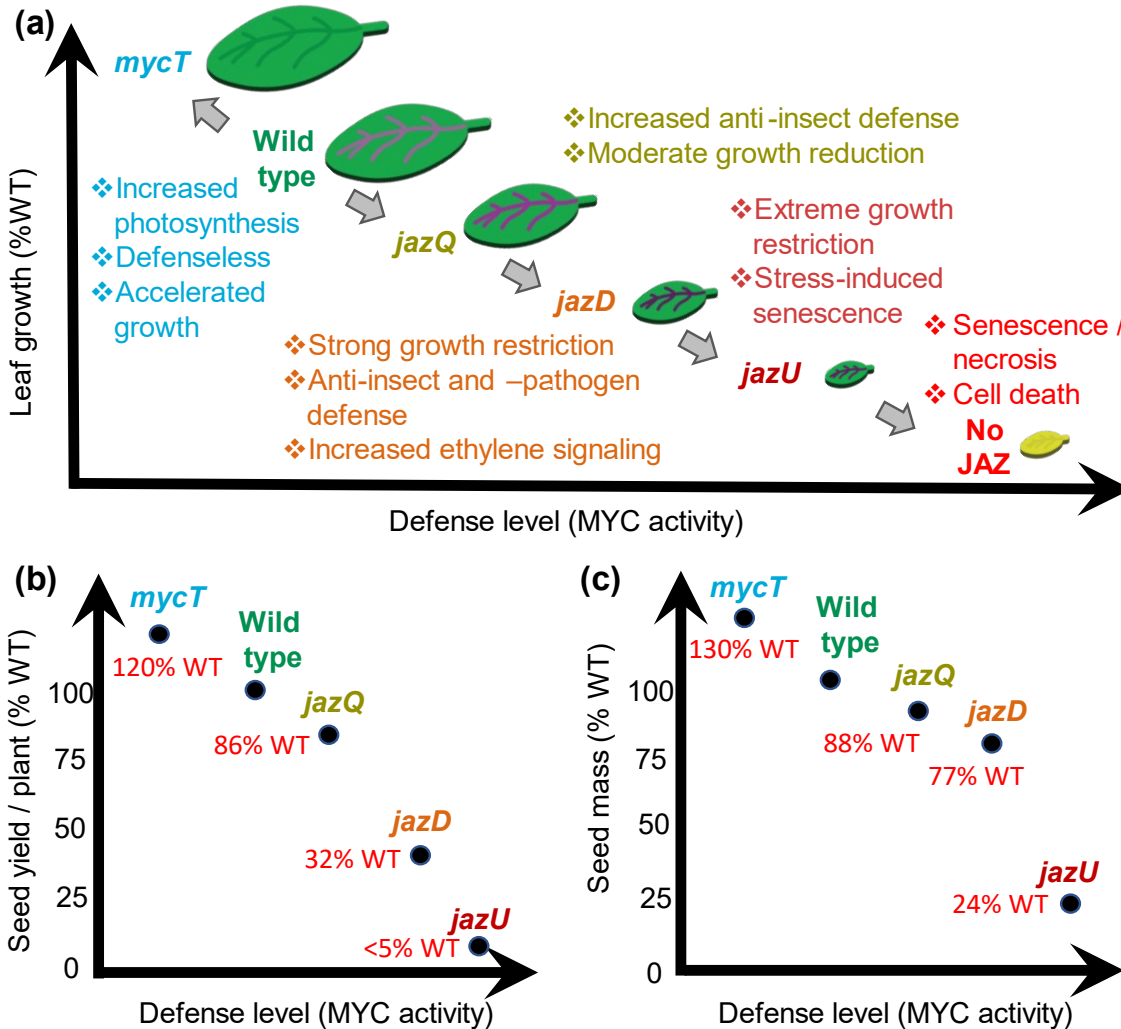


Figure 1.2 Growth-defense tradeoffs in *jaz* mutants.

(a) Leaf growth negatively correlates with increasing MYC activity as JAZ proteins are depleted. As the number of *jaz* mutations increases, the strength of JA-related phenotypes increases in unstressed tissue. No JAZ indicates *jazD* tissue treated with coronatine, which likely acts through depleting the remaining JAZ. (b) Seed yield and mass (c) are negatively impacted by increasing defense levels. *mycT* mutants have larger seed mass and yield than WT plants, while *jaz* mutants have increasingly negative fitness penalties as more JAZ are depleted. *mycT*, *myc2/3/4*; *jazQ*, *jaz1/3/4/9/10*; *jazD*, *jaz1/2/3/4/5/6/7/9/10/13*; *jazU*, *jaz1/2/3/4/5/6/7/8/9/10/13*.

ROLE OF JASMONATE IN THE CONTROL OF GROWTH-DEFENSE BALANCE

Growth and defense trade-offs are a well-characterized aspect of stress responses but the mechanisms underlying this phenomenon are not fully elucidated (Huot et al. 2014; Ballaré and Austin 2019; Havko et al. 2016; Kliebenstein 2016). Inhibition of root growth by exogenous JA or methyl-JA is a common assay to identify altered JA responses and many components of JA signaling were identified in this manner (Staswick et al. 1992; Feys et al. 1994; Lorenzo et al. 2004; Guo et al. 2018). JA inhibits mitosis through regulation of cell cycle proteins both through regulation of the B-type CYCLIN DEPENDENT KINASE (CDKB) and cyclin B, which regulates the G₂ checkpoint of the cell cycle (Swiatek et al. 2002; Dewitte and Murray 2003; Swiatek et al. 2004; Zhang and Turner 2008). In root tissue, JA inhibits cell division and elongation and represses the transcription of the PLETHORA transcription factors to alter stem cell patterning (Chen et al. 2011). Notably, defense phenotypes in the higher order *jaz* mutants correlate tightly with decreases in growth and fertility (Guo et al. 2018) (Fig 1.2a). The enhanced JA responses are predominantly coordinated by the MYC transcription factors. The introduction of the *myc* triple mutant (*mycT*, consisting of *myc2 myc3 myc4*) into higher order *jaz* mutants restores both defense and vegetative growth phenotypes (Major et al. 2017; Guo et al. 2022). This suggests the pleiotropic effects exacerbated in *jazD* can be attributed to further increases in MYC activity by depletion of JAZs relative to *jazQ*. Several studies show that MYCs are involved in repressing seed size and yield, and it was recently shown that MYCs repress ovule and integument cell proliferation to regulate seed size (Gao et al. 2016; Liu et al. 2020; Hu et al. 2021; Guo et al. 2022). This suggests that MYCs are required for proper male reproductive development, while playing an opposing role in suppressing growth in maternal tissues. While *jazQ* has relatively minor fitness penalties in terms of seed yield, the *jazD* mutant has

significantly reduced seed yield and seed mass that inversely correlates with increases in resistance phenotypes (Fig 1.2b-c). Modulating MYC activity is a potential mechanism to boost stress resilience without yield losses, such as through tissue-specific modifications that would allow for enhanced vegetative responses while differentially affecting floral responses. Levels of defense could be tuned to provide increased resistance to stressors without significant yield loss.

Growth and defense tradeoffs are also regulated through pathway crosstalk. Growth regulators such as the hormone gibberellic acid (GA) and the light and temperature sensor PHYTOCHROME B (PHYB) regulate growth through the PIF transcription factors (Schwechheimer 2011; Kim et al. 2021). The GA-regulated DELLA proteins interact with the JAZ proteins to balance growth and defense cues. Once DELLA proteins are degraded upon GA signaling activation, the JAZ are released and can then interact with the MYCs and other TFs to repress JA responses and promote growth. Conversely, JAZ proteins inhibit DELLA repression of downstream TFs, and upon activation of a JA response, JAZ degradation allows for DELLA interactions to inhibit growth (Hou et al. 2010; Yang et al. 2012). At the interface of light cues, growth, and defense, low red/far-red light ratios, which inactivate PHYB, promote DELLA turnover and increase JAZ10 abundance, suggesting that light cues alter JA/GA crosstalk to promote growth and suppress defense (Leone et al. 2014). PHYB has also been identified as a growth regulator in genetic screens to identify factors involved in jasmonate-induced growth inhibition (Campos et al. 2016; Major et al. 2020). The *phyB* mutant does not fully restore the impaired growth in *jazD*, suggesting that there are other growth-defense regulatory mechanisms yet to be uncovered (Major et al. 2020).

While studies have identified several molecular mechanisms of growth-defense regulation, the complex interaction between growth and defense still remains enigmatic (Hou et al. 2010;

Leone et al. 2014; Campos et al. 2016; Major et al. 2020). JA signaling is an intriguing model to study the effects of metabolism on growth due to the regulation of diverse defense compounds through reprogramming of metabolism (Guo et al. 2018; Wasternack and Strnad 2019; Savchenko et al. 2019). Recent work suggests the primary JA transcriptional regulators, the MYC transcription factors, are responsible for metabolic and reproductive output and therefore provide targets for understanding the regulation of these tradeoffs through a central hub (Hu et al. 2021; Guo et al. 2022). JA has also been implicated in the regulation of senescence, but the physiological relevance is unclear as JA signaling and biosynthesis mutants do not display obvious senescence phenotypes (Xiao et al. 2004; Seltsmann et al. 2010). Further work is needed to determine whether there is a connection between JA-induced senescence and the regulation of metabolism.

MOLECULAR MECHANISMS OF JA-INDUCED SENESCENCE

In Arabidopsis, *coi1* mutants are often used to identify JA dependence for senescence programs (He et al. 2002; Xiao et al. 2004). Regulation of senescence programs is important for the prevention of untimely senescence, and in JA signaling, the JAZ repressors are critical for inhibiting errant JA signaling (Guo et al. 2018). Several studies across species have uncovered roles of JAZ proteins in repressing senescence signaling. The Arabidopsis *jaz* quintuple mutant, *jazQ*, shows increased chlorophyll degradation in excised leaves treated with methyl-jasmonate compared to WT plants (Major et al. 2017). In Arabidopsis, a non-loss-of-function mutation of *JAZ7* led to enhanced senescence phenotypes (Yu et al. 2016). Additionally, mutations in *jaz4* and *jaz8* show more severe senescence phenotypes in detached leaf assays and these transcripts are elevated in these senescence promoting conditions in wild-type plants, suggesting that these JAZ proteins are synthesized to inhibit senescence programs (Jiang et al. 2014). In rice, overexpression of a Jas domain-truncated *OsJAZ8* reduces chlorophyll loss of rice leaf blade

segments in dark-induced senescence conditions (Uji et al. 2017). The apple MdBt2 protein was shown to interact with MdJAZ1, 2, 3, 4, and 8 to regulate JA-induced senescence phenotypes. BT2 stabilizes the JAZ proteins to inhibit the senescence programs activated by MYC2 (An et al. 2021). These studies show that JAZ proteins are a conserved mechanism to repress senescence signaling across species.

JA-related senescence phenotypes can be altered by mutations in the *MYC* gene family. The MYC TFs promote senescence by regulating genes such as *SENESCENCE ASSOCIATED GENES (SAGs)* while the related bHLH IIIId (“JAM”) transcription factors antagonize MYC binding of *SAG* promoters to inhibit the activation of senescence transcriptional programs (Qi et al. 2015). Additionally, studies with the higher-order *jaz* mutants show that the JA senescence phenotype is dependent upon the MYC transcription factors. The introduction of the triple *myc* mutant, *mycT* (*myc2*, 3, and 4), into the *jazQ* mutant completely inhibits the enhanced sensitivity to methyl-JA- plus dark treatment to induce senescence (Major et al. 2017). These studies show that the jasmonate-driven senescence program is predominantly regulated by the *MYC* gene family. This is seen in other species as well, such as more severe senescence in *OsMYC2* overexpression rice leaf blade segments in dark-induced senescence conditions (Uji et al. 2017).

Other transcription factors implicated in JA-regulated senescence may play a role downstream or in parallel with the MYCs. For instance, the *Dof2.1* transcription factor was recently shown to enhance senescence by sustaining a *MYC2-Dof2.1* feed-forward transcriptional loop (Zhuo et al. 2020). *WRKY57* has been shown to negatively regulate JA-induced senescence through comparisons of detached wild type and *wrky57* mutant and overexpression lines. Interestingly, JA induces *WRKY57* transcription but degradation of the *WRKY57* protein through the 26S proteasome occurs after JA application, potentially through the interaction with JAZ

proteins (Jiang et al. 2014). This negative feedback of JA-induced *WRKY57* expression may reflect a mechanism to attenuate senescence signaling. Post-transcriptional regulation of jasmonate biosynthesis and senescence programs by the mi319/TEOSINTE BRANCHED/CYCLOIDEA/PCF (TCP) module is yet another point of regulation to control jasmonate-induced senescence (Schommer et al. 2008). Recently, the circadian clock has been connected to the regulation of JA-induced senescence. The Evening Complex (EC) regulates JA-driven senescence by repressing MYC2 activity through direct binding of the MYC2 promoter (Zhang et al. 2018). Given the diverse transcription factors that interact with MYCs, these combinatorial regulatory components likely function to integrate various external cues that modulate the timing of senescence. Additionally, regulation at the level of COI1 or JAZ provides additional control over senescence induction to prevent unnecessary or untimely cell death.

Ethylene is a well-known senescence regulator and is regulated in part by light and circadian signaling through PIF4/5 activation of the transcription factor, ETHYLENE INSENSITIVE 3 (EIN3) (Sakuraba et al. 2014). JA and ethylene signaling have been shown to act both antagonistically and synergistically (Zhu et al. 2011; Li et al. 2013; Song et al. 2014; Qiu et al. 2015). JAZ repressors physically interact with the ETHYLENE INSENSITIVE 3 (EIN3) transcription factor and JA/ET responses to *Botrytis cinerea* are enhanced by the addition of JA (Zhu et al. 2011). In a study elucidating the role of EIN3 in senescence, the *ein3* mutation inhibited MeJA-driven senescence in excised leaf assays, indicating an important role for ethylene signaling components in JA-driven senescence (Li et al. 2013). In the *jaz* decuple mutant, *jazD*, ethylene signaling is strongly transcriptionally activated and associated defense responses against *B. cinerea* are elevated as well, suggesting that this synergy remains when the *JAZ* genes are mutated as well as relieved by degradation through JA application (Guo et al.

2018). In untreated *jazD* tissue, senescence-associated genes such as the chlorophyll catabolism enzymes and *SAGs* have increased expression compared to wild-type plants, while these changes in expression are not seen in the quintuple mutant, *jazQ*. Interestingly, the *jazD* mutant senescences and eventually becomes necrotic upon treatment with coronatine, while the only visible response in WT and *jazQ* plants is the accumulation of anthocyanins (Guo et al. 2018). This sensitivity to coronatine may be attributed to the reduced pool of JAZ proteins in *jazD*, while the *jazQ* mutant may contain a sufficient level of JAZs to prevent excessive signaling activation. Additionally, the synergy between JA and ethylene signaling through EIN3 regulation may explain why the *jazD* mutant displays chlorosis and necrosis when treated with coronatine, in contrast to the *jazQ* mutant and wild-type plants which require an additional environmental stressor (Major et al. 2017; Guo et al. 2018). Further characterization of the JA/ethylene connection, such as examination of temporal changes in signaling and other TFs involved, will provide insight into the drivers of JA-induced senescence.

PHYSIOLOGICAL RELEVANCE OF JA-REGULATED SENESCENCE

Jasmonate was first implicated as a senescence regulator after *Artemisia absinthium* extracts induced senescence in segments of oat leaves (Ueda and Kato 1980). Coronatine, a JA agonist, was also shown to induce chlorosis in tomato leaves (Palmer and Bender 1995). Senescence transcripts identified in dark-induced senescence conditions were differentially stimulated by JA compared to two other senescence promoters, abscisic acid (ABA) and ethylene, suggesting these hormones regulate unique senescence programs (Park et al. 1998). JA levels correlate with the catabolism of both plastid lipids and chlorophyll, and JA transcription factors regulate important chlorophyll breakdown enzymes as well as *SAGs* (He et al. 2002; Seltmann et al. 2010; Zhu et al. 2015). JA has also been linked to abiotic stress-induced

senescence such as nutrient deprivation (Cao et al. 2006; Diaz et al. 2006). Despite the well-established fact that high concentrations of exogenous JA accelerate senescence-like phenotypes, the biological relevance and molecular mechanisms are not fully elucidated. Moreover, there is little evidence that mutants defective in JA biosynthesis or signaling exhibit alterations in natural, age-dependent senescence (Parthier 1990; Selmann et al. 2010; Shan et al. 2011). Many JA senescence studies replicate the early experiments on excised leaf segments in the dark under “starvation conditions”- a highly artificial environment- or require high concentrations of exogenous JA. Together with the lack of developmental senescence phenotypes, this suggests JA primarily drives stress-induced senescence but a direct link to a causal stressor has not been identified, such as ABA and drought-induced senescence. It is unclear whether JA control of senescence relates to its roles in defense and specialized metabolism, but control of plastid status may provide a valuable link to nutrient recycling to support resource-costly defense processes.

Jasmonate biosynthesis begins with the release of α -linolenic acid from plastid membrane lipids and thus JA could behave as a retrograde signal between the chloroplast and nucleus after damage (Fig 1.3). A recent study implicates jasmonate signaling in a plastid-nuclear feedback loop to regulate the breakdown of chlorophyll. A dexamethasone-inducible *STAY GREEN* (*SGRI*) magnesium dechelataase gene shows that JA levels increase upon chlorophyll degradation (Ono et al. 2019). After DEX treatment, the expression levels of JA biosynthesis genes increased, as well as the levels of the transcription factors *MYC2* and *MYC3*, several *JAZ* genes, and *SGRI* expression, indicating that jasmonate signaling is activated by disruption of chlorophyll. Chlorophyll degradation may lead to the destabilization of thylakoid membranes by disrupting the stability of the pigment-protein complexes, which generates pools of linolenic acid for jasmonate biosynthesis (Ono et al. 2019). Similarly, the destabilization of the thylakoid

membrane via the overexpression of two ABA-inducible plastid lipases has also been shown to promote jasmonate biosynthesis (Wang et al. 2018). In addition to chlorophyll catabolism, JA represses *RUBISCO ACTIVASE* transcription (Shan et al. 2011). The inhibition of carbon fixation clearly impacts leaf function and plant growth, as *rca* mutants senesce early and mimics the starvation conditions created by dark-induced senescence. Interestingly, in a “non-starvation” model of long-term MeJA-treated *Nicotiana tabacum*, common senescence markers such as *SAG12* and *RCA* were not upregulated and the senescence phenotype was reversible (Wang et al. 2022). An estimated 75% of leaf nitrogen is accounted for by photosynthesis-related proteins such as Rubisco, LHCs, and cytochrome b6f complexes, and under certain conditions such as carbon starvation, plants may use plastidial macromolecules as alternative respiratory substrates (Araújo et al. 2011; Evans and Clarke 2019). Plastid dismantling could provide necessary resources when conditions are limiting, but under non-starvation conditions, these phenotypic extremes are not achieved, or the mechanisms to attenuate the signaling pathway remain intact. Additional studies of non-starvation models will provide insight into the role of JA-induced senescence on nutrient recycling for stress responses.

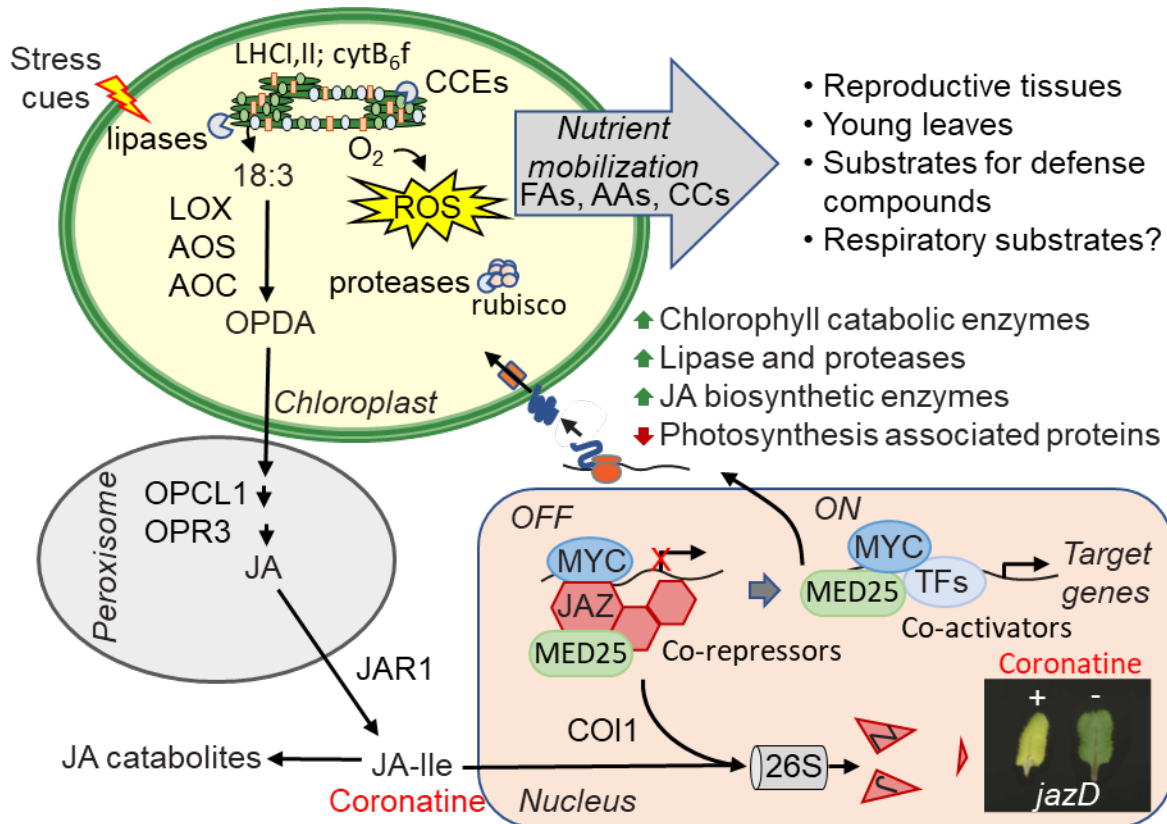


Figure 1.3 Plastid-to-nuclear signaling scheme for JA-mediated nutrient mobilization in response to stress.

Damage to chloroplast membranes releases fatty acid (e.g., linolenic acid, 18:3) precursors of jasmonic acid (JA), which is converted to jasmonoyl-L-isoleucine (JA-Ile) by the cytosolic JAR1 enzyme. Elevated JA-Ile levels promote COI1-JAZ interaction, leading to the degradation of JAZ and relief of repression on MYC transcription factors. JA signaling may perpetuate a feedback loop through the increased expression of genes encoding chlorophyll catabolic enzymes (CCEs) and the downregulation of photosynthesis-related genes. Metabolic intermediates (i.e., nutrients) generated by the breakdown of pigment-protein complexes, plastid membranes, or abundant proteins (e.g., rubisco, LHCl, LHCII, cytB₆f) may be remobilized to sink tissues as chloroplastic macromolecules are dismantled. These catabolic intermediates may also be routed to biosynthetic pathways for the biosynthesis of defense compounds or used as alternative respiratory substrates during the decline of photosynthetic capacity. Photograph in lower right shows senescence-like symptoms in a *jazD* leaf four days after treatment with coronatine (COR), which is a molecular mimic of JA-Ile. OPDA, 12-oxo-phytodienoic acid; LOX, lipoxygenase; AOS, allele oxide synthase; AOC allele oxide cyclase; OPR3, 12-OPDA reductase3; OPCL1, OPC-8:0 CoA ligase; JAR1, JASMONATE RESISTANT 1; JA-Ile, jasmonoyl-L-isoleucine; 26S, 26S PROTEASOME; MED25, MEDIATOR 25; LHCl,II, LIGHT HARVESTING COMPLEX I OR II; cytB₆f, cytochrome B₆f; CCEs, Chlorophyll Catabolic Enzymes; AAs, amino acids; FAs, fatty acids; CCs, chlorophyll catabolites.

JA AS A LINK BETWEEN METABOLISM AND CHLOROPLAST SIGNALING

The concept of plasticity in resource allocation to competing physiological tasks pervades current models of growth-defense balance (Guo et al. 2018; Monson et al. 2021). A significant gap in all such theories is the lack of mechanistic insight into how re-partitioning of specific metabolic resources to defense pathways is coordinated with primary metabolic processes that fuel other aspects of plant growth and development. Jasmonate signaling regulates transcriptional shifts in primary metabolic pathways such as the pentose phosphate pathway, towards specialized metabolism, such as the upregulation of tryptophan biosynthesis and other amino acids to support the production of defense-related specialized metabolites (Guo et al. 2018; Savchenko et al. 2019). Specialized metabolites have been implicated in primary metabolic processes through the reintegration of catabolic products and regulation of growth (Erb and Kliebenstein 2020; Bai et al. 2021; Berger et al. 2022). Kaempferol and coumarate provide precursor material, 4-hydroxybenzoate, for ubiquinone biosynthesis to support respiratory electron transfer (Berger et al. 2022). Mutations in the biosynthetic pathway of the Arabidopsis triterpene, thalianol, display altered auxin responses using the DR5 reporter. However, a clear mechanism for the regulation of auxin by thalianol metabolism was not established and further work is necessary to elucidate the role of terpenes on plant root growth and development (Bai et al. 2021). The full extent of how specialized metabolism signals to regulate primary metabolic processes is unclear, but recent work suggests a role for a glucosinolate species, 3-hydroxypropylglucosinolate, in inhibiting TOR signaling to restrict growth (Malinovsky et al. 2017; Erb and Kliebenstein 2020). TOR signaling serves as an intriguing convergence point between primary and secondary metabolism, as it additionally acts as a sensor for glucose and amino acid abundance (Cao et al. 2019). Considering the role of TOR as a central energy regulator, a potential mechanism for JA signaling to integrate

this mechanism of energy sensing and regulate growth is through the release of free amino acids via proteolysis of plastid-based proteins, as well as through signaling through the production of specialized metabolites. The biosynthesis of many metabolites is localized, in part, in the chloroplast. Thus, JA control of the plastid status through regulation of chlorophyll degradation, photosynthesis, and metabolites could relate to balancing energy sources towards primary versus secondary metabolism (Fig 1.4).

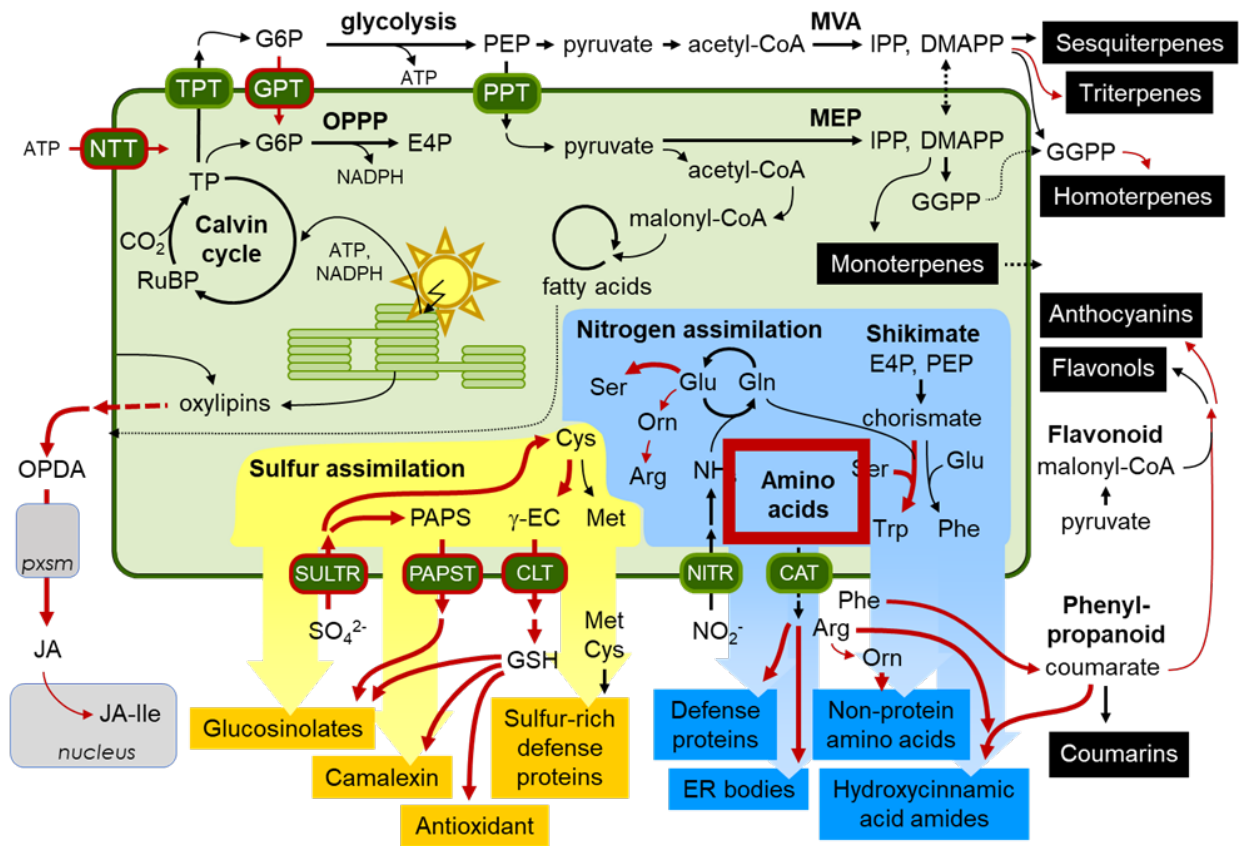


Figure 1.4 Chloroplast-derived metabolites regulated by JA.

Generalized schematic of metabolic pathways localized in the chloroplast. Carbon, sulfur, and nitrogen assimilation in the chloroplast provides precursors for defense-related compounds. Red arrows and boxes denote which pathways are upregulated in the *jazD* mutant. Pxsm, peroxisome; SULTR, SULFATE TRANSPORTER; PAPS, 3-phosphoadenosine-5-phosphosulfate; PAPST, PAPS TRANSPORTER; γ -EC, γ -glutamyl cysteine; CLT, CHLOROQUINE-RESISTANCE TRANSPORTER-LIKE TRANSPORTER; Met, methionine; Cys, cysteine; GSH, glutathione; SO₄²⁻, sulfate; NITR, Nitrate transporter; CAT, CATIONIC AMINO ACID TRANSPORTER; Arg, arginine; Phe, phenylalanine; Orn, ornithine; Ser, Serine; Trp, tryptophan; Glu, glutamate;

Figure 1.4 (cont'd)

RuBP, ribulose 1,5-bisphosphate; E4P, erythrose-4-phosphate; PEP, phosphoenolpyruvate; Gln, glutamine; IPP, isopentenyl diphosphate; DMAPP, dimethylallyl diphosphate; GGPP, geranylgeranyl pyrophosphate; NTT, ATP/ADP transporter; TPT, triose phosphate translocator; GPT, glucose-6-phosphate translocator; G6P, glucose-6-phosphate; PPT, PEP translocator; MVA, mevalonate pathway.

Further mechanistic insights into the molecular pathways associated with specialized metabolite signaling will provide valuable information on how defense and developmental cues can be integrated. For example, understanding the role of jasmonate-induced senescence and how it may connect with resource availability or nutrient recycling may have post-harvest or yield implications. Elucidation of systems such as the non-starvation system in tobacco or global -omics of *jazD* treated with coronatine will provide valuable insights into the regulatory mechanisms of JA-induced senescence, such as understanding where major carbon and nitrogen shifts are occurring and how primary and secondary metabolism change throughout the senescence process (Guo et al. 2018; Wang et al. 2022). In addition to global examinations of JA-induced changes, further study of JA function in single cells or tissue types could elucidate how specific JA responses are achieved and provide mechanisms to alter JA signaling without the pleiotropic effects seen in the higher order *Arabidopsis* mutants. Recent analysis of single-cell RNA sequencing suggests that *JAZ5* and *JAZ6* are differentially expressed in root cell types, and *JAZ2* has been implicated in controlling stomatal dynamics during defense responses (Gimenez-Ibanez et al. 2017; Lewsey et al. 2022).

THESIS RATIONALE AND OVERVIEW

The work presented here expands our knowledge of JA control of metabolism, the growth-defense balance, and senescence. A fundamental question in plant hormone signaling is how response specificity is achieved by limited sets of signaling components. JAZs and MYCs are often described as redundant due to the additive effects of mutations in these families, and a lack of

phenotypes in single mutants. Chapter 2 describes how JA signaling components coordinate specific tryptophan metabolism and defense outputs. This work identified a JAZ-MYC regulon that regulates tryptophan metabolism and responses to necrotrophic pathogens and more broadly, suggests that subfunctionalization of the JAZ and MYC families contributes to JA response specificity. This dissertation additionally aimed to address how the growth-defense balance and transition to senescence is regulated in the context of JA signaling. Chapter 3 explores the use of genetic screens to identify genes that regulate JA-induced growth inhibition and senescence. These screens identified components of the JA signaling pathway, which supports the idea that attenuation of JA signaling is critical for maintaining growth-defense tradeoffs and the promotion of senescence. Finally, Chapter 4 describes results using a JA-hypersensitive Arabidopsis mutant (*jazD*) to systematically study the process of JA-induced leaf senescence under physiological conditions. Using transcriptomics, biochemical analyses of metabolites, and visualization techniques, this work shows JA targets degradation of chloroplasts and plastid-associated metabolites. This work demonstrates how JA controls chloroplast metabolism during the growth-defense transition.

REFERENCES

- An C, Li L, Zhai Q, You Y, Deng L, Wu F, Chen R, Jiang H, Wang H, Chen Q, et al. 2017. Mediator subunit MED25 links the jasmonate receptor to transcriptionally active chromatin. *Proceedings of the National Academy of Sciences* **114**: E8930–E8939.
- Araújo WL, Tohge T, Ishizaki K, Leaver CJ, Fernie AR. 2011. Protein degradation - an alternative respiratory substrate for stressed plants. *Trends in Plant Science* **16**: 489–498.
- Attaran E, Major IT, Cruz JA, Rosa BA, Koo AJK, Chen J, Kramer DM, He SY, Howe GA. 2014. Temporal dynamics of growth and photosynthesis suppression in response to jasmonate signaling. *Plant Physiology* **165**: 1302–1314.
- Bai Y, Fernández-Calvo P, Ritter A, Huang AC, Morales-Herrera S, Bicalho KU, Karady M, Pauwels L, Buyst D, Njo M, et al. 2021. Modulation of *Arabidopsis* root growth by specialized triterpenes. *New Phytologist* **230**: 228–243.
- Bai Y, Meng Y, Huang D, Qi Y, Chen M. 2011. Origin and evolutionary analysis of the plant-specific TIFY transcription factor family. *Genomics* **98**: 128–136.
- Ballaré CL, Austin AT. 2019. Recalculating growth and defense strategies under competition: Key roles of photoreceptors and jasmonates. *Journal of Experimental Botany* **70**: 3425–3436.
- Bell E, Creelman RA, Mullet JE. 1995. A chloroplast lipoxygenase is required for wound-induced jasmonic acid accumulation in *Arabidopsis*. *Proceedings of the National Academy of Sciences* **92**: 8675–8679.
- Berger A, Latimer S, Stutts LR, Soubeyrand E, Block AK, Basset GJ. 2022. Kaempferol as a precursor for ubiquinone (coenzyme Q) biosynthesis: An atypical node between specialized metabolism and primary metabolism. *Current Opinion in Plant Biology* **66**: 102165.
- Campos ML, Yoshida Y, Major IT, de Oliveira Ferreira D, Weraduwage SM, Froehlich JE, Johnson BF, Kramer DM, Jander G, Sharkey TD, et al. 2016. Rewiring of jasmonate and phytochrome B signalling uncouples plant growth-defense tradeoffs. *Nature Communications* **7**: 12570.
- Cao P, Kim S-J, Xing A, Schenck CA, Liu L, Jiang N, Wang J, Last RL, Brandizzi F. 2019. Homeostasis of branched-chain amino acids is critical for the activity of TOR signaling in *Arabidopsis*. *Elife* **8**: e50747.
- Cao S, Su L, Fang Y. 2006. Evidence for involvement of jasmonic acid in the induction of leaf senescence by potassium deficiency in *Arabidopsis*. *Canadian Journal of Botany* **84**: 328–333.

- Chauvin A, Caldelari D, Wolfender J-L, Farmer EE. 2013.** Four 13-lipoxygenases contribute to rapid jasmonate synthesis in wounded *Arabidopsis thaliana* leaves: a role for lipoxygenase 6 in responses to long-distance wound signals. *New Phytologist* **197**: 566–575.
- Chen R, Jiang H, Li L, Zhai Q, Qi L, Zhou W, Liu X, Li H. 2012.** The *Arabidopsis* mediator subunit MED25 differentially regulates jasmonate and abscisic acid signaling through interacting with the MYC2 and ABI5 transcription factors. *The Plant Cell* **24**: 2898–2916.
- Chen Q, Sun J, Zhai Q, Zhou W, Qi L, Xu L, Wang B, Chen R, Jiang H, Qi J, et al. 2011.** The Basic Helix-Loop-Helix transcription factor MYC2 directly represses PLETHORA expression during jasmonate-mediated modulation of the root stem cell niche in *Arabidopsis*. *The Plant Cell* **23**: 3335–3352.
- Chini A, Fonseca S, Chico JM, Fernández-Calvo P, Solano R. 2009.** The ZIM domain mediates homo- and heteromeric interactions between *Arabidopsis* JAZ proteins. *Plant Journal* **59**: 77–87.
- Chini A, Fonseca S, Fernández G, Adie B, Chico JM, Lorenzo O, García-Casado G, López-Vidriero I, Lozano FM, Ponce MR, et al. 2007.** The JAZ family of repressors is the missing link in jasmonate signalling. *Nature* **448**: 666–671.
- Chung HS, Howe GA. 2009.** A critical role for the TIFY motif in repression of jasmonate signaling by a stabilized splice variant of the JASMONATE ZIM-domain protein JAZ10 in *Arabidopsis*. *The Plant Cell* **21**: 131–145.
- Cruz Castillo M, Martínez C, Buchala A, Métraux J-P, León J. 2004.** Gene-specific involvement of beta-oxidation in wound-activated responses in *Arabidopsis*. *Plant Physiology* **135**: 85–94.
- Dewitte W, Murray JAH. 2003.** The plant cell cycle. *Annual Review of Plant Biology* **54**: 235–264.
- Diaz C, Saliba-Colombani V, Loudet O, Belluomo P, Moreau L, Daniel-Vedele F, Morot-Gaudry J-F, Masclaux-Daubresse C. 2006.** Leaf yellowing and anthocyanin accumulation are two genetically independent strategies in response to nitrogen limitation in *Arabidopsis thaliana*. *Plant and Cell Physiology* **47**: 74–83.
- Dombrecht B, Xue GP, Sprague SJ, Kirkegaard JA, Ross JJ, Reid JB, Fitt GP, Sewelam N, Schenk PM, Manners JM, et al. 2007.** MYC2 differentially modulates diverse jasmonate-dependent functions in *Arabidopsis*. *The Plant Cell* **19**: 2225–2245.
- Erb M, Kliebenstein DJ. 2020.** Plant secondary metabolites as defenses, regulators, and primary metabolites: the blurred functional trichotomy. *Plant Physiology* **184**: 39–52.
- Evans JR, Clarke VC. 2019.** The nitrogen cost of photosynthesis. *Journal of Experimental Botany* **70**: 7–15.

- Fernández-Calvo P, Chini A, Fernández-Barbero G, Chico J-M, Gimenez-Ibanez S, Geerinck J, Eeckhout D, Schweizer F, Godoy M, Franco-Zorrilla JM, et al. 2011.** The *Arabidopsis* bHLH transcription factors MYC3 and MYC4 are targets of JAZ repressors and act additively with MYC2 in the activation of jasmonate responses. *The Plant Cell* **23**: 701–715.
- Feys BJF, Benedetti CE, Penfold CN, Turner JG. 1994.** *Arabidopsis* mutants selected for resistance to the phytotoxin coronatine are male sterile, insensitive to methyl jasmonate, and resistant to a bacterial pathogen. *The Plant Cell* **6**: 751–759.
- Fonseca S, Chini A, Hamberg M, Adie B, Porzel A, Kramell R, Miersch O, Wasternack C, Solano R. 2009.** (+)-7-iso-Jasmonoyl-L-isoleucine is the endogenous bioactive jasmonate. *Nature Chemical Biology* **5**: 344–350.
- Gao C, Qi S, Liu K, Li D, Jin C, Li Z, Huang G, Hai J, Zhang M, Chen M. 2016.** MYC2, MYC3, and MYC4 function redundantly in seed storage protein accumulation in *Arabidopsis*. *Plant Physiology and Biochemistry* **108**: 63–70.
- Gimenez-Ibanez S, Boter M, Ortigosa A, Garcia-Casado G, Chini A, Lewsey MG, Ecker JR, Ntoukakis V, Solano R. 2017.** JAZ2 controls stomata dynamics during bacterial invasion. *New Phytologist* **213**: 1378–1392.
- Glauser G, Dubugnon L, Mousavi SAR, Rudaz S, Wolfender J-L, Farmer EE. 2009.** Velocity estimates for signal propagation leading to systemic jasmonic acid accumulation in wounded *Arabidopsis*. *Journal of Biological Chemistry* **284**: 34506–34513.
- Guan L, Denkert N, Eisa A, Lehmann M, Sjuts I, Weiberg A, Soll J, Meinecke M, Schwenkert S. 2019.** JASSY, a chloroplast outer membrane protein required for jasmonate biosynthesis. *Proceedings of the National Academy of Sciences* **116**: 10568–10575.
- Guo Q, Major IT, Howe GA. 2018a.** Resolution of growth-defense conflict: mechanistic insights from jasmonate signaling. *Current Opinion in Plant Biology* **44**: 72–81.
- Guo Q, Major IT, Kapali G, Howe GA. 2022.** MYC transcription factors coordinate tryptophan-dependent defense responses and compromise seed yield in *Arabidopsis*. *New Phytologist* **236**: 132-145.
- Guo Q, Yoshida Y, Major IT, Wang K, Sugimoto K, Kapali G, Havko NE, Benning C, Howe GA. 2018b.** JAZ repressors of metabolic defense promote growth and reproductive fitness in *Arabidopsis*. *Proceedings of the National Academy of Sciences* **115**: E10768–E10777.
- Havko NE, Major IT, Jewell JB, Attaran E, Browse J, Howe GA. 2016.** Control of carbon assimilation and partitioning by jasmonate: An accounting of growth-defense tradeoffs. *Plants* **5**: 7.

- He Y, Fukushige H, Hildebrand DF, Gan S. 2002.** Evidence supporting a role of jasmonic acid in *Arabidopsis* leaf senescence. *Plant Physiology* **128**: 876–884.
- Hou X, Lee LYC, Xia K, Yan Y, Yu H. 2010.** DELLAs modulate jasmonate signaling via competitive binding to JAZs. *Developmental Cell* **19**: 884–894.
- Howe GA, Major IT, Koo AJ. 2018.** Modularity in jasmonate signaling for multistress resilience. *Annual Review of Plant Biology* **69**: 387–415.
- Hu Y, Jiang L, Wang F, Yu D. 2013.** Jasmonate regulates the inducer of cbf expression-C-repeat binding factor/DRE binding factor1 cascade and freezing tolerance in *Arabidopsis*. *The Plant Cell* **25**: 2907–2924.
- Hu S, Yang H, Gao H, Yan J, Xie D. 2021.** Control of seed size by jasmonate. *Science China Life Sciences* **64**: 1215–1226.
- Huot B, Yao J, Montgomery BL, He SY. 2014.** Growth-defense tradeoffs in plants: A balancing act to optimize fitness. *Molecular Plant* **7**: 1267–1287.
- Hyun Y, Choi S, Hwang H-J, Yu J, Nam S-J, Ko J, Park J-Y, Seo YS, Kim EY, Ryu SB, et al. 2008.** Cooperation and functional diversification of two closely related galactolipase genes for jasmonate biosynthesis. *Developmental Cell* **14**: 183–192.
- Ingle RA, Stoker C, Stone W, Adams N, Smith R, Grant M, Carré I, Roden LC, Denby KJ. 2015.** Jasmonate signalling drives time-of-day differences in susceptibility of *Arabidopsis* to the fungal pathogen *Botrytis cinerea*. *Plant Journal* **84**: 937–948.
- Ishiguro S, Kawai-Oda A, Ueda J, Nishida I, Okada K. 2001.** The *DEFECTIVE IN ANTHIER DEHISCENCE* gene encodes a novel phospholipase A1 catalyzing the initial step of jasmonic acid biosynthesis, which synchronizes pollen maturation, anther dehiscence, and flower opening in *Arabidopsis*. *The Plant Cell* **13**: 2191–2209.
- Jiang Y, Liang G, Yang S, Yu D. 2014.** *Arabidopsis* WRKY57 functions as a node of convergence for jasmonic acid- and auxin-mediated signaling in jasmonic acid-induced leaf senescence. *The Plant Cell* **26**: 230–245.
- Kagale S, Links MG, Rozwadowski K. 2010.** Genome-wide analysis of ethylene-responsive element binding factor-associated amphiphilic repression motif-containing transcriptional regulators in *Arabidopsis*. *Plant Physiology* **152**: 1109–1134.
- Kidd BN, Edgar CI, Kumar KK, Aitken EA, Schenk PM, Manners JM, Kazan K. 2009.** The mediator complex subunit PFT1 is a key regulator of jasmonate-dependent defense in *Arabidopsis*. *The Plant Cell* **21**: 2237–2252.
- Kim JY, Lee J-H, Park C-M. 2021.** A multifaceted action of phytochrome B in plant environmental adaptation. *Frontiers in Plant Science* **12**: 659712.

- Kliebenstein DJ. 2016.** False idolatry of the mythical growth versus immunity tradeoff in molecular systems plant pathology. *Physiological and Molecular Plant Pathology* **95**: 55–59.
- Koo AJK, Chung HS, Kobayashi Y, Howe GA. 2006.** Identification of a peroxisomal acyl-activating enzyme involved in the biosynthesis of jasmonic acid in *Arabidopsis*. *Journal of Biological Chemistry* **281**: 33511–33520.
- Koo AJK, Gao X, Jones AD, Howe GA. 2009.** A rapid wound signal activates the systemic synthesis of bioactive jasmonates in *Arabidopsis*. *Plant Journal* **59**: 974–986.
- Laudert D, Pfannschmidt U, Lottspeich F, Holländer-Czytko H, Weiler EW. 1996.** Cloning, molecular and functional characterization of *Arabidopsis thaliana* allene oxide synthase (CYP74), the first enzyme of the octadecanoid pathway to jasmonates. *Plant Molecular Biology* **31**: 323–335.
- Leone M, Keller MM, Cerrudo I, Ballaré CL. 2014.** To grow or defend? Low red : far-red ratios reduce jasmonate sensitivity in *Arabidopsis* seedlings by promoting DELLA degradation and increasing JAZ10 stability. *New Phytologist* **204**: 355–367
- Lewsey MG, Yi C, Berkowitz O, Ayora F, Bernado M, Whelan J. 2022.** scCloudMine: A cloud-based app for visualization, comparison, and exploration of single-cell transcriptomic data. *Plant Communications* **3**: 100302.
- Li Z, Luo X, Ou Y, Jiao H, Peng L, Fu X, Macho AP, Liu R, He Y. 2021.** JASMONATE-ZIM DOMAIN proteins engage Polycomb chromatin modifiers to modulate jasmonate signaling in *Arabidopsis*. *Molecular Plant* **14**: 732–747.
- Li C, Shi L, Wang Y, Li W, Chen B, Zhu L, Fu Y. 2020.** *Arabidopsis* ECAP is a new adaptor protein that connects JAZ repressors with the TPR2 co-repressor to suppress jasmonate-responsive anthocyanin accumulation. *Molecular Plant* **13**: 246–265.
- Li Q, Zheng J, Li S, Huang G, Skilling SJ, Wang L, Li L, Li M, Yuan L, Liu P. 2017.** Transporter-mediated nuclear entry of jasmonoyl-isooleucine is essential for jasmonate signaling. *Molecular Plant* **10**: 695–708.
- Liu Z, Li N, Zhang Y, Li Y. 2020.** Transcriptional repression of GIF1 by the KIX-PPD-MYC repressor complex controls seed size in *Arabidopsis*. *Nature Communications* **11**: 1846.
- Liu B, Seong K, Pang S, Song J, Gao H, Wang C, Zhai J, Zhang Y, Gao S, Li X, et al. 2021.** Functional specificity, diversity, and redundancy of *Arabidopsis* JAZ family repressors in jasmonate and COI1-regulated growth, development, and defense. *New Phytologist* **231**: 1525–1545.
- Long JA, Ohno C, Smith ZR, Meyerowitz EM. 2006.** TOPLESS regulates apical embryonic fate in *Arabidopsis*. *Science* **312**: 1520–1523.

- Lorenzo O, Chico JM, Sánchez-Serrano JJ, Solano R. 2004.** JASMONATE-INSENSITIVE1 encodes a MYC transcription factor essential to discriminate between different jasmonate-regulated defense responses in *Arabidopsis*. *The Plant Cell* **16**: 1938–1950.
- Major IT, Guo Q, Zhai J, Kapali G, Kramer DM, Howe GA. 2020.** A phytochrome B-independent pathway restricts growth at high levels of jasmonate defense. *Plant Physiology* **183**: 733–749.
- Major IT, Yoshida Y, Campos ML, Kapali G, Xin X-F, Sugimoto K, Ferreira DDO, He SY, Howe GA. 2017.** Regulation of growth – defense balance by the JASMONATE ZIM-DOMAIN (JAZ) -MYC transcriptional module. *New Phytologist* **215**: 1533–1547.
- Malinovsky FG, Thomsen M-LF, Nintemann SJ, Jagd LM, Bourguine B, Burow M, Kliebenstein DJ. 2017.** An evolutionarily young defense metabolite influences the root growth of plants via the ancient TOR signaling pathway. *Elife* **6**: e29353.
- Monte I, Franco-Zorrilla JM, Garcia-Casado G, Zamarreno AM, Garcia-Mina JM, Nishihama R, Kohchi T, Solano R. 2019.** A single JAZ repressor controls the jasmonate pathway in *Marchantia polymorpha*. *Molecular Plant* **12**: 185–198.
- Moreno JE, Shyu C, Campos ML, Patel LC, Chung HS, Yao J, He SY, Howe GA. 2013.** Negative feedback control of jasmonate signaling by an alternative splice variant of JAZ10. *Plant Physiology* **162**: 1006–1017.
- Ono K, Kimura M, Matsuura H, Tanaka A, Ito H. 2019.** Jasmonate production through chlorophyll a degradation by Stay-Green in *Arabidopsis thaliana*. *Journal of Plant Physiology* **238**: 53–62.
- Palmer D, Bender CL. 1995.** Ultrastructure of tomato leaf tissue treated with the pseudomonad phytotoxin coronatine and comparison with methyl jasmonate. *Molecular Plant Microbe Interactions* **8**: 683–692.
- Park JH, Oh SA, Kim YH, Woo HR, Nam HG. 1998.** Differential expression of senescence-associated mRNAs during leaf senescence induced by different senescence-inducing factors in *Arabidopsis*. *Plant Molecular Biology* **37**: 445–454.
- Parthier B. 1990.** Jasmonates: hormonal regulators or stress factors in leaf senescence? *Journal of Plant Growth Regulation* **9**: 57.
- Pauwels L, Barbero GF, Geerinck J, Tilleman S, Grunewald W, Pérez AC, Chico JM, Bossche RV, Sewell J, Gil E, et al. 2010.** NINJA connects the co-repressor TOPLESS to jasmonate signalling. *Nature* **464**: 788–791.
- Qi T, Huang H, Song S, Xie D. 2015.** Regulation of jasmonate-mediated stamen development and seed production by a bHLH-MYB complex in *Arabidopsis*. *The Plant Cell* **27**: 1620–1633.

- Savchenko TV, Rolletschek H, Dehesh K. 2019.** Jasmonates-mediated rewiring of central metabolism regulates adaptive responses. *Plant and Cell Physiology* **60**: 2613–2620.
- Schillmiller AL, Koo AJK, Howe GA. 2007.** Functional diversification of acyl-coenzyme A oxidases in jasmonic acid biosynthesis and action. *Plant Physiology* **143**: 812–824.
- Schommer C, Palatnik JF, Aggarwal P, Chételat A, Cubas P, Farmer EE, Nath U, Weigel D. 2008.** Control of jasmonate biosynthesis and senescence by miR319 targets. *PLoS Biology* **6**: e230.
- Schwechheimer C. 2011.** Gibberellin signaling in plants - the extended version. *Frontiers in Plant Science* **2**: 107.
- Schweizer F, Fernandez-Calvo P, Zander M, Diez-Diaz M, Fonseca S, Glauser G, Lewsey MG, Ecker JR, Solano R, Reymond P. 2013.** *Arabidopsis* basic Helix-Loop-Helix transcription factors MYC2, MYC3, and MYC4 regulate glucosinolate biosynthesis, insect performance, and feeding behavior. *The Plant Cell* **25**: 3117–3132.
- Seltmann MA, Hussels W, Berger S. 2010a.** Jasmonates during senescence. *Plant Signaling and Behavior* **5**: 1493–1496.
- Seltmann MA, Stingl NE, Lautenschlaeger JK, Krischke M, Mueller MJ, Berger S. 2010b.** Differential impact of lipoxygenase 2 and jasmonates on natural and stress-induced senescence in *Arabidopsis*. *Plant Physiology* **152**: 1940–1950.
- Shan X, Li C, Peng W, Gao B. 2011a.** New perspective of jasmonate function in leaf senescence. *Plant Signaling and Behavior* **6**: 575–577.
- Shan X, Wang J, Chua L, Jiang D, Peng W, Xie D. 2011b.** The role of *Arabidopsis* Rubisco activase in jasmonate-induced leaf senescence. *Plant Physiology* **155**: 751–764.
- Shyu C, Figueroa P, Depew CL, Cooke TF, Sheard LB, Moreno JE, Katsir L, Zheng N, Browse J, Howe GA. 2012.** JAZ8 lacks a canonical degron and has an EAR motif that mediates transcriptional repression of jasmonate responses in *Arabidopsis*. **24**: 536–550.
- Song S, Huang H, Wang J, Liu B, Qi T, Xie D. 2017.** MYC5 is involved in jasmonate-regulated plant growth, leaf senescence and defense responses. *Plant and Cell Physiology* **58**: 1752–1763.
- Song S, Qi T, Huang H, Ren Q, Wu D, Chang C, Peng W, Liu Y, Peng J, Xie D. 2011.** The JASMONATE-ZIM DOMAIN proteins interact with the R2R3-MYB transcription factors MYB21 and MYB24 to affect jasmonate-regulated stamen development in *Arabidopsis*. *The Plant Cell* **23**: 1000–1013.
- Staswick PE, Su W, Howell SH. 1992.** Methyl jasmonate inhibition of root growth and induction of a leaf protein are decreased in an *Arabidopsis thaliana* mutant. *Proceedings of the National Academy of Sciences* **89**: 6837–6840.

- Staswick PE, Tiriyaki I. 2004.** The oxylipin signal jasmonic acid is activated by an enzyme that conjugates it to isoleucine in *Arabidopsis*. *The Plant Cell* **16**: 2117–2127.
- Stintzi A, Browse J. 2000.** The *Arabidopsis* male-sterile mutant, opr3, lacks the 12-oxophytodienoic acid reductase required for jasmonate synthesis. *Proceedings of the National Academy of Sciences* **97**: 10625–10630.
- Swiatek A, Azmi A, Stals H, Inzé D, Van Onckelen H. 2004.** Jasmonic acid prevents the accumulation of cyclin B1;1 and CDK-B in synchronized tobacco BY-2 cells. *FEBS Letters* **572**: 118–122.
- Swiatek A, Lenjou M, Van Bockstaele D, Inzé D, Van Onckelen H. 2002.** Differential effect of jasmonic acid and abscisic acid on cell cycle progression in tobacco BY-2 cells. *Plant Physiology* **128**: 201–211.
- Thines B, Katsir L, Melotto M, Niu Y, Mandaokar A, Liu G, Nomura K, He SY, Howe GA, Browse J. 2007.** JAZ repressor proteins are targets of the SCF^{COI1} complex during jasmonate signalling. *Nature* **448**: 661–665.
- Thireault C, Shyu C, Yoshida Y, St Aubin B, Campos ML, Howe GA. 2015.** Repression of jasmonate signaling by a non-TIFY JAZ protein in *Arabidopsis*. *Plant Journal* **82**: 669–679.
- Toledo-Ortiz G, Huq E, Quail PH. 2003.** The *Arabidopsis* basic/helix-loop-helix transcription factor family. *The Plant Cell* **15**: 1749–1770.
- Ueda J, Kato J. 1980.** Isolation and identification of a senescence-promoting substance from wormwood (*Artemisia absinthium* L.). *Plant Physiology* **66**: 246–249.
- Uji Y, Akimitsu K, Gomi K. 2017.** Identification of OsMYC2-regulated senescence-associated genes in rice. *Planta* **245**: 1241–1246.
- Wang C, Ding Y, Wang W, Zhao X, Liu Y, Timko MP, Zhang Z, Zhang H. 2022.** Insights into gene regulation of jasmonate-induced whole-plant senescence of tobacco under non-starvation conditions. *Plant and Cell Physiology* **63**: 45–56.
- Wang K, Guo Q, Froehlich JE, Hersh HL, Zienkiewicz A, Howe GA, Benning C. 2018.** Two abscisic acid-responsive plastid lipase genes involved in jasmonic acid biosynthesis in *Arabidopsis thaliana*. *The Plant Cell* **30**: 1006–1022.
- Wang H, Li S, Li Y, Xu Y, Wang Y, Zhang R, Sun W, Chen Q, Wang XJ, Li C, et al. 2019.** MED25 connects enhancer–promoter looping and MYC2-dependent activation of jasmonate signalling. *Nature Plants* **5**: 616–625.
- Wasternack C, Strnad M. 2019.** Jasmonates are signals in the biosynthesis of secondary metabolites — Pathways, transcription factors and applied aspects — A brief review. *New Biotechnology* **48**: 1–11.

- Wu F, Deng L, Zhai Q, Zhao J, Chen Q, Li C. 2020.** Mediator subunit MED25 couples alternative splicing of JAZ genes with fine-tuning of jasmonate signaling. *The Plant Cell* **32**: 429–448.
- Wu K, Zhang L, Zhou C, Yu C-W, Chaikam V. 2008.** HDA6 is required for jasmonate response, senescence and flowering in *Arabidopsis*. *Journal of Experimental Botany* **59**: 225–234.
- Xiao S, Dai L, Liu F, Wang Z, Peng W, Xie D. 2004.** COS1: an *Arabidopsis* coronatine insensitive suppressor essential for regulation of jasmonate-mediated plant defense and senescence. *The Plant Cell* **16**: 1132–1142.
- Xie DX, Feys BF, James S, Nieto-Rostro M, Turner JG. 1998.** COI1: an *Arabidopsis* gene required for jasmonate-regulated defense and fertility. *Science* **280**: 1091–1094.
- Yang D-L, Yao J, Mei C-S, Tong X-H, Zeng L-J, Li Q, Xiao L-T, Sun T-P, Li J, Deng X-W, et al. 2012.** Plant hormone jasmonate prioritizes defense over growth by interfering with gibberellin signaling cascade. *Proceedings of the National Academy of Sciences* **109**: E1192–E1200.
- Yu J, Zhang Y, Di C, Zhang Q, Zhang K, Wang C, You Q, Yan H, Dai SY, Yuan JS, et al. 2016.** JAZ7 negatively regulates dark-induced leaf senescence in *Arabidopsis*. *Journal of Experimental Botany* **67**: 751–762.
- Zander M, Lewsey MG, Clark NM, Yin L, Bartlett A, Saldierna Guzmán JP, Hann E, Langford AE, Jow B, Wise A, et al. 2020.** Integrated multi-omics framework of the plant response to jasmonic acid. *Nature Plants* **6**: 290–302.
- Zhang Y, Turner JG. 2008.** Wound-induced endogenous jasmonates stunt plant growth by inhibiting mitosis. *PLoS One* **3**: e3699.
- Zhang F, Yao J, Ke J, Zhang L, Lam VQ, Xin X-F, Zhou XE, Chen J, Brunzelle J, Griffin PR, et al. 2015.** Structural basis of JAZ repression of MYC transcription factors in jasmonate signalling. *Nature* **525**: 269–273.
- Zhu Z, An F, Feng Y, Li P, Xue L, A M, Jiang Z, Kim J-M, To TK, Li W, et al. 2011.** Derepression of ethylene-stabilized transcription factors (EIN3/EIL1) mediates jasmonate and ethylene signaling synergy in *Arabidopsis*. *Proceedings of the National Academy of Sciences* **108**: 12539–12544.
- Zhu X, Chen J, Xie Z, Gao J, Ren G, Gao S, Zhou X, Kuai B. 2015.** Jasmonic acid promotes degreening via MYC2/3/4- and ANAC019/055/072-mediated regulation of major chlorophyll catabolic genes. *Plant Journal* **84**: 597–610.
- Ziegler J, Stenzel I, Hause B, Maucher H, Hamberg M, Grimm R, Ganai M, Wasternack C. 2000.** Molecular cloning of allene oxide cyclase. The enzyme establishing the stereochemistry of octadecanoids and jasmonates. *Journal of Biological Chemistry* **275**: 19132–19138.

**CHAPTER 2: SUBFUNCTIONALIZATION OF JAZ REPRESSORS IN PLANT
IMMUNITY AND METABOLISM**

Leah Y.D. Johnson,* Ian T. Major,* Yani Chen, Changxian Yang, Leidy J. Vanegas-Cano, and
Gregg A. Howe

Author contributions: YC generated the MYC overexpression lines and CY performed the 5-MT assays with the MYC overexpression lines in fig 2.4. LJVC performed the experiment in fig 2.1. ITM performed the experiments for figures 2.2 and 2.3. LYDJ performed the remaining experiments. LYDJ, ITM, and GAH wrote the manuscript.

ABSTRACT

Jasmonate re-programs metabolism to confer resistance to diverse plant consumers. Jasmonate stimulates the degradation of JAZ proteins that repress the activity of MYC transcription factors (TFs). In *Arabidopsis thaliana*, JAZ and MYC are encoded by 13 (*JAZ1-13*) and four (*MYC2-5*) genes, respectively. The extent to which individual JAZ and MYC proteins act redundantly or uniquely to regulate specific defense traits is not well understood. Here, we investigated the role of *MYC* and *JAZ* paralogs in controlling the production of defense compounds derived from aromatic amino acids. Analysis of loss-of-function and dominant *myc* mutations identified MYC3 and MYC4 as the major regulators of jasmonate-induced tryptophan metabolism. We developed a *JAZ* family-based, forward genetics approach to screen randomized *jaz* polymutants for allelic combinations that enhance tryptophan biosynthetic capacity. We found that mutants defective in all members (*JAZ1/2/5/6*) of JAZ subclade I over-accumulate aromatic amino acid-derived defense compounds, constitutively express marker genes for the jasmonate-ethylene branch of immunity and have enhanced resistance to necrotrophic pathogens but not insect herbivores. In defining a subset of *JAZ* and *MYC* paralogs that regulate the production of amino acid-derived defense compounds, our results provide insight into the response specificity of JA signaling.

INTRODUCTION

Plant innate immunity depends on a large repertoire of receptors which, upon perceiving foreign or endogenous “danger” signals, trigger metabolic changes that thwart attack by invading organisms. Our current understanding of how immune activation re-programs plant metabolism comes mainly from the study of secondary metabolites that exert toxic or repellent effects on herbivores (Mithöfer and Boland 2012). Recent research in animal systems has spawned the field of immunometabolism, which seeks to understand how primary metabolic pathways such as glycolysis, the TCA cycle, and amino acid metabolism support host defense by modulating the behavior of immune cells (Mathis and Shoelson 2011; Makowski et al. 2020). Links between primary metabolism in plant immunity are also well documented and generally reflect the increased demand during defense responses for energy, reducing power, and simple organic building blocks (Bolton 2009). Fundamental differences between plants and animals have likely shaped the interface between host immunity and metabolism in these two kingdoms of life. Chief among these are the absence of mobile immune cells in plants, the proliferation in plants of metabolic pathways dedicated to the production of defensive compounds (i.e., secondary metabolites), and ability of plants to photosynthetically assimilate organic skeletons containing carbon, nitrogen, and sulfur. The precise mechanisms by which plants coordinate the production and allocation of primary resources with the changing demand for defense compounds remain largely unknown.

Nearly one third of assimilated CO₂ in plants is partitioned to the shikimate pathway for the production of the aromatic amino acids (AAAs) phenylalanine (Phe), tyrosine (Tyr), and tryptophan (Trp) (Maeda and Dudareva 2012). In addition to their use in protein synthesis, AAAs are precursors for lignin and lignan, phytohormones such as auxin, and a myriad of secondary

metabolites that protect plants from environmental insults (Glawischnig et al. 2004; Mashiguchi et al. 2011; Macoy et al. 2015; Liu et al. 2018). Given the high metabolic cost of producing AAAs and their derivatives (Arnold and Nikoloski 2014), it is reasonable to hypothesize that the cellular demand for these compounds is tightly coordinated with primary metabolic pathways that supply AAAs, namely the shikimate pathway and photosynthetic assimilation of carbon and nitrogen. Recent studies show, for example, that genetic modification of enzymes controlling the flux of carbon into the shikimate pathway not only increase AAA production but also boost rates of CO₂ assimilation (Yokoyama et al. 2022). Elucidation of the mechanisms that integrate metabolic sink demand with requisite supply-side pathways may inform strategies for sustainable production of plant-based aromatics from atmospheric CO₂.

The importance of Trp for animal health and as a precursor of various plant defense compounds (e.g., indole glucosinolates) and phytohormones (e.g., auxin) has sparked interest in understanding how the biosynthesis of this essential amino acid is regulated. The amenability of the model plant *Arabidopsis thaliana* to genetic analysis has been particularly useful for these efforts (Gilchrist and Kosuge 1974; Bender and Fink 1998; Herrmann and Weaver 1999; Maeda and Dudareva 2012; Yokoyama et al. 2021). For example, genetic screens have identified mutants of *Arabidopsis* that are defective in the negative feedback inhibition of ANTHRANILATE SYNTHASE 1 (AS) (Bender and Fink 1998; Kreps et al. 1996; Li and Last 1996). As the committed step in Trp biosynthesis, AS is feedback inhibited by Trp (Fig 2.1a). Various synthetic analogs of Trp, including 5-methyl Trp (5-MT), also exert feedback inhibition on AS and impair growth by depleting tryptophan (Fig. 1b). Interestingly, genetic modifications that increase the expression of AS confer resistance to growth inhibition by 5-MT (Bender and Fink 1998; Smolen et al. 2002; Celenza et al. 2005; Guo et al. 2018). Such mutants have been instrumental for

identifying transcriptional regulators of Trp metabolism (Bender and Celenza 2009). Included among these regulators is the transcription factor MYB34, which plays a major role in coordinating the production of indole glucosinolates with the availability of Trp and assimilated forms of sulfur.

The jasmonate (JA) signaling pathway has also been implicated as a positive regulator of the expression of anthranilate synthase (AS) and other enzymes in the Trp biosynthetic pathway (Niyogi and Fink 1992; Bohlmann et al. 1996; Brader et al. 2001; Memelink et al. 2001; Celenza et al. 2005; Ishihara et al. 2008). Genetic screens for 5-MT-resistant mutants provided key insights into the mechanism by which the JA pathway promotes Trp biosynthesis. The dominant *atr2D* mutant was shown to harbor a single amino acid substitution (D94N) in the conserved JAZ-interacting domain (JID) of the bHLH-type transcription factor MYC3 (Smolen et al. 2002; Zhang et al. 2015). By attenuating JAZ binding to MYC3, *atr2D* appears to increase the constitutive activity of MYC3, leading to increased expression of *AS* and other Trp biosynthetic genes. Consistent with this notion, an Arabidopsis *jaz* decuple mutant (*jazD*) lacking 10 of 13 JAZ family members is highly resistant to growth inhibition by 5-MT (Major et al. 2020). Moreover, *jazD* plants accumulate elevated levels of free Trp and Trp-derived defense compounds via a signaling pathway that depends on MYC transcription factors (Guo et al. 2022).

In all vascular plant species examined to date, JAZ proteins are encoded by multigene families that typically exceed a dozen members, with alternative splicing of *JAZ* pre-mRNA further expanding the structural repertoire of JAZ in a given cell (Chung et al. 2010; Bai et al. 2011; Howe et al. 2018). The extent to which individual JAZ proteins exert transcriptional repression on specific *versus* redundant (or overlapping) physiological processes remains an active area of investigation (Chini et al. 2016; Guo et al. 2018; Liu et al. 2021). Efforts to delineate

specificity of response among *JAZ* paralogs are further complicated by the fact that most *JAZ* physically interact with and repress most members of the MYC TF family, which in Arabidopsis consists of four proteins (MYC2-5) (Fernández-Calvo et al. 2011; Song et al. 2017). Nevertheless, increasing evidence supports the view that *JAZ* proteins control at least some specific responses, including processes associated with stomatal behavior, senescence, and defense (Yu et al. 2016; Gimenez-Ibanez et al. 2017; Oblessuc et al. 2020; Liu et al. 2021). A critical test of functional specificity among *JAZ* paralogs or groups of paralogs is the emergence of specific phenotypes in the corresponding *jaz* loss-of-function mutants (Guo et al. 2018; Liu et al. 2021).

Interestingly, although the level of Trp and Trp-derived defense compounds is elevated in the *jazD* mutant lacking *JAZ1/2/3/4/5/6/7/9/10/13*, a *jaz* quintuple mutant (*jazQ*) defective in *JAZ1/3/4/9/10* does not exhibit this phenotype (Guo et al. 2018; Major et al. 2020). It was also reported that *jazD* strongly increases resistance to both the chewing insect *Trichoplusia ni* and the necrotrophic fungal pathogen *Botrytis cinerea*, whereas *jazQ* moderately protects against *T. ni* feeding but compromises resistance to *B. cinerea* (Guo et al. 2018). These well-defined metabolic and biological phenotypes of *jazD* and *jazQ* provide a tractable system with which to investigate the extent of *JAZ* specificity and redundancy of JA responses mediated by MYC TFs. Here, we used higher-order *myc* and *jaz* mutants as a starting point to address this question. First, screening of all possible *myc* mutant combinations identified MYC2 (and to a lesser extent MYC3) as the major regulators of 5-MT resistance. Next, we generated a population of Arabidopsis that segregates for the ten *jaz* alleles in *jazD* and screened this population for root growth resistance to 5-MT as a proxy for Trp pathway activity. This approach, which combines the power of both reverse and forward genetics in a single screen, showed that lines harboring loss-of-function mutations in all four members of *JAZ* sub-clade I (*JAZ1/2/5/6*) were more resistant to 5-MT than

wild type but less resistant than *jazD*. Biochemical and physiological studies indicate that JAZ1/2/5/6 repress immune responses to infection by *B. cinerea*, including the production of several anti-fungal metabolites whose biosynthesis depends on AAAs. We also provide evidence that JAZ1/2/5/6 control resistance to *B. cinerea* through selective repression of the JA-ethylene branch of immunity, whereas JAZ1/3/4/9/10 attenuate defense responses to insect attack through selective repression on the JA branch of immunity that mainly promotes responses to wounding. Overall, this study illustrates a novel genetic approach to identify functional specificity within multigene families, and further suggests that specific JAZ-MYC modules exert both specific and overlapping roles in plant defense.

MATERIALS AND METHODS

Plant Material and Growth Conditions

Arabidopsis thaliana accession Columbia-0 (Col-0) was used as the wild-type (WT) control for all experiments. The construction of *jazQ* and *jazD* mutants was previously described (Campos et al. 2016; Guo et al. 2018). Plants were grown in soil at 21°C under a long-day light regime of 16 h light (100 $\mu\text{mol m}^{-2}\text{s}^{-1}$) and 8 h dark. For insect and pathogen bioassays, plants were grown under short-day conditions of 8 h light (100 $\mu\text{mol m}^{-2}\text{s}^{-1}$) and 16 h dark. Site-directed mutagenesis was used to construct *MYC*^{DN} variants as previously described (Fisher and Pei 1997) using Phusion® High-Fidelity DNA Polymerase (NEB, M0530S), with all mutations verified by Sanger sequencing. Gateway cloning technology was used to insert *MYC* cDNAs into vector pGWB517, which uses a *Cauliflower Mosaic Virus* 35S promoter and adds a *c-Myc* epitope tag to the C-terminus of the MYC TF. Constructs were transformed into *Agrobacterium tumefaciens* strain GV3101 using the floral dip method (Clough and Bent 1998). Transformed plants were selected on media containing half-strength Linsmaier and Skoog (LS; Caisson Labs), 0.8% (w/v) sucrose,

0.8% (w/v) phytoblend agar (Caisson Labs), and 50 $\mu\text{g}/\text{mL}$ hygromycin. Fifteen independent T_1 lines were selected for each construct and two homozygous lines were advanced to the T_3 generation.

Root Growth Assays

Seeds were sterilized for five minutes in 70% (v/v) ethanol, five minutes in 30% (v/v) bleach, and rinsed in sterile deionized water six to eight times. Seeds were then stratified at 4°C for three to four days. Seeds were plated onto media containing half-strength Linsmaier and Skoog (LS; Caisson Labs), 0.8% (w/v) sucrose, 0.8% (w/v) phytoblend agar (Caisson Labs), and the indicated concentrations of 5-DL-methyltryptophan (5-MT) (Millipore Sigma) and methyl-jasmonate (MeJA; Sigma Aldrich). Stock solutions of 5-MT and MeJA were prepared in 0.5 N hydrochloric acid and 70% ethanol, respectively. Plates were incubated under 16 h light (80 $\mu\text{mol m}^{-2}\text{s}^{-1}$) / 8 h dark conditions at 21°C. Roots were scanned after 10 days of growth and measured using ImageJ software (<https://imagej.nih.gov/ij/>).

Growth Measurements

Plants of the indicated genotypes were grown side-by-side for four weeks under long-day conditions. The entire rosette was excised above the soil and weighed immediately to obtain total fresh weight. The projected leaf area was measured as previously described (Guo *et al.* 2018).

Screen for 5-methyl tryptophan-resistant mutants

We crossed *jazD* to WT to create a population that segregates for *jaz1*, *jaz2*, *jaz3*, *jaz4*, *jaz5*, *jaz6*, *jaz7*, *jaz9*, *jaz10*, and *jaz13* mutations. A single F_1 plant was self-pollinated to generate the segregating F_2 population. Approximately 7,500 F_2 seedlings were grown in Petri plates under 16 h light (80 $\mu\text{mol m}^{-2}\text{s}^{-1}$) and 8 h dark at 21°C on medium containing half-strength LS salts, 0.8% (w/v) sucrose, 0.8% (w/v) phytoblend agar (Caisson Labs), and 15 μM 5-DL-methyltryptophan

(5-MT) (Millipore Sigma). Parental WT and *jazD* lines were included on each plate as controls. Petri plates were incubated vertically to easily assess root length after 10 days of growth post-germination. F₂ seedlings exhibiting long roots relative to WT were transferred to soil for genotyping at each of the 10 segregating *JAZ* loci and F₃ seed collection.

PCR-based genotyping

PCR-based genotyping of *jaz* mutations was performed with two primers flanking the DNA insertion site and one primer that annealed to the T-DNA border (see Fig. A2.1). Primer sequences are provided in Table A2.1. PCR reaction conditions were as follows: 95°C for 5 min, 35 cycles of denaturation (95°C, 30 s), annealing (56°C, 30 s), elongation (72°C, 1.5 min), and one final elongation step at 72°C for 5 min. Reactions were held at 12°C until removed from the PCR instrument and analyzed on a 1% agarose gel with DNA standards (1 kb plus DNA ladder, Invitrogen).

Insect and Pathogen Bioassays

Plant-insect bioassays were performed as previously described (Herde et al. 2013) with minor modifications. *Trichoplusia ni* (cabbage looper) eggs (Benzon Research) were incubated at room temperature for 3 days on moist filter paper. Once hatched, 3-4 larvae were placed on 7- to 8-week-old, short-day-grown plants. Larval weights were determined 8-10 day after the start of feeding. For pathogen assays, leaves from short-day grown plants were excised at the petiole and placed in a Petri dish containing moist filter paper. *Botrytis cinerea* (strain B05.10) spores were suspended in 1:1 water:grape juice at a concentration of 10,000 spores/mL. Four µL of the spore suspension were applied onto each excised leaf. Plates were sealed with micropore tape (3M Health Care) and placed in the same growth chamber used for plant growth. Leaves were imaged

four days after inoculation and the necrotic lesion areas were measured using ImageJ (<https://imagej.nih.gov/ij/>).

Gene Expression Analysis

RNA extraction was performed with the Nucleospin RNA Plant kit (Machery-Nagel). cDNA was synthesized using a High-Capacity cDNA Reverse Transcription kit (Applied Biosciences, ABI) according to the manufacturer's instructions. cDNA was diluted to 0.5 ng/ μ L in nuclease-free water. Quantitative reverse-transcription PCR (qPCR) reactions contained 5 μ L 2x Power SYBR Green (ABI), 1 μ L 5 μ M combined forward and reverse primers, 2 μ L cDNA, and 2 μ L nuclease-free water to achieve a 10 μ L reaction volume. The sequence of qPCR primers is provided in Table A2.2. qPCR reactions were performed using an Applied Biosystems 7500 Fast qPCR instrument programmed as follows: hold at 50°C for 2 min; hold at 95°C for 10 min; 40 cycles between 95°C (15 s) and 60°C (1 min). LinReg v 12.18 was used to calculate efficiencies for each primer pair. Transcription abundance for each sample was normalized to that of *PROTEIN PHOSPHATASE 2A (PP2A)*.

Metabolite Analysis

The entire rosette from four-week-old, long-day grown plants was harvested and weighed prior to freezing in liquid nitrogen. Tissue was homogenized using a TissueLyserII (Qiagen). Target metabolites were extracted upon addition of 500 μ L per 50-100 mg FW tissue 80% (v/v) methanol, followed by vortexing for 5 min. Samples were heated at 80°C for 10 min and then centrifuged for 5 min at maximum speed. Metabolite analysis was performed at the Michigan State University Mass Spectrometry Facility. A 1:10 dilution in water of the extract was analyzed using ultrahigh pressure liquid chromatography (UPLC) coupled to quadrupole time-of-flight mass-spectrometry (QTOFMS) on the Waters Xevo G2-XS instrument fitted with an Acquity UPLC CSH C18 1.7

µm column. QuantLynx software was used to obtain peak area. Peaks were normalized to a telmisartan internal standard for positive electrospray ionization (ESI) mode compounds (camalexin and HCAAs) and sinigrin for negative ESI mode compounds (glucosinolates). Normalized peak area was then normalized to fresh weight to obtain relative compound levels per gram fresh weight.

Accession numbers

Genes described here have the following Arabidopsis Genome Initiative (AGI) gene accession numbers: *JAZ1* (AT1G19180), *JAZ2* (AT1G74950), *JAZ3* (AT3G17860), *JAZ4* (AT1G48500), *JAZ5* (AT1G17380), *JAZ6* (AT1G72450), *JAZ7* (AT2G34600), *JAZ9* (AT1G70700), *JAZ10* (AT5G13220), *JAZ13* (AT3G22275), *MYC2* (AT1G32640), *MYC3* (AT5G46760), *MYC4* (AT4G17880), *MYC5* (AT5G46830), *TSA1* (AT3G54640), *ASA1* (AT5G05730), *TRP1* (AT5G17990), *PDF1.2* (AT5G44420), *PP2A* (AT1G13320), *VSP2* (AT5G24770), *ORA59* (AT1G06160), and *ACT* (AT5G61160).

RESULTS

MYC3 and MYC4 promote resistance to 5-methyl tryptophan

Root growth in the presence of 5-MT provides a facile, quantitative proxy for tryptophan biosynthetic capacity. As a prelude to investigating the contribution of *JAZ* and *MYC* paralogs to 5-MT resistance in Arabidopsis, we first assessed the root growth of wild-type (WT) seedlings treated with a low, inductive concentration of methyl-JA (MeJA) together with increasing doses of 5-MT. Treatment with either MeJA or 5-MT alone was necessary to disentangle the effects of each compound, which inhibit root growth by distinct mechanisms (Fig 2.1b). In the absence of 5-MT, supplementation of the growth medium with 2.5 µM MeJA inhibited root growth by 27% relative to the mock (no MeJA) control (Fig A2.2). This concentration (2.5 µM) of MeJA

completely rescued root growth inhibition by 20 μM 5-MT and partially rescued growth inhibition by 50 μM 5-MT (Fig 2.1c). Similar results were obtained using medium supplemented with 5 μM MeJA, which in the absence of 5-MT inhibited root growth by 54% relative to a mock control (Fig 2.1d and Fig A2.2). These data are consistent with a model (Fig 2.1b) in which activation of MYC TFs with exogenous MeJA reduces the sensitivity of WT plants to 5-MT.

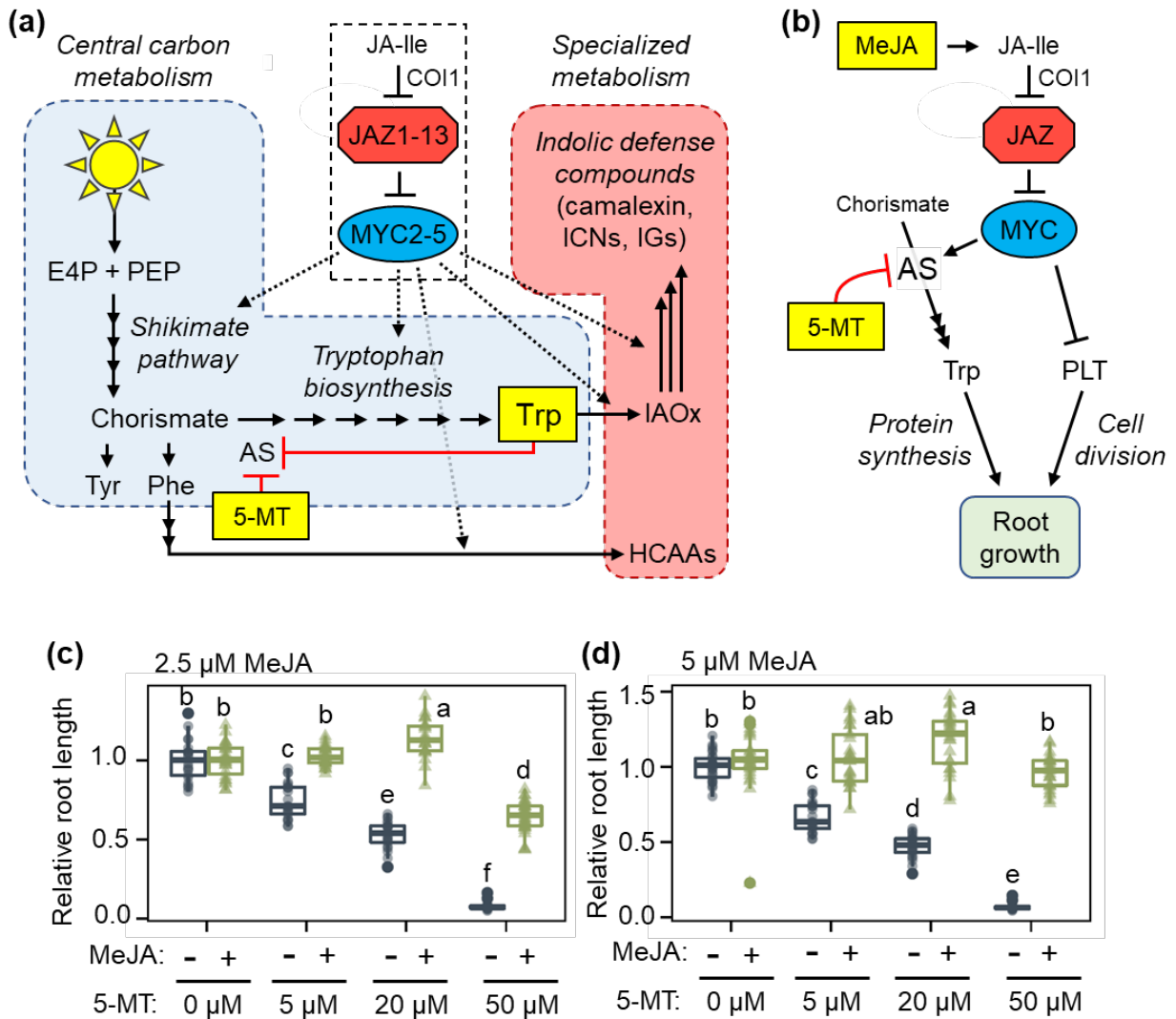


Figure 2.1 Regulation of tryptophan biosynthesis by the jasmonate signaling pathway.

(a) Within the JA signaling pathway, COI1 promotes the degradation of JAZ proteins (JAZ1-13) in the presence of JA-Ile, thus relieving repression on MYC transcription factors (MYC2-5). Dashed arrows indicate points of positive regulation by JA on the shikimate pathway, HCAA biosynthesis, tryptophan (Trp) biosynthesis and defense metabolites derived from Trp, including

Figure 2.1 (cont'd)

camalexin, indole-3-carbonyl nitriles (ICNs), and indole glucosinolates (IGs). Yellow boxes and red lines represent feedback inhibition on ANTHRANILATE SYNTHASE (AS) by Trp or the toxic Trp analog, 5-methyl Trp (5-MT). (b) Schematic of root growth regulation by JA signaling. Inhibition of root growth by methyl jasmonate (MeJA) depends on MYC-mediated inhibition of PLETHORA (PLT). Root growth inhibition in response to 5-MT presumably results from depletion of Trp, which is required for protein synthesis. (c-d) Relative root length of Arabidopsis seedlings grown on media containing various concentrations of 5-MT or a combination of 5-MT and MeJA. Inclusion of (c) 2.5 μ M or (d) 5.0 μ M MeJA in the medium reduced root growth inhibition by 5-MT. + and – symbols denote the presence or absence of MeJA in the growth media. Root length values are scaled relative to the 0 μ M 5-MT for mock or MeJA treatment. Data show 18-33 seedlings per treatment. Letters indicate significant differences at $P < 0.05$ according to Tukey's honestly significant difference (HSD) test. Absolute root length data is shown in Figure A2.2.

To directly assess the contribution of individual MYC TFs to tryptophan metabolism under conditions of basal (i.e., JAZ replete cells) JA signaling, we used root growth assays to measure the sensitivity of *myc2*, *myc3*, *myc4*, and *myc5* single mutants and all possible *myc* polymutant combinations to 5-MT. Dose-response profiles showed that the 16 genotypes segregated into three distinct groups relative to the WT control: low (i.e., WT) sensitivity to 5-MT (group I), moderate hypersensitivity to 5-MT (group II), and strong hypersensitivity to 5-MT (group III) (Fig 2.2a). Group I included WT and all other genotypes harboring the WT *MYC3* allele. All moderately hypersensitive genotypes in group II were homozygous for the loss-of-function *myc3* allele. Group III included genotypes containing both *myc3* and *myc4* mutations, indicating that *myc4* enhances the *myc3* phenotype. The separation of genotypes into three 5-MT-response phenotypes was supported by unbiased hierarchical clustering of the root growth data (Fig 2.2b), as well as statistical analysis of root growth responses to a single concentration of 5-MT (e.g., 10 μ M; Fig 2.2c). These data indicate that, in cells containing a full complement of JAZ proteins, MYC3 is the major positive regulator of 5-MT resistance and that MYC4 also performs this role in a *myc3* mutant background. *MYC2* and *MYC5* did not contribute to 5-MT resistance under these experimental conditions.

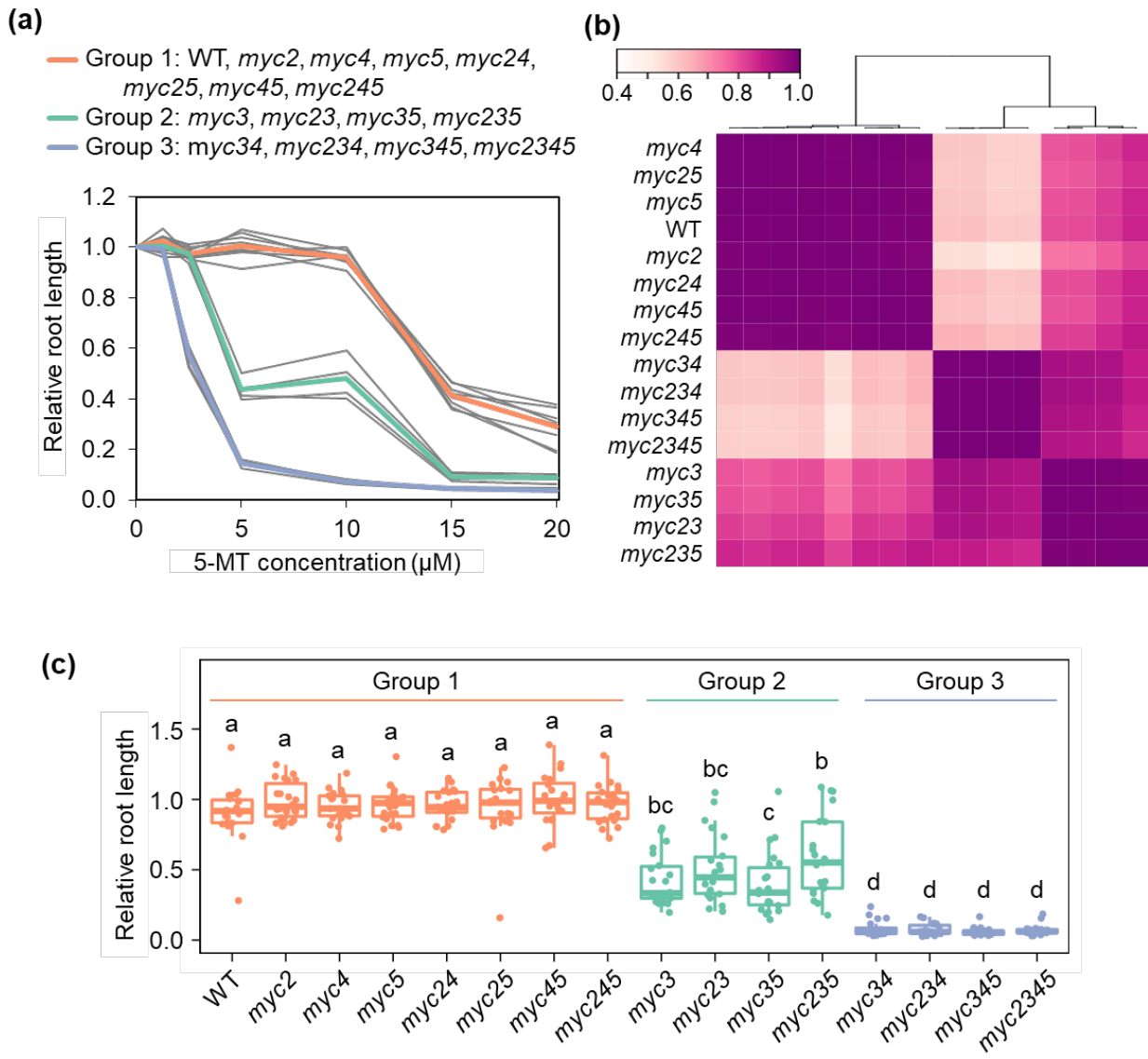


Figure 2.2 Loss of MYC3 and MYC4 results in hypersensitivity to root growth inhibition by 5-methyl tryptophan (5-MT) in Arabidopsis seedlings.

(a) 5-MT dose-response curves for the indicated 16 genotypes. Grey lines show individual genotypes, which clustered into three distinct groups (color lines). Relative root lengths were obtained by normalizing to root lengths on medium lacking (0 μM) 5-MT. (b) The data shown in panel (a) were used to generate a pairwise Pearson correlation matrix of root lengths. Matrix order was determined by hierarchical clustering and is represented by a dendrogram. (c) Root lengths of wild type (WT) and *myc* polymutant seedlings grown on plates supplemented with 10 μM 5-MT. Data show 19-22 seedlings per genotype and are shaded orange for group 1 genotypes, turquoise for group 2 genotypes, and light blue for group 3 genotypes. Root lengths in (c) were normalized to medium without (0 μM) 5-MT for each genotype. Letters indicate significant differences at $P < 0.05$ according to Tukey's honestly significant difference (HSD) test.

We next used the 5-MT assay to study the regulation of tryptophan metabolism by MYC TFs under conditions in which JA signaling was constitutively activated by genetic depletion of JAZ. As shown in Fig 2.3 and previous studies, mutation of 10 *JAZ* genes in the *jazD* mutant constitutively activates the expression of tryptophan biosynthetic genes and confers strong resistance to 5-MT (Guo et al. 2018). We used genetic crosses (Guo et al. 2022) to combine *jazD* with all six *myc* polymutant combinations: three *myc* single mutants, three *myc* double mutants, and the *myc2 myc3 myc4* triple mutant, referred to as *mycT* (Fig 2.3). The *jazD mycT* combinatorial mutant was as hypersensitive to 5-MT as *mycT* seedlings, indicating that increased tryptophan metabolism *jazD* strictly requires the combined action of MYC2/3/4. Among the *myc* single mutants (*jazD myc2*, *jazD myc3*, and *jazD myc4*), only *myc3* enhanced the sensitivity of *jazD* to 5-MT. Analysis of *myc* double mutants showed that *myc2* and *myc4* did not further enhance sensitivity of *jazD myc3* to 5-MT. Unexpectedly, however, the combination of *myc2* and *myc4* modestly (but statistically significant) increased the sensitivity of *jazD* to 5-MT (Fig 2.3). These data support the notion that MYC3 is the major positive regulator of tryptophan metabolism in JAZ-depleted cells. Under these conditions, MYC2 and MYC4 appear to exert a weak positive effect on tryptophan biosynthetic capacity.

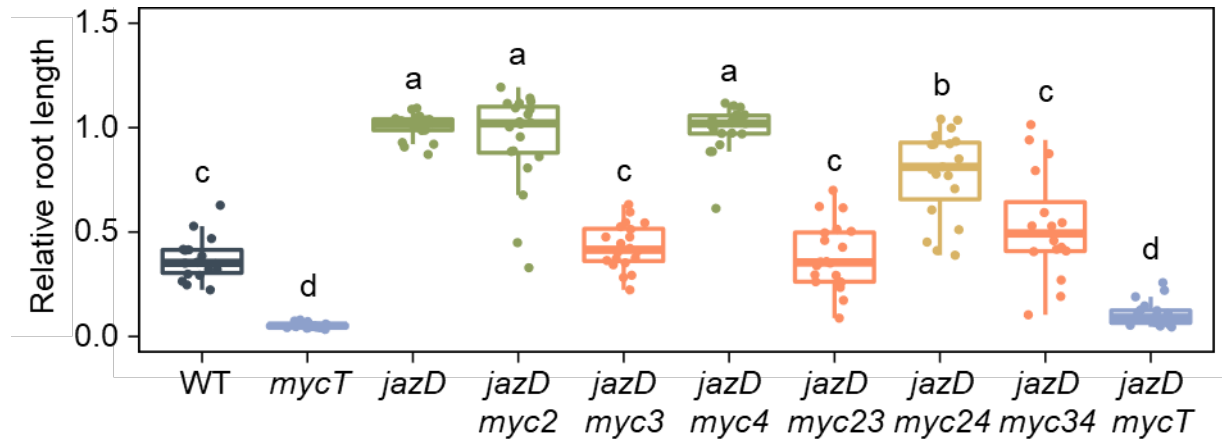


Figure 2.3 Genes encoding MYC TFs are required for resistance of the *jazD* decuple mutant (*jazD*) to 5-methyl tryptophan (5-MT).

Data show the root lengths of wild type (WT), *mycT* (*myc2/3/4* triple mutant), *jazD*, and *jazD myc* (*jaz* decuple mutant with *myc* single, double, or triple mutant combinations) seedlings grown on medium supplemented with 15 μ M 5-MT. Root lengths for each genotype were normalized to root growth on medium lacking (0 μ M) 5-MT. Data show 20 seedlings per genotype. Letters indicate significant differences at $P < 0.05$ according to Tukey's honestly significant difference (HSD) test.

In addition to analysis of *myc* loss-of-function mutants, we developed transgenic lines that overexpress dominant MYC variants with attenuated JAZ-binding capacity. This approach was based on the previous observation that a point mutation (D94N) in the JAZ-interacting domain of MYC3 abolishes interaction with most JAZ proteins and confers resistance to 5-MT through upregulation of tryptophan biosynthetic genes (Smolen et al. 2002; Goossens et al. 2015; Zhang et al. 2015). We found that overexpression of MYC3^{D94N} and MYC4^{D102N}, but not the MYC3^{WT} and MYC4^{WT} proteins, conferred resistance to 5-MT at a level comparable to *jazD* (Fig 2.4b, c). Overexpression of neither MYC2^{WT} nor MYC2^{D105N} affected 5-MT resistance (Fig 2.4a).

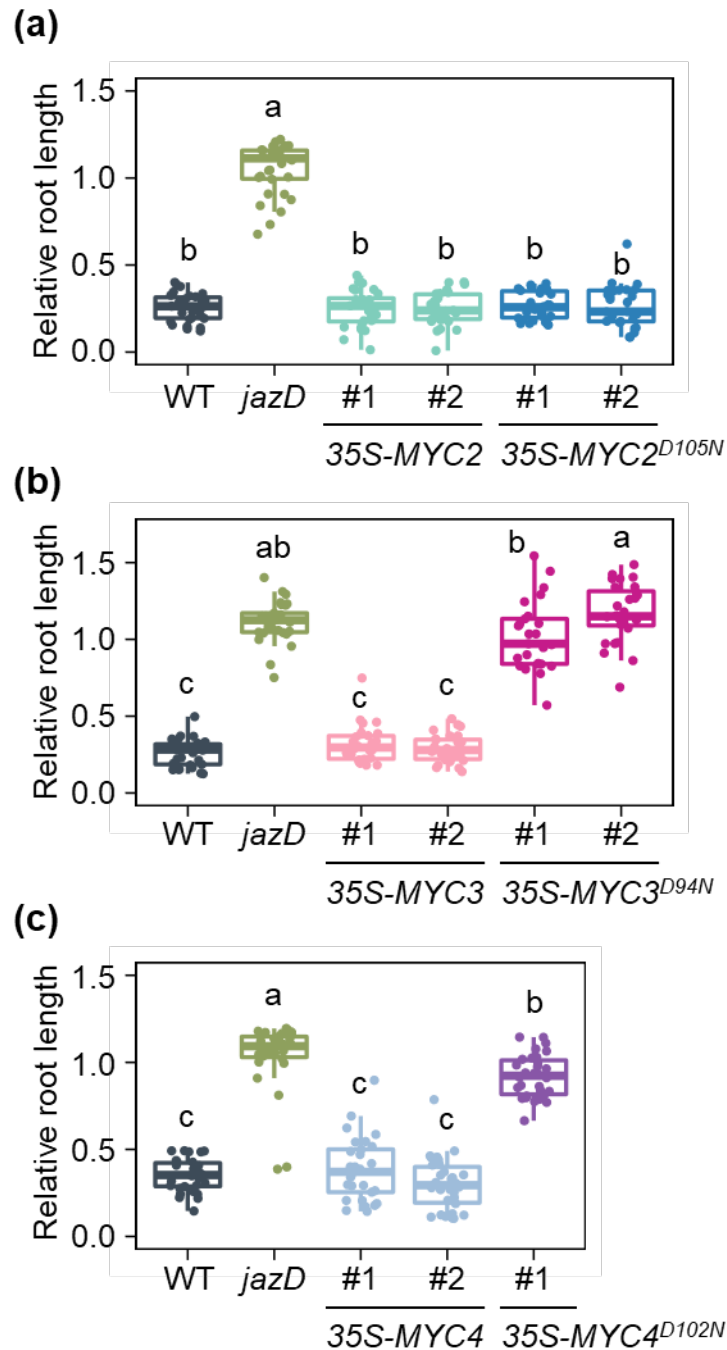


Figure 2.4 Overexpression of dominant MYC3 and MYC4 variants confer increased resistance to growth inhibition by 5-methyl tryptophan (5-MT).

(a-c) Data show the root lengths of wild type (WT), *jaz* decuple (*jazD*), and transgenic lines overexpressing WT or dominant “DN” variants (mutation resulting in substitution of conserved aspartate to asparagine) of MYC2 (a), MYC3 (b), and MYC4 (c) grown on medium supplemented with 15 μ M 5-MT. Root lengths for each genotype were normalized to root growth on medium lacking (0 μ M) 5-MT. Data show 28-30 seedlings per genotype. Letters

Figure 2.4 (cont'd)

indicate significant differences at $P < 0.05$ according to Tukey's honestly significant difference (HSD) test.

Resistance to 5-methyl tryptophan is associated with loss of group I JAZ genes

The epistatic relationship between *mycT* and *jazD* (Fig 2.3) is consistent with the hypothesis that one or more JAZ proteins repress the ability of MYCs to bolster tryptophan metabolism in response to increased demand for defense compounds (Fig 2.1a). We used *jaz* loss-of-function (i.e., insertional) mutants to test whether 5-MT resistance is controlled by specific JAZ subtypes or whether JAZs act additively to perform this function. Given the large size of the *JAZ* family in *Arabidopsis*, however, systematic construction of thousands of possible *jaz* polymutant combinations was not practical. As an alternative approach, we exploited the strong 5-MT resistance of *jazD* to identify lower-order combinations of *jaz* mutations that alter tryptophan biosynthetic capacity. We reasoned that segregation of 10 *jaz* mutations in an F_2 population derived from a cross between *jazD* and WT would generate allelic combinations that confer resistance to 5-MT (Fig 2.5a). Among ~7,500 F_2 seedlings screened on medium supplemented with 15 μ M 5-MT, we identified 97 F_2 progeny having longer roots than WT (Fig 2.5b). Genotyping of these 97 lines at each of the 10 segregating *JAZ* loci showed that homozygous mutations in *JAZ1*, *JAZ2*, *JAZ5*, *JAZ6*, and *JAZ9* were significantly associated with 5-MT resistance, whereas mutations in *JAZ3*, *JAZ4*, *JAZ7*, *JAZ10*, and *JAZ13* were much less frequent among the resistant lines (Fig 2.5b; Fig A2.3; Table A2.3). Three F_2 progeny (#11, #36, and #93) with increased 5-MT resistance were selected for further characterization. Genotyping of F_3 progeny showed that these three lines contained a common set of homozygous mutations affecting all four members (*JAZ1/2/5/6*) of the *JAZ* phylogenetic clade I: line 11-19, *jaz1/2/5/6/9*; line 36-14, *jaz1/2/5/6/7/10*; and line 93-30, *jaz1/2/5/6* (Fig A2.4). Dose-response curves performed with F_4 -generation plants showed that the 5-MT resistance of all three lines was intermediate between *jazD* and WT (Fig 2.5c).

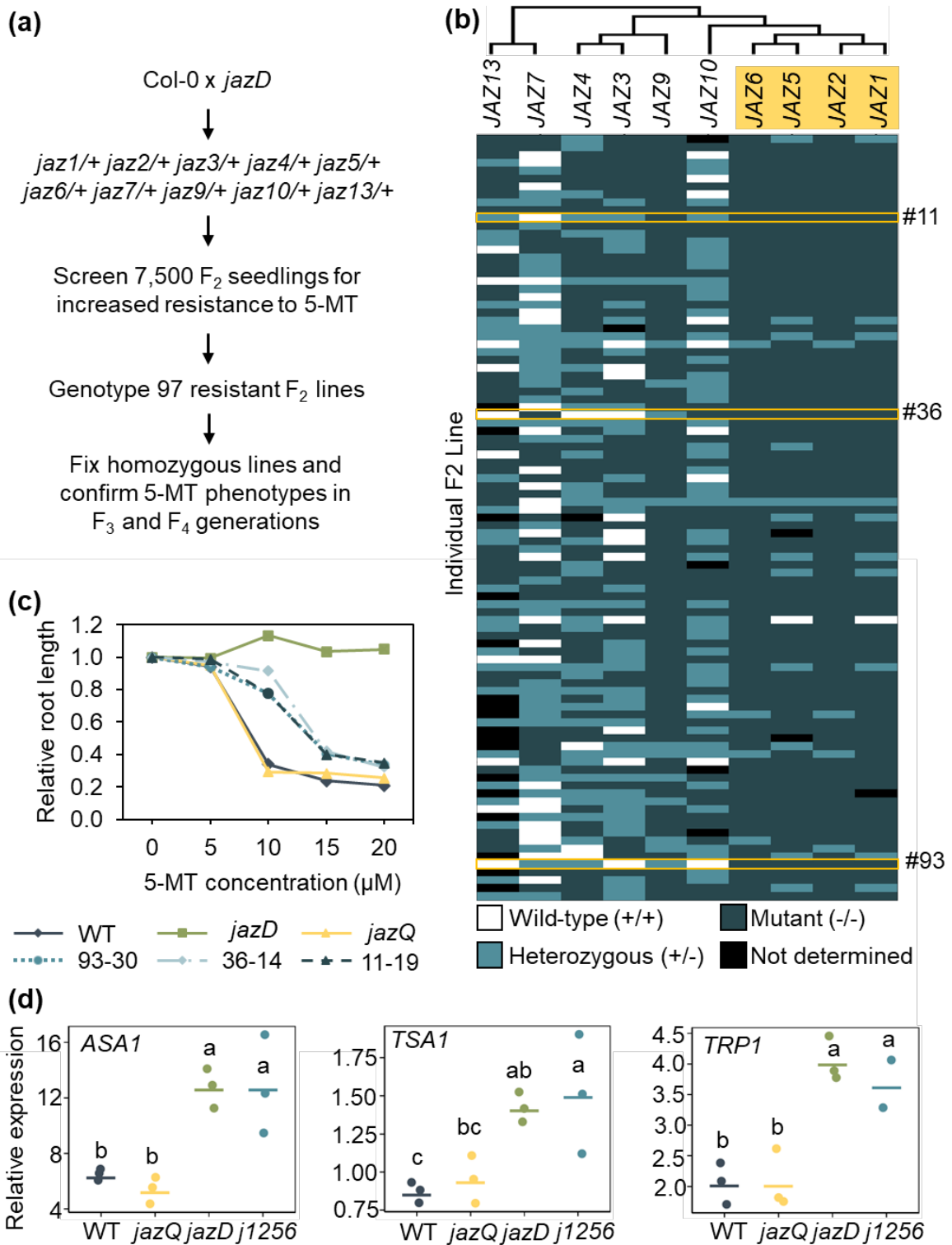


Figure 2.5 Identification of *jaz* mutations associated with resistance to 5-methyl tryptophan (5-MT).

Figure 2.5 (cont'd)

(a) Summary of the screening procedure. (b) Heat map of genotyping results for 97 F₂ seedlings exhibiting increased resistance to 5-MT relative to WT. Rows and columns correspond to individual F₂ plants and the corresponding genotype, respectively: white, homozygous wild-type (+/+); medium shading, heterozygous (+/-); dark shading; homozygous *jaz* allele (-/-); black, undetermined. Highlighted F₂ progeny #11, 36, and 93 were selected for further study. The phylogenetic tree was constructed using the Maximum Likelihood method and JTT-based matrix model in MEGA X, based on the predicted amino-acid sequences of full-length JAZ proteins. The *JAZ* group I clade is highlighted in yellow. (c) 5-MT dose-response curves of the indicated genotypes grown for 10 days on media supplemented with increasing concentrations of 5-MT. F₄ progeny of lines 11, 36, and 93, in which *jaz* alleles were fixed, were used for this experiment. Root lengths were normalized to that of seedlings not treated (0 μM) with 5-MT. (d) Quantitative PCR analysis of gene expression in roots of 16-day old seedlings of the indicated genotype. *ASAI*, ANTHRANILATE SYNTHASE ALPHA SUBUNIT 1; *TSA1*, TRYPTOPHAN SYNTHASE ALPHA CHAIN 1; *TRP1*, TRYPTOPHAN BIOSYNTHESIS 1. Gene expression values were normalized to the reference gene, *PP2A*. Dots represent individual data points and bars represent the mean. Letters indicate significant differences at P<0.05 according to Tukey's honestly significant difference (HSD) test.

Subsequent experiments were focused on detailed phenotypic analysis of line 93 (henceforth referred to as *j1256*) through comparisons to parental WT and *jazD*, as well as a *jaz* quintuple mutant (*jazQ*; *jaz1/3/4/9/10*) that is fully sensitive to 5-MT (Major et al. 2020, Fig 2.5c). Quantitative PCR analysis of RNA isolated from roots of WT, *jazQ*, *jazD*, and *j1256* seedlings showed that the expression of *ASAI* and two additional tryptophan biosynthetic genes (*TSA1* and *TRP1*) was increased in *jazD* and *j1256* relative to WT, but was not elevated in the 5-MT-sensitive *jazQ* mutant (Fig 2.5d). These data suggest a JAZ subtype-specific function for group I JAZs in the control of tryptophan biosynthetic capacity. Growth of plants in soil showed that the leaf biomass of *j1256* was intermediate between WT and *jazD* but lower than that of *jazQ* (Fig 2.6), consistent with the role of JAZ in growth promotion (Guo et al. 2018).

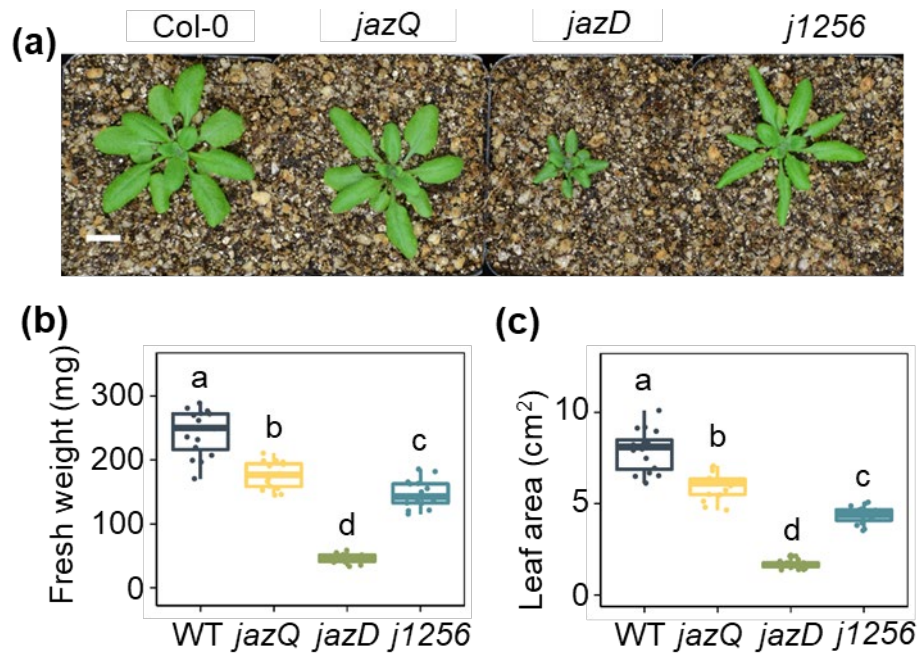


Figure 2.6 *j1256* mutant plants exhibit a moderate reduction in leaf growth.

(a) Photograph of 26-d-old wild-type (WT), *jaz* quintuple mutant (*jazQ*), *jaz* decuple mutant (*jazD*), and *jaz1/2/5/6* (*j1256*) plants. Scale bar represents 1 cm. (b-c) Fresh weight (b) and projected leaf area (c) of 26-day-old WT, *jazQ*, *jazD*, and *j1256* rosettes. Letters indicate significant differences at $P < 0.05$ according to Tukey's honestly significant difference (HSD) test.

***j1256* plants constitutively accumulate anti-fungal defense compounds derived from the shikimate pathway**

We hypothesized that that the increased resistance of *j1256* plants to 5-MT may be accompanied by constitutive accumulation of tryptophan-derived secondary metabolites, which serve a key role in protecting *Arabidopsis* from various biotic attackers (Clay et al. 2009; Müller et al. 2019). We tested whether leaves of untreated *j1256* plants over-accumulate indolic defense compounds such as indole glucosinolates (IGs) and camalexin (Fig 2.1a). Analysis of leaf extracts using liquid chromatography-mass spectrometry (LC-MS) showed that the total glucosinolate profile, as determined from principal component analysis (PCA), of *j1256* leaves was more similar to WT than *jazD* (Fig 2.7a). Indeed, with the exception of a single IG derivative (4MOI3M) that

was slightly more abundant (1.8-fold) in *j1256* than WT, the level of bulk IGs (including I3M, the most abundant IG) (Brown et al. 2003) was unchanged in *j1256* compared to WT (Fig 2.7b and Fig A2.6). The content of aliphatic glucosinolates (AGs) in *j1256*, including the most abundant 4MSOB derivative, was also comparable to WT (Fig 2.7c and Fig A2.6). In contrast to glucosinolates, we found that *j1256* leaves constitutively accumulate higher levels of camalexin than WT and *jazQ*, with camalexin levels in *jazD* trending higher than WT as well (Fig 2.7d). Thus, 5-MT resistance in *j1256* is associated with increased production of some (e.g., camalexin) but not all (e.g., I3M) tryptophan-derived secondary metabolites.

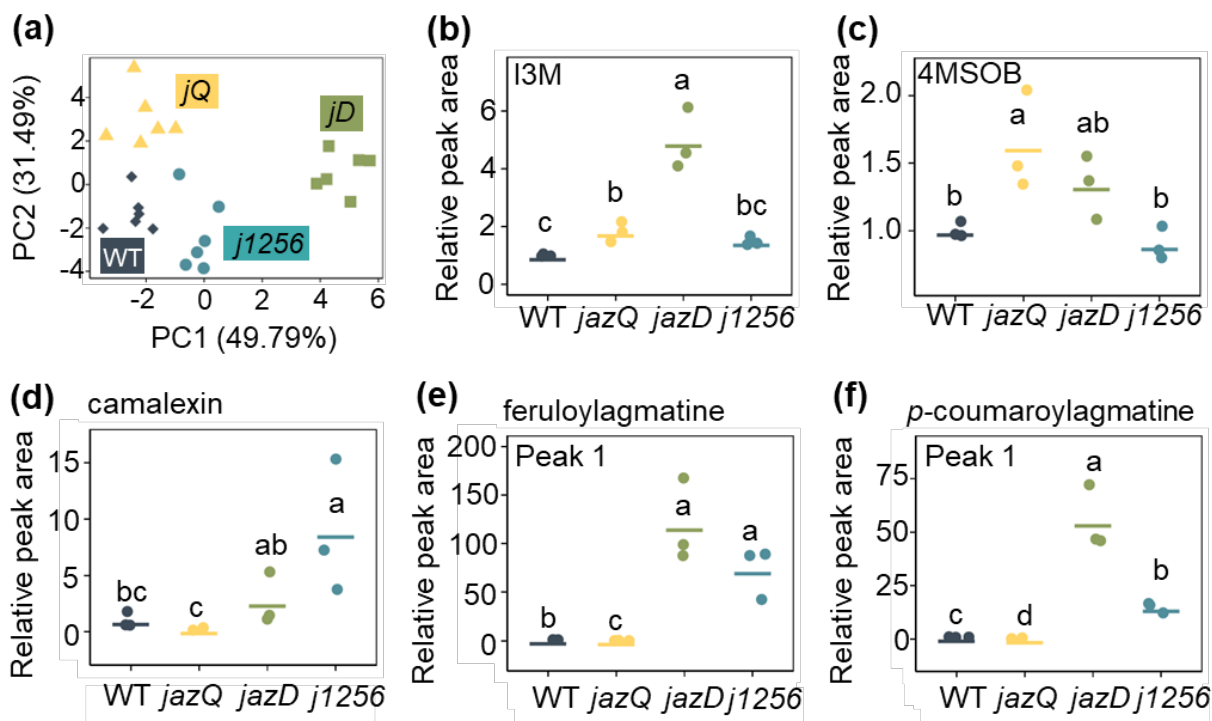


Figure 2.7 Constitutive accumulation of select defense compounds in the *j1256* mutant.

(a) Principal component analysis of 18 glucosinolate metabolites in leaves of 26-day-old wild-type (WT), *jaz1/2/5/6* (*j1256*), *jaz* quintuple (*jQ*), *jaz* decuple (*jD*) mutant plants. (b-c) Relative levels of the most abundant (b) indole (indol-3-ylmethyl-, I3M) and (c) aliphatic (4-methylsulphinylbutyl-, 4MSOB) glucosinolate species in leaves of untreated 26-day-old plants. Peak areas were normalized to the WT. (d-f) Relative levels of (d) camalexin and two hydroxycinnamic acid amides, (e) feruloylagmatine and (f) *p*-coumaroylagmatine in leaves of 26-day-old leaves of the indicated genotypes. Peak areas were normalized to the WT. A second

Figure 2.7 (cont'd)

peak having an identical mass was also detected for the two HCAAs (Fig A2.5). Letters indicate significant differences at $P < 0.05$ according to Tukey's honestly significant difference (HSD) test.

We next tested whether the *j1256* mutant constitutively accumulates secondary metabolites derived from non-tryptophan branches of the shikimate pathway. Hydroxycinnamic acid amides (HCAAs), including feruloylagmatine and *p*-coumaroylagmatine, constitute a class of anti-fungal compounds whose biosynthesis from phenylalanine is dependent on synergistic interactions between the JA and ethylene signaling pathways (Muroi et al. 2009; Li et al. 2018). WT and *jazQ* leaves accumulated low but detectable levels of both HCAAs (Fig 2.7e, f). These compounds accumulated to much higher levels (>14-fold higher than WT) in *jazD* and *j1256* leaves. During the course of these measurements, we noted that each HCAA eluted as two discrete LC peaks (peak 1 and 2) having identical mass and similar genotype-dependent accumulation pattern, which likely indicates the presence of structural isomers (Fig A2.5). These data demonstrate that 5-MT resistance in *jazD* and *j1256* plants is associated with increased constitutive accumulation of anti-fungal compounds produced from multiple aromatic amino acids.

The jasmonate-ethylene branch of immunity is selectively activated in *j1256* plants

The bifurcated JA and JA-ethylene (JA-ET) signaling pathways in *Arabidopsis* confer resistance to wounding by chewing insects and necrotrophic-type colonization by fungal pathogens, respectively (Glazebrook 2005; Penninckx et al. 1998). We used qPCR analysis of pathway-specific marker genes to assess whether the JA and JA-ET sector of defense are constitutively activated in *j1256* plants. In comparison to WT, expression of the *VEGETATIVE STORAGE PROTEIN2* (*VSP2*) marker of the JA-dependent wound response pathway was induced in *jazD* and *jazQ* but not *j1256* (Fig 2.8a). By contrast, the *PLANT DEFENSIN1.2* (*PDF1.2*) marker of the JA-ET response pathway was highly induced in *jazD* and *j1256* but not in *jazQ* or WT (Fig 2.8b). A similar pattern was observed for two additional markers of the JA-

ET pathway: *ORA59*, which coordinates HCAA production via the JA-ET pathway (Li et al. 2018) and *ACT*, which encodes the acyltransferase catalyzing the rate-limiting step in HCAA biosynthesis (Muroi et al. 2009) (Fig 2.8c, d).

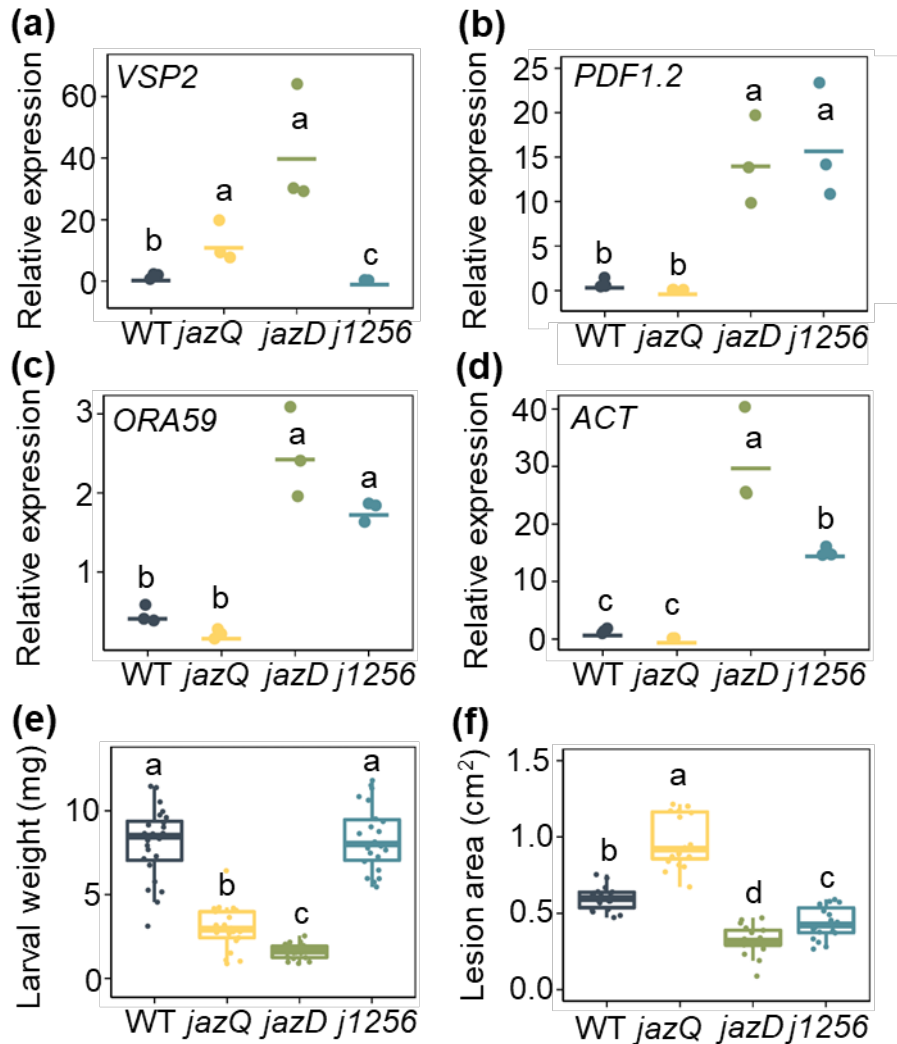


Figure 2.8 The jasmonate-ethylene branch of immunity is selectively activated in *j1256* plants.

(a-d) Abundance of (a) *VEGETATIVE STORAGE PROTEIN 2 (VSP2)*, (b) *PLANT DEFENSIN 1.2 (PDF1.2)*, (c) *OCTADECANOID-RESPONSIVE ARABIDOPSIS AP2/ERF 59 (ORA59)*, and (d) *ANTHOCYANIN 5-AROMATIC ACYLTRANSFERASE 1 (ACT)* transcripts in untreated leaves of 26-day-old wild-type (WT), *jaz* quintuple (*jazQ*), *jaz* decuple (*jazD*), and *jaz1/2/5/6 (j1256)* plants. Transcript levels were normalized to a *PROTEIN PHOSPHATASE 2A (PP2A)* reference gene. (e) Performance of *Trichoplusia ni* larvae on the indicated host genotype. Newly hatched larvae were placed on seven-week-old WT, *jazQ*, *jazD*, and *j1256* plants and weighed

Figure 2.8 (cont'd)

after eight days of feeding (n = 21-24). (f) Leaf disease symptoms caused by infection of *Botrytis cinerea* on the indicated host genotype. The lesion area on excised leaves was measured four days after pathogen inoculation with a 4 μ L drop of 10,000 spores/ml (n = 18). Letters indicate significant differences at P<0.05 according to Tukey's honestly significant difference (HSD) test.

These observations led us to test the level of biotic stress resistance in *j1256* plants. In agreement with previous studies (Guo et al. 2018), *jazD* was highly resistant to both the chewing insect *Trichopulsia ni* and the necrotrophic-type fungal pathogen *Botrytis cinerea*, whereas *jazQ* is moderately resistant to *T. ni* but hypersusceptible to *B. cinerea* (Fig 2.8e, f). Strikingly, *j1256* plants exhibited a WT-level of susceptibility to insect herbivory but were more resistant than WT to *B. cinerea* infection. These findings indicate that JAZ1/2/5/6 repress the biosynthesis of select amino acid-derived defense compounds that confer resistance to a necrotrophic fungal pathogen.

DISCUSSION**Screening of a segregating mutant population identifies JAZ subtype involved in tryptophan metabolism**

A common genetic approach to resolve the individual roles of genes from small multigene families is to generate combinatorial mutations, however the large number of polymutant combinations made this impractical for the 13-member JAZ family. As an alternative, we generated a segregating F₂ population of *jaz* mutants and found that mutations in *JAZ1*, *JAZ2*, *JAZ5*, and *JAZ6* were associated with control of tryptophan metabolism and the production of anti-fungal compounds. The robust long-root phenotype associated with 5-MT resistance was important to the success of our screen, consistent with the benefits of simple screening procedures with few false positives (Page and Grossniklaus 2002). Our F₂ screen is unbiased and uses biological phenotypes to discriminate the roles of individual contributions of multigene families, in contrast to other approaches that prioritize specific mutant combinations based on phylogeny or molecular interactions to investigate the function of large gene families (Overvoorde et al. 2005;

Campos et al. 2016; Liu et al. 2021). Our approach may be broadly applicable to other plants using CRISPR, for which multiplex editing and counter-selection markers permit the rapid generation of non-transgenic mutants of entire gene families (Zhao et al. 2018; Stuttmann et al. 2021; Ursache et al. 2021; Zhang et al. 2021).

We note that genetic linkage is a caveat of our approach and may limit the resolution of linked genes. The tight linkage of the *JAZ2-JAZ6-JAZ9* and *JAZ1-JAZ5* loci likely influenced their segregation ratios in our screen (Fig. A2.4) and impedes further genetic dissection of the *jl256* mutant. It is possible that *JAZ1*, *JAZ2*, *JAZ5*, and *JAZ6* contribute unequally to the *jl256* mutant phenotypes since the single *jaz6* mutant has a reported subtle increase in fungal resistance (Ingle et al. 2015; Liu et al. 2021). The weaker *jl256* phenotypes relative to *jazD* also suggest that other JAZs may contribute to repression of fungal resistance and tryptophan metabolism (Fig. 2.7; Fig. 2.8; Table A2.3). Our screen showed that homozygous mutations in *JAZ3*, *JAZ4*, and *JAZ13* were significantly associated with 5-MT resistance and may provide some additive resistance to 5-MT in *jazD* (Table A2.3). Considering that *JAZ3*, *JAZ4*, and *JAZ9* form the JAZ phylogenetic clade V, it is difficult to distinguish whether the *JAZ9* mutation contributes some 5-MT resistance and is masked by the *JAZ2-JAZ6-JAZ9* linkage.

Resolving JAZ-MYC redundancy and specificity

Our genetic analyses add to growing evidence that the JAZ and MYC regulators have specific functions (Gasparini et al. 2015; Zander et al. 2020; Liu et al. 2021). While we do not address how the group I JAZ1/2/5/6 are primary regulators of 5-MT resistance and necrotroph immunity, this specificity may act through subtleties in expression patterns or protein sequence that influence protein-protein interactions. Some JAZs have distinct domains, such as the Cryptic MYC Interacting Domain (CMID) that binds with higher affinity to the MYCs or an Ethylene-

responsive Amphiphilic Repression motif (EAR) that directly recruits the repressor TOPLESS (Kagale et al. 2010; Shyu et al. 2012; Moreno et al. 2013). Protein-protein interaction studies show that almost all of the JAZ proteins bind to MYC2, MYC3, and MYC4 and the co-repressor, NINJA (Chini et al. 2016). Differential binding of groups of JAZs with the MYC transcription factors may regulate outputs through mechanisms such as the additional recruitment of histone modifiers or the binding capacity of the JAZs, such as through the CMID. The JAZ proteins additionally recruit chromatin modifiers and co-repressor proteins, which may provide an additional level of response specificity. While some JAZs are able to interact directly with the corepressor, TOPLESS, other JAZs require an adaptor protein such as NINJA. A novel adaptor protein, ECAP, contributes to JA-regulated anthocyanin production, and *ecap* mutants display elevated *Botrytis* resistance, suggesting that these responses are regulated in part by co-repressors (Li et al. 2020). Many studies have been performed with systems such as yeast-two-hybrid, but additional work identifying interactions through pull-down assays *in planta* may clarify how these JAZs work with other regulatory components to provide specific outputs. Additionally, single-cell sequencing or other tissue specificity studies may help clarify how specific JAZs may coordinate responses across cell types and throughout development (Gasperini et al. 2015; Gimenez-Ibanez et al. 2017; Lewsey et al. 2022).

While single *jaz1*, *jaz2*, *jaz5*, and *jaz6* mutants are not resistant to 5-MT-induced root growth inhibition, combinations of these four JAZs may be more important for the 5-MT phenotype than others, as well as for regulating the responses to *Botrytis*. JAZ1 and JAZ2 are more closely related, while JAZ5 and JAZ6 are more closely related based on sequence identity. This may suggest further subfunctionalization between the two subclades of Group I. While Ingle et al. show that JAZ6 contributes to circadian-related responses to *Botrytis*, their *jaz5,6,10* triple mutant

does not appear to be more resistant to *Botrytis* than their *jaz6* single mutant, although this was not confirmed with statistical analysis (Ingle et al. 2015). Additionally, Liu et al. show that a *jaz6* single mutant is slightly more resistant to lesion formation compared to *jaz1*, *jaz2*, and *jaz5*, but *Botrytis* resistance is the strongest in the *jaz1/2/5/6* mutant (Liu et al. 2021). Future work to dissect the contributions of the Group I JAZs would elucidate whether specific combinations of these four JAZs contribute more than others in regulating the plant responses to *Botrytis* and 5-MT resistance. Creating new combinatorial mutants through CRISPR or transforming WT sequences into the existing mutant background could be effective approaches to addressing this question, as genetic linkage makes it difficult to isolate the pairs in the *jaz1/2/5/6* mutant.

JAZ subsets regulate separate branches of plant immunity and metabolism

Many compounds have been associated with defense responses after various biotic challenges but how JA signaling regulates specific metabolic shifts to promote defense is not well understood (Ferrari et al. 2003; Muroi et al. 2009; Schweizer et al. 2013). Our expression and metabolic data suggest that the Group I JAZs, *JAZ1/2/5/6*, negatively regulate *ASAI* expression and shikimate pathway-derived defense compounds, as indicated by the increased abundance of Trp-derived camalexin and Phe-derived HCAAs. Additionally, the separation of metabolic output between *jazQ* and *jaz1/2/5/6* suggests that regulation of specialized metabolism is partially tuned by the JAZs to provide specific defense responses such as the differential regulation of enzymes that produce glucosinolates versus necrotroph-induced specialized metabolites. The higher levels of resistance against 5-MT and in the biotic assays between *jazQ* and *jaz1256* compared to *jazD* suggest that while the JAZ subsets within *jazQ* and *j1256* are the predominant repressors involved in the responses to insects and necrotrophic pathogens, other JAZ proteins are involved as well. For example, while JAZ9 is not required to maintain the 5-MT resistance of *jaz1/2/5/6*, JAZ9 is

able to selectively activate ORA59/ERF1 signaling when treated with a modified coronatine agonist, suggesting that JAZ9 is capable of activating the JA/ET signaling branch (Saito et al. 2018). The selective activation of JAZ-COII interactions through altered signaling molecules may also hint at another level of specificity regulation, where the JAZs may have altered binding affinities for JA-Ile.

In certain contexts, the JA and ethylene pathways are interdependent, such as the requirement for intact JA or ethylene signaling pathways in responses to necrotrophic pathogens (Zhu et al. 2011). While we establish here that MYC3 and MYC4 act additively to regulate Trp biosynthesis, the regulation of aromatic amino acids and their derivatives may be driven by this JA/ET branch of jasmonate signaling through a variety of ethylene-related transcription factors coordinating with the MYC transcription factors. For instance, JAZ proteins are able to bind and inhibit ERF109 activation of *ASAI* during de novo root regeneration in Arabidopsis (Zhang et al. 2019). Additionally, JA and ethylene act synergistically through the ORA59 transcription factor to regulate genes involved in HCAA biosynthesis, and through the ERF1 transcription factor to regulate camalexin biosynthesis (Li et al. 2018; Zhou et al. 2022). These studies and our data provide the basis for a model in which JAZ1/2/5/6 repress MYC3 and MYC4 as well as ethylene transcription factors to regulate the production of certain classes of defense compounds and aromatic amino acid metabolism to support defense against necrotrophic pathogens.

REFERENCES

- Arnold A, Nikoloski Z. 2014.** Bottom-up Metabolic Reconstruction of Arabidopsis and Its Application to Determining the Metabolic Costs of Enzyme Production. *Plant Physiology* **165**: 1380–1391.
- Bai Y, Meng Y, Huang D, Qi Y, Chen M. 2011.** Origin and evolutionary analysis of the plant-specific TIFY transcription factor family. *Genomics* **98**: 128–136.
- Bender J, Celenza JL. 2009.** Indolic glucosinolates at the crossroads of tryptophan metabolism. *Phytochemistry Reviews* **8**: 25–37.
- Bender J, Fink GR. 1998.** A MYB homologue, ATR1, activates tryptophan gene expression in Arabidopsis. *Proceedings of the National Academy of Sciences* **95**: 5655–5660.
- Campos ML, Yoshida Y, Major IT, De Oliveira Ferreira D, Weraduwage SM, Froehlich JE, Johnson BF, Kramer DM, Jander G, Sharkey TD, et al. 2016.** Rewiring of jasmonate and phytochrome B signalling uncouples plant growth-defense tradeoffs. *Nature Communications* **7**: 1–10.
- Chini A, Gimenez-Ibanez S, Goossens A, Solano R. 2016.** Redundancy and specificity in jasmonate signalling. *Current Opinion in Plant Biology* **33**: 147–156.
- Chung HS, Cooke TF, Depew CL, Patel LC, Ogawa N, Kobayashi Y, Howe GA. 2010.** Alternative splicing expands the repertoire of dominant JAZ repressors of jasmonate signaling. *Plant Journal* **63**: 613–622.
- Clough SJ, Bent AF. 1998.** Floral dip: a simplified method for *Agrobacterium*-mediated transformation of *Arabidopsis thaliana*. *Plant Journal* **16**: 735–743.
- Cusack SA, Wang P, Lotreck SG, Moore BM, Meng F, Conner JK, Krysan PJ, Lehti-Shiu MD, Shiu S-H. 2021.** Predictive Models of Genetic Redundancy in *Arabidopsis thaliana*. *Molecular Biology and Evolution* **38**: 3397–3414.
- Dombrecht B, Xue GP, Sprague SJ, Kirkegaard JA, Ross JJ, Reid JB, Fitt GP, Sewelam N, Schenk PM, Manners JM, et al. 2007.** MYC2 Differentially Modulates Diverse Jasmonate-Dependent Functions in *Arabidopsis*. *The Plant Cell* **19**: 2225–2245.
- Fernández-Calvo P, Chini A, Fernández-Barbero G, Chico J-M, Gimenez-Ibanez S, Geerinck J, Eeckhout D, Schweizer F, Godoy M, Franco-Zorrilla JM, et al. 2011.** The *Arabidopsis* bHLH transcription factors MYC3 and MYC4 are targets of JAZ repressors and act additively with MYC2 in the activation of jasmonate responses. *The Plant Cell* **23**: 701–715.
- Ferrari S, Plotnikova JM, De Lorenzo G, Ausubel FM. 2003.** *Arabidopsis* local resistance to *Botrytis cinerea* involves salicylic acid and camalexin and requires EDS4 and PAD2, but not SID2, EDS5 or PAD4. *Plant Journal* **35**: 193–205.

- Gasperini D, Chételat A, Acosta IF, Goossens J, Pauwels L, Goossens A, Dreos R, Alfonso E, Farmer EE. 2015.** Multilayered organization of jasmonate signalling in the regulation of root growth. *PLoS Genetics* **11**: e1005300.
- Gilchrist DG, Kosuge T. 1974.** Regulation of aromatic amino acid biosynthesis in higher plants. Properties of an aromatic amino acid-sensitive chorismate mutase (CM-1) from mung bean. *Archives of Biochemistry and Biophysics* **164**: 95–105.
- Gimenez-Ibanez S, Boter M, Ortigosa A, Garcia-Casado G, Chini A, Lewsey MG, Ecker JR, Ntoukakis V, Solano R. 2017.** JAZ2 controls stomata dynamics during bacterial invasion. *New Phytologist* **213**: 1378–1392.
- Glawischnig E, Hansen BG, Olsen CE, Halkier BA. 2004.** Camalexin is synthesized from indole-3-acetaldoxime, a key branching point between primary and secondary metabolism in *Arabidopsis*. *Proceedings of the National Academy of Sciences* **101**: 8245–8250.
- Guo Q, Major IT, Kapali G, Howe GA. 2022.** MYC transcription factors coordinate tryptophan-dependent defense responses and compromise seed yield in *Arabidopsis*. *New Phytologist* **236**: 135-142.
- Guo Q, Yoshida Y, Major IT, Wang K, Sugimoto K, Kapali G, Havko NE, Benning C, Howe GA. 2018.** JAZ repressors of metabolic defense promote growth and reproductive fitness in *Arabidopsis*. *Proceedings of the National Academy of Sciences* **115**: E10768-10777.
- Han Y, Luthe D. 2021.** Identification and evolution analysis of the JAZ gene family in maize. *BMC Genomics* **22**: 256.
- Herrmann KM, Weaver LM. 1999.** The shikimate pathway. *Annual Review of Plant Physiology and Plant Molecular Biology* **50**: 473–503.
- Howe GA, Major IT, Koo AJ. 2018.** Modularity in jasmonate signaling for multistress resilience. *Annual Review of Plant Biology* **69**: 387–415.
- Ingle RA, Stoker C, Stone W, Adams N, Smith R, Grant M, Carré I, Roden LC, Denby KJ. 2015.** Jasmonate signalling drives time-of-day differences in susceptibility of *Arabidopsis* to the fungal pathogen *Botrytis cinerea*. *Plant Journal* **84**: 937–948.
- Kagale S, Links MG, Rozwadowski K. 2010.** Genome-wide analysis of ethylene-responsive element binding factor-associated amphiphilic repression motif-containing transcriptional regulators in *Arabidopsis*. *Plant Physiology* **152**: 1109–1134.
- Kreps JA, Ponappa T, Dong W, Town CD. 1996.** Molecular basis of alpha-methyltryptophan resistance in *amt-1*, a mutant of *Arabidopsis thaliana* with altered tryptophan metabolism. *Plant Physiology* **110**: 1159–1165.

- Lewsey MG, Yi C, Berkowitz O, Ayora F, Bernado M, Whelan J. 2022.** scCloudMine: A cloud-based app for visualization, comparison, and exploration of single-cell transcriptomic data. *Plant Communications* **3**: 100302.
- Li J, Last RL. 1996.** The *Arabidopsis thaliana* trp5 mutant has a feedback-resistant anthranilate synthase and elevated soluble tryptophan. *Plant Physiology* **110**: 51–59.
- Li C, Shi L, Wang Y, Li W, Chen B, Zhu L, Fu Y. 2020.** *Arabidopsis* ECAP is a new adaptor protein that connects JAZ repressors with the TPR2 co-repressor to suppress jasmonate-responsive anthocyanin accumulation. *Molecular Plant* **13**: 246–265.
- Liu Q, Luo L, Zheng L. 2018.** Lignins: biosynthesis and biological functions in plants. *International Journal of Molecular Sciences* **19**: 335.
- Liu B, Seong K, Pang S, Song J, Gao H, Wang C, Zhai J, Zhang Y, Gao S, Li X, et al. 2021.** Functional specificity, diversity, and redundancy of *Arabidopsis* JAZ family repressors in jasmonate and COI1-regulated growth, development, and defense. *New Phytologist* **231**: 1525–1545.
- Macoy DM, Kim W-Y, Lee SY, Kim MG. 2015.** Biosynthesis, physiology, and functions of hydroxycinnamic acid amides in plants. *Plant Biotechnology Reports* **9**: 269–278.
- Maeda H, Dudareva N. 2012.** The shikimate pathway and aromatic amino Acid biosynthesis in plants. *Annual Reviews of Plant Biology* **63**: 73–105.
- Major IT, Guo Q, Zhai J, Kapali G, Kramer DM, Howe GA. 2020.** A phytochrome B-independent pathway restricts growth at high levels of jasmonate defense. *Plant Physiology* **183**: 733–749.
- Major IT, Yoshida Y, Campos ML, Kapali G, Xin X-F, Sugimoto K, Ferreira DDO, He SY, Howe GA. 2017.** Regulation of growth – defense balance by the JASMONATE ZIM-DOMAIN (JAZ) -MYC transcriptional module. *New Phytologist* **215**: 1533–1547.
- Mashiguchi K, Tanaka K, Sakai T, Sugawara S, Kawaide H, Natsume M, Hanada A, Yaeno T, Shirasu K, Yao H, et al. 2011.** The main auxin biosynthesis pathway in *Arabidopsis*. *Proceedings of the National Academy of Sciences* **108**: 18512–18517.
- Monte I, Franco-Zorrilla JM, Garcia-Casado G, Zamarreno AM, Garcia-Mina JM, Nishihama R, Kohchi T, Solano R. 2019.** A single JAZ repressor controls the jasmonate pathway in *Marchantia polymorpha*. *Molecular Plant*: 185–198.
- Moreno JE, Shyu C, Campos ML, Patel LC, Chung HS, Yao J, He SY, Howe GA. 2013.** Negative feedback control of jasmonate signaling by an alternative splice variant of JAZ10. *Plant Physiology* **162**: 1006–1017.

- Muroi A, Ishihara A, Tanaka C, Ishizuka A, Takabayashi J, Miyoshi H, Nishioka T. 2009.** Accumulation of hydroxycinnamic acid amides induced by pathogen infection and identification of agmatine coumaroyltransferase in *Arabidopsis thaliana*. *Planta* **230**: 517–527.
- Oblessuc PR, Obulareddy N, DeMott L, Matioli CC, Thompson BK, Melotto M. 2020.** JAZ4 is involved in plant defense, growth, and development in *Arabidopsis*. *Plant Journal* **101**: 371–383.
- Overvoorde PJ, Okushima Y, Alonso JM, Chan A, Chang C, Ecker JR, Hughes B, Liu A, Onodera C, Quach H, et al. 2005.** Functional genomic analysis of the AUXIN/INDOLE-3-ACETIC ACID gene family members in *Arabidopsis thaliana*. *The Plant Cell* **17**: 3282–3300.
- Page DR, Grossniklaus U. 2002.** The art and design of genetic screens: *Arabidopsis thaliana*. *Nature Reviews Genetics* **3**: 124–136.
- Peñuelas M, Monte I, Schweizer F, Vallat A, Reymond P, García-Casado G, Franco-Zorrilla JM, Solano R. 2019.** Jasmonate-related MYC transcription factors are functionally conserved in *Marchantia polymorpha*. *The Plant Cell* **31**: 2491–2509.
- Schweizer F, Fernandez-Calvo P, Zander M, Diez-Diaz M, Fonseca S, Glauser G, Lewsey MG, Ecker JR, Solano R, Reymond P. 2013.** *Arabidopsis* basic helix-loop-helix transcription factors MYC2, MYC3, and MYC4 regulate glucosinolate biosynthesis, insect performance, and feeding behavior. *The Plant Cell* **25**: 3117–3132.
- Sehr EM, Agusti J, Lehner R, Farmer EE, Schwarz M, Greb T. 2010.** Analysis of secondary growth in the *Arabidopsis* shoot reveals a positive role of jasmonate signalling in cambium formation. *Plant Journal* **63**: 811–822.
- Shyu C, Figueroa P, Depew CL, Cooke TF, Sheard LB, Moreno JE, Katsir L, Zheng N, Browse J, Howe GA. 2012.** JAZ8 lacks a canonical degron and has an EAR motif that mediates transcriptional repression of jasmonate responses in *Arabidopsis*. *The Plant Cell* **24**: 536–550.
- Smolen GA, Pawlowski L, Wilensky SE, Bender J. 2002.** Dominant alleles of the basic helix-loop-helix transcription factor ATR2 activate stress-responsive genes in *Arabidopsis*. *Genetics* **161**: 1235–1246.
- Song S, Huang H, Wang J, Liu B, Qi T, Xie D. 2017.** MYC5 is involved in jasmonate-regulated plant growth, leaf senescence and defense responses. *Plant and Cell Physiology* **58**: 1752–1763.
- Stuttman J, Barthel K, Martin P, Ordon J, Erickson JL, Herr R, Ferik F, Kretschmer C, Berner T, Keilwagen J, et al. 2021.** Highly efficient multiplex editing: one-shot generation of 8x *Nicotiana benthamiana* and 12x *Arabidopsis* mutants. *Plant Journal* **106**: 8–22.

- Ursache R, Fujita S, Dénervaud Tendon V, Geldner N. 2021.** Combined fluorescent seed selection and multiplex CRISPR/Cas9 assembly for fast generation of multiple *Arabidopsis* mutants. *Plant Methods* **17**: 111.
- Yokoyama R, de Oliveira MVV, Kleven B, Maeda HA. 2021.** The entry reaction of the plant shikimate pathway is subjected to highly complex metabolite-mediated regulation. *The Plant Cell* **33**: 671–696.
- Yokoyama R, de Oliveira MVV, Takeda-Kimura Y, Ishihara H, Alseekh S, Arrivault S, Kukshal V, Jez JM, Stitt M, Fernie AR, et al. 2022.** Point mutations that boost aromatic amino acid production and CO₂ assimilation in plants. *Science Advances* **8**: eabo3416.
- Yu J, Zhang Y, Di C, Zhang Q, Zhang K, Wang C, You Q, Yan H, Dai SY, Yuan JS, et al. 2016.** JAZ7 negatively regulates dark-induced leaf senescence in *Arabidopsis*. *Journal of Experimental Botany* **67**: 751–762.
- Zander M, Lewsey MG, Clark NM, Yin L, Bartlett A, Saldierna Guzmán JP, Hann E, Langford AE, Jow B, Wise A, et al. 2020.** Integrated multi-omics framework of the plant response to jasmonic acid. *Nature Plants* **6**: 290–302.
- Zhang Y, Ren Q, Tang X, Liu S, Malzahn AA, Zhou J, Wang J, Yin D, Pan C, Yuan M, et al. 2021.** Expanding the scope of plant genome engineering with Cas12a orthologs and highly multiplexable editing systems. *Nature Communications* **12**: 1944.
- Zhang F, Yao J, Ke J, Zhang L, Lam VQ, Xin X-F, Zhou XE, Chen J, Brunzelle J, Griffin PR, et al. 2015.** Structural basis of JAZ repression of MYC transcription factors in jasmonate signalling. *Nature* **525**: 269–273.
- Zhao Y, Zhang Z, Gao J, Wang P, Hu T, Wang Z, Hou Y-J, Wan Y, Liu W, Xie S, et al. 2018.** *Arabidopsis* duodecuple mutant of PYL ABA receptors reveals PYL repression of ABA-independent SnRK2 activity. *Cell Reports* **23**: 3340-3351.e5.

APPENDIX

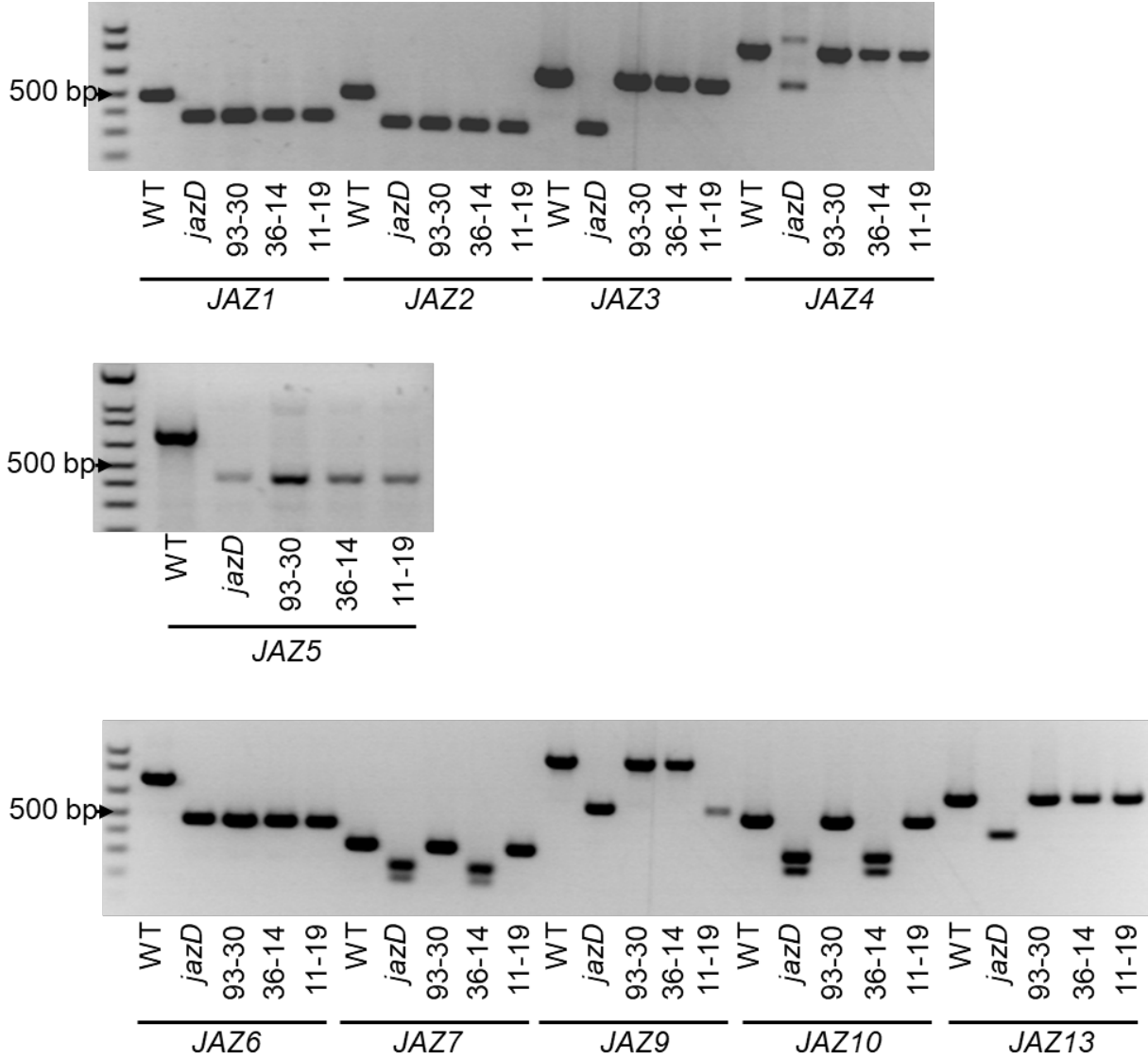


Figure A2.1 PCR-based genotyping of ten *jaz* mutations segregating in the *jazD* x Col-0 F₂ population.

DNA extracted from leaves of wild type (WT), *jazD*, and selected F₄ lines (93-30, *jaz1/2/5/6*; 11-19, *jaz1/2/5/7/9*; 36-14, *jaz1/2/5/6/7/10*) was used as a template for PCR reactions with the *JAZ*-specific primer sets are listed in Table A2.1. Nucleic acid molecular weight markers (1 kb ladder) are shown in the leftmost lane.

Table A2.1 Oligonucleotide primers used for genotyping *JAZ* loci.

Mutation ¹	Mutant line ²	Fwd primer ³	Rev primer ³	T-DNA primer ³
<i>jaz1-2</i>	SM_3.22668	ACCGAGACACA TTCCCGATT	CATCAGGCTTGCA TGCCATT	ACGAATAAGAGCG TCCATTTTAGAG
<i>jaz2-2</i>	RIKEN_13- 5433-1	TCTTCCTCGTGA CAAACGCA	CCAAACACAGAAC CATCTCCACA	CCGGATCGTATCG GTTTTCG
<i>jaz3-4</i>	097F09	ACGGTTCCTCTA TGCTCAAGTC	GTGGAGTGGTCTA AAGCAACCTTC	ATAACGCTGCGGA CATCTACATT
<i>jaz4-1</i>	SALK_141628	TCAGGAAGACA GAGTGTTCCC	TGCGTTTTCTCTAA GAACCGAG	TTGGGTGATGGTT CACGTAG
<i>jaz5-1</i>	SALK_053775	GCTTATACCGAA AACCCGATTCCA G	GGCTCATTGAGAT CAGGAAGAACCA	TTGGGTGATGGTT CACGTAG
<i>jaz6-1</i>	CSHL_ET30	GACACACATCA CTGTCACTTC	AGTTTCTGAGGTC TCTACCTTC	CCGTTTTGTATAT CCCGTTTCCGT
<i>jaz7-1</i>	WiscDsLox7H 11	ATGCGACTTGG AACTTCGCC	GGAGGATCCGAA CCGTCTG	ACGTCCGCAATGT GTTATTA
<i>jaz9-4</i>	265H05	TACCGCATAATC ATGGTCGTC	TCATGCTCATTGC ATTAGTCG	CTTTGAAGACGTG GTTGGAACG
<i>jaz10-1</i>	SAIL_92_D08	ATTTCTCGATCG CCGTCGTAGT	GCCAAAGAGCTTT GGTCTTAGAGTG	GTCTAAGCGTCAA TTTGTTTACACC
<i>jaz13-1</i>	193G07	GCACGTGACCA AATTTGCAGA	TGAAGAGAGGAG GATGATGAGGA	AAACCTCCTCGGA TTCCATTGC

¹Allele designation of *jaz* mutations employed in this study.

²Original name of the DNA insertion (T-DNA or transposon) line.

³Primer sequences are written in the 5' to 3' direction. Forward (Fwd) and reverse (Rev) primers were used to detect the wild-type *JAZ* allele, whereas the border primer was specific for amplification of the mutant DNA-insertion allele. All three primers were combined in equal concentrations for a single PCR reaction.

Table A2.2 Primers used for gene expression analysis by quantitative PCR (qPCR).

AGI accession ¹	Gene name ²	Primer 1 ³	Primer 2 ³
AT1G13220	<i>PP2A</i>	AAGCAGCGTAATCG GTAGG	GCACAGCAATCGG GTATAAAG
AT5G05730	<i>ASA1</i>	TCAGCTTACTCCTG TTCTTGCTTACC	GCTATAACGACCAA CGCTAGACATCTG
AT5G17990	<i>TRP1</i>	GGTTGATCTATCTG AAACTGAGGCTG	ACCCCAATCTCT TCGTATGTCT
AT3G54640	<i>TSA1</i>	ACAAGGCAAAGTA GCATTCATACCA	GAGTAAGGAACACC CAATTCGATTATGTC
AT5G24770	<i>VSP2</i>	GTTAGGGACCGGA GCATCAACC	TCTTCCACAACCTC CAACGGTCACT
AT5G44420	<i>PDF1.2</i>	GGGGTTTGCGGAA ACAGTAAT	AATACACACGATTTA GCACCAAAGATTA
AT1G06160	<i>ORA59</i>	AAAAGAAGAAGGA AAAGAAGCCAC	GTGTCGAATGTCCC AAGCCA
AT5G61160	<i>ACT</i>	CGCTGCTGATTTTA GGAACC	CGCTGCTGATTTTA GGAACC

¹AGI accession indicates the locus identifier provided by The Arabidopsis Information Resource (TAIR) database and the Arabidopsis Genome Initiative (AGI).

²Gene name indicates the common gene symbol.

³Primer sequences used for qPCR are written in the 5' to 3' direction.

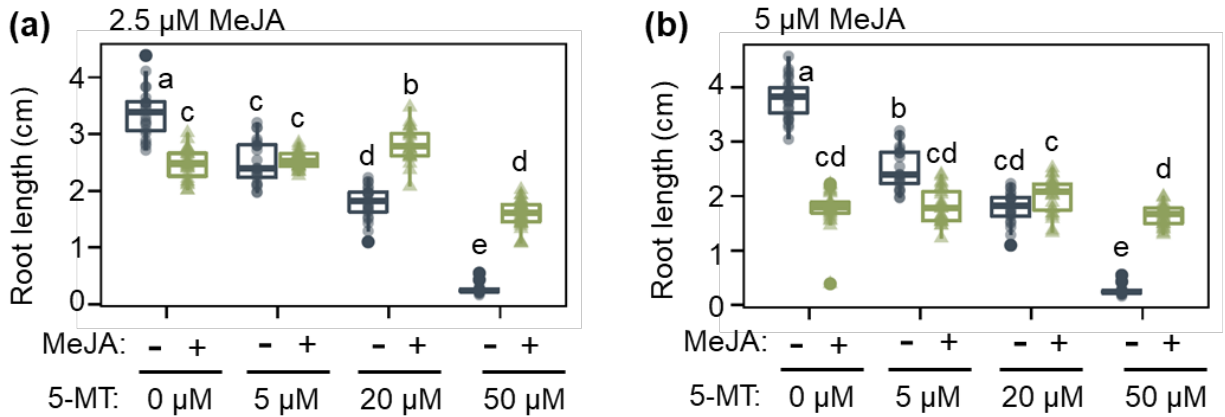


Figure A2.2 Root lengths of Arabidopsis seedlings grown on media supplemented with 5-methyl tryptophan (5-MT) or 5-MT and methyl jasmonate (MeJA).

The data show the absolute root lengths of seedlings used for the experiment described in Figure 1c-d. Seedlings were simultaneously treated with either 2.5 μM MeJA (a) or 5 μM MeJA (b) plus the indicated concentration of 5-MT. Data show 18-33 seedlings per treatment. Letters indicate significant differences at $P < 0.05$ according to Tukey's honestly significant difference (HSD) test.

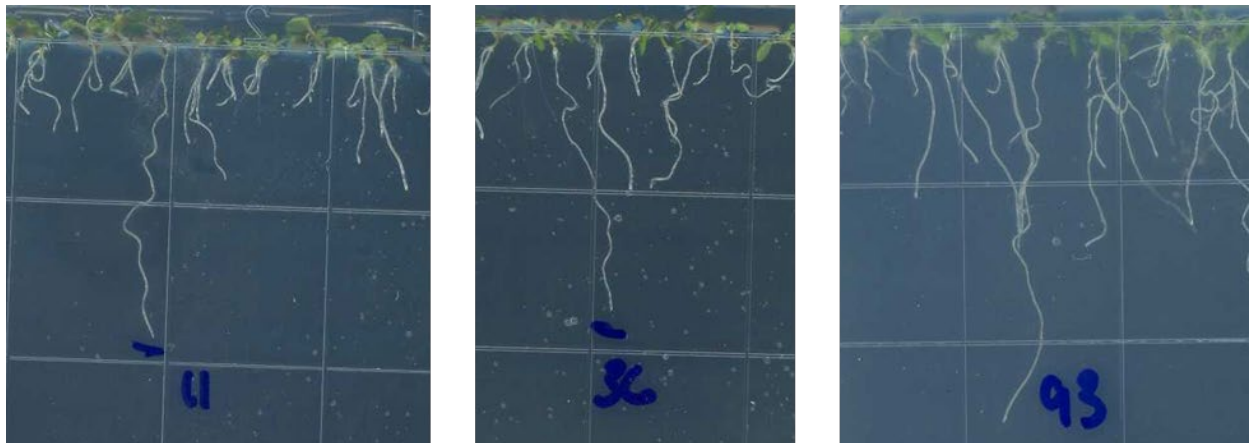


Figure A2.3 Photographs of representative F2 seedlings exhibiting resistance to 5-methyl-tryptophan (5-MT).

F₂ seedlings derived from a cross between WT and *jazD* were grown for 10 days on media containing 15 μM 5-MT. Left, middle, and right images show the identification of lines 11, line 36, and line 93, respectively.

Table A2.3 Segregation frequency of *jaz* mutations in an F₂ population derived from a cross between wild type and the *jaz* decuple mutant (*jazD*).

	JAZ1	JAZ2	JAZ3	JAZ4	JAZ5	JAZ6	JAZ7	JAZ9	JAZ10	JAZ13
+/+	0.01	0.00	0.12	0.04	0.01	0.00	0.28	0.00	0.10	0.10
+/-	0.10	0.05	0.39	0.37	0.12	0.05	0.40	0.12	0.48	0.30
-/-	0.88	0.95	0.47	0.58	0.85	0.95	0.32	0.88	0.37	0.42
ND	0.01	0.00	0.01	0.01	0.02	0.00	0.00	0.00	0.04	0.18
P-value	7.71E-19	1.32E-24	0.015	4.58E-05	2.16E-17	1.32E-24	1	1.58E-18	0.582	0.011

PCR was used to determine the genotype of 97 individual F₂ progeny at each of the 10 segregating *JAZ* loci in Fig 2.5. +/+, homozygous for wild-type allele; +/-, heterozygous; -/-, homozygous for *jaz* mutant allele; ND, not determined due to ambiguous PCR results. P-values represent a Fisher's exact test with Bonferroni's correction for multiple testing to determine whether the number of homozygous mutations differed from the expected proportion for an unlinked, recessive mutation of 0.25 of genotyped seedlings.

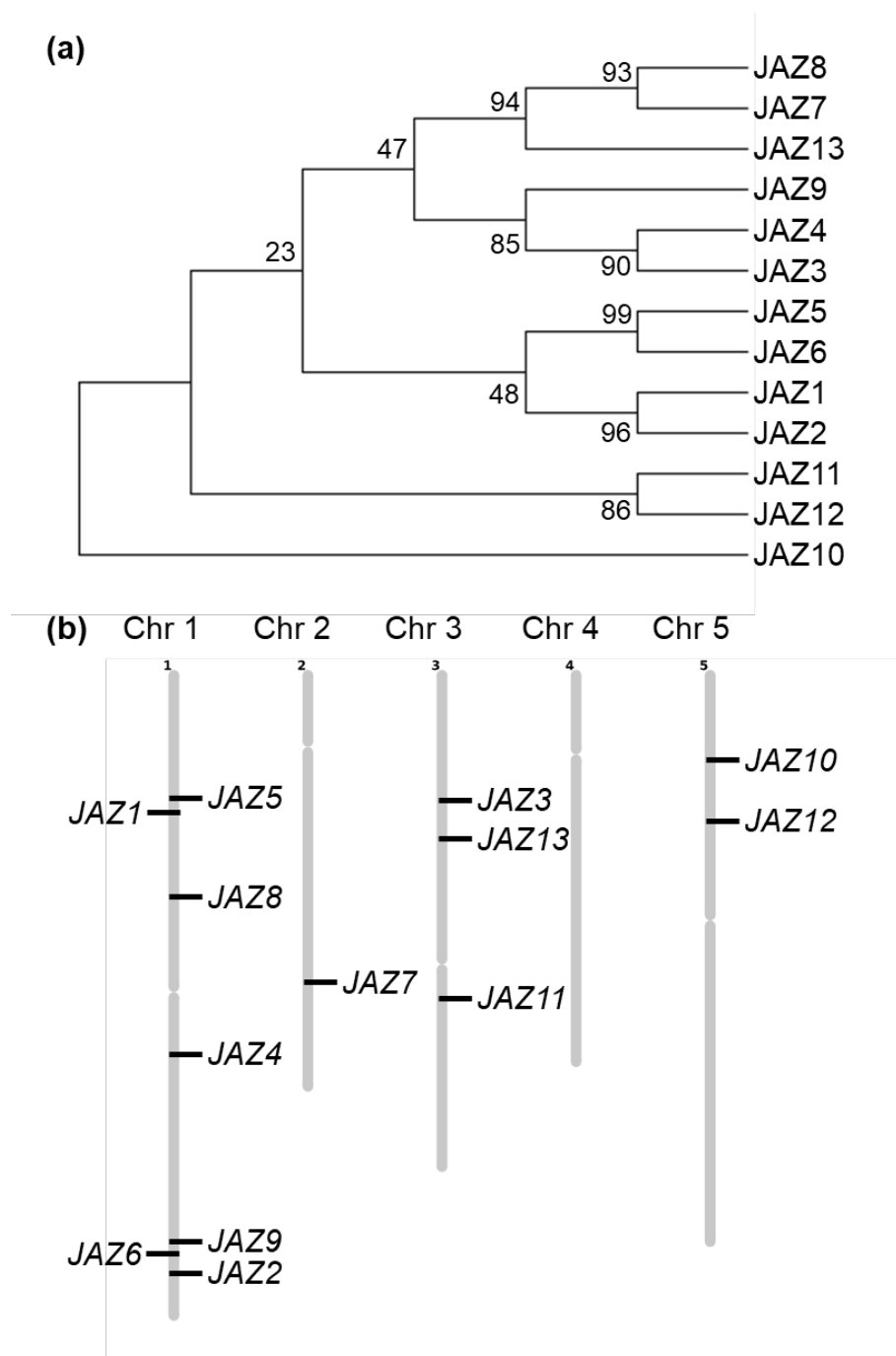


Figure A2.4 Phylogenetic tree and genome location of members of the Arabidopsis JAZ family.

(a) The phylogenetic tree was constructed using the Maximum Likelihood method and JTT-based matrix model in MEGA X and is based on the predicted amino-acid sequences of full-length JAZ proteins. Numbers denote the bootstrap consensus inferred from 500 replicates. (b) Chromosomal map location of Arabidopsis *JAZ* genes based on information at The Arabidopsis Information Resource (TAIR).

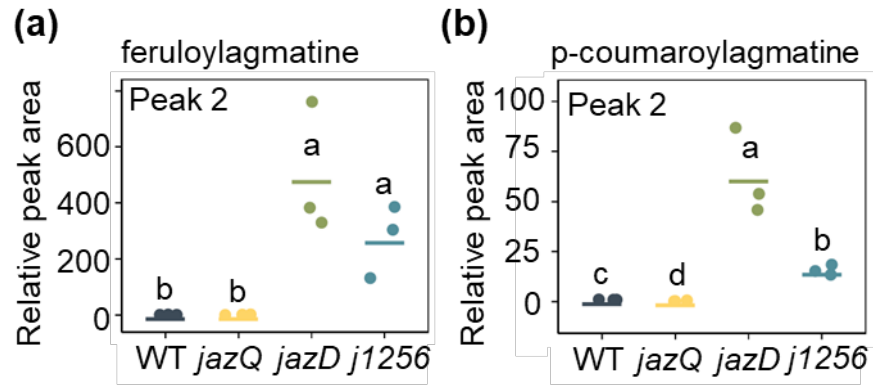


Figure A2.5 Secondary peak detected for the hydroxycinnamic acid amides.

Relative levels of (a) feruloylagmatine and (b) *p*-coumaroylagmatine in leaves of 26-day-old leaves of the indicated genotypes. Peak areas were normalized to the WT. Letters indicate significant differences at $P < 0.05$ according to Tukey's honestly significant difference (HSD) test.

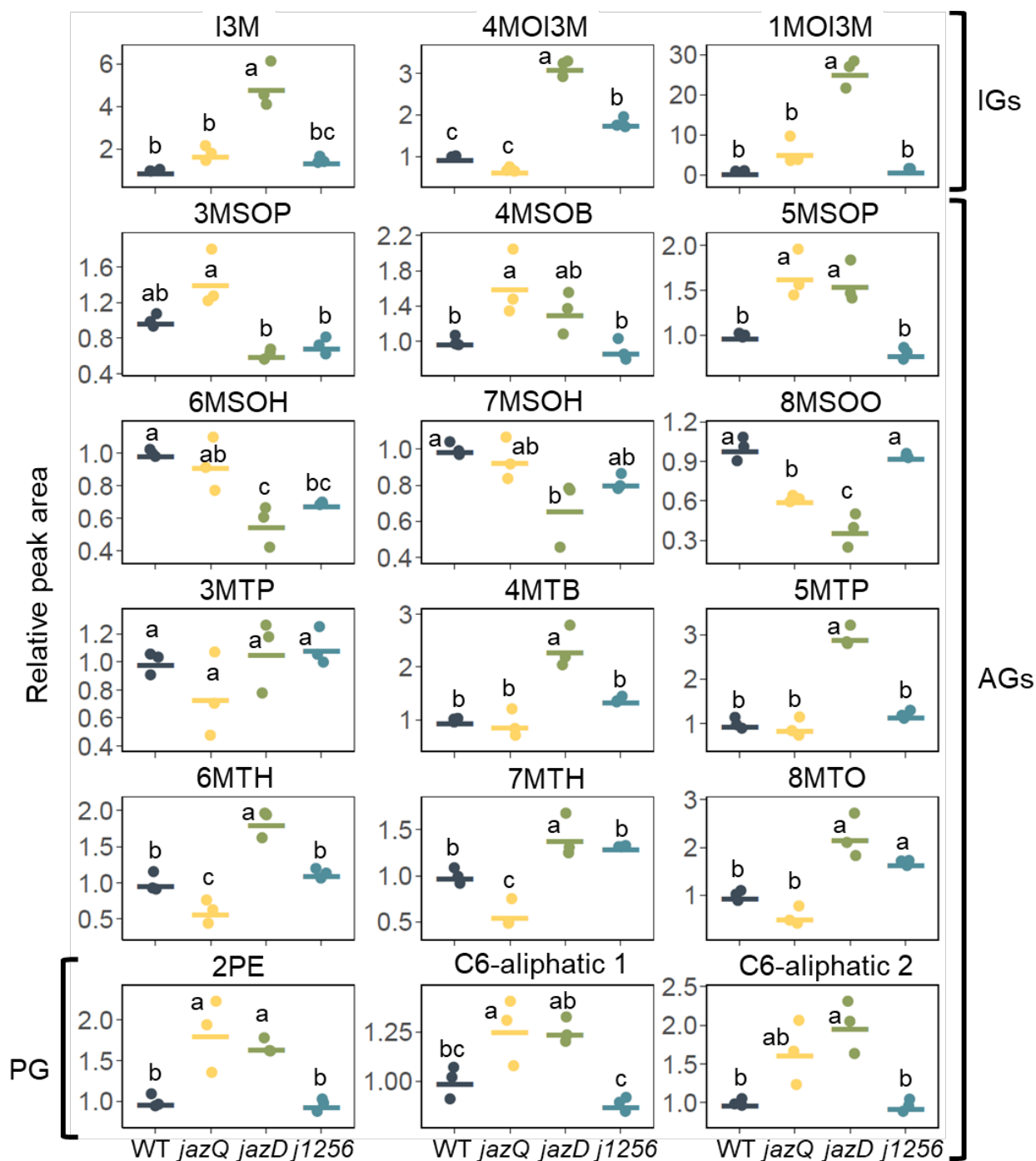


Figure A2.6 Levels of various glucosinolate derivatives in untreated leaves of 26-day-old wild-type (WT), *jaz* quintuple (*jazQ*), *jaz* decuple (*jazD*), and *jaz1/2/5/6* (*j1256*) plants.

Peak areas were normalized to the WT average peak areas for each compound. Brackets denote indole (IG), aliphatic (AG), and phenolic (PG) glucosinolates. Letters indicate significant differences at $P < 0.05$ according to Tukey's honestly significant difference (HSD) test. I3M = Indol-3-ylmethyl (glucobrassicin); 4MOI3M = 4-Methoxyindol-3-ylmethyl (methoxyglucobrassicin); 1MOI3M = 1-Methoxyindol-3-ylmethyl (neoglucobrassicin); 3MSOP

Figure A2.6 (cont'd)

= 3-Methylsulphinylpropyl (glucoiberin); 4MSOB = 4-Methylsulphinylbutyl (glucoraphanin); 5MSOP = 5-Methylsulphinylpentyl (glucoalyssin); 6MSOH = 6-Methylsulphinylhexyl (glucohesperin); 7MSOH = 7-Methylsulphinylheptyl (glucoibarin); 8MSOO = 8-Methylsulphinyl-octyl (glucohirsutin); 3MTP = 3-Methylthiopropyl (glucoiberverin); 4MTB = 4-Methylthiobutyl (glucoerucin); 5MTP = 5-Methylthiopentyl (glucoberteroin); 6MTH = 6-Methylthiohexyl (glucosquerellin); 7-MTH = 7-Methylthioheptyl; 8MTO = 8-Methylthiooctyl; 2PE = 2-Phenylethyl (gluconasturtiin); C6-aliphatic 1 and 2 formula = $C_{13}H_{24}NO_9S_2$, appears as two peaks on extracted ion chromatogram.

**CHAPTER 3: GENETIC SUPPRESSOR SCREENS IDENTIFY REGULATORS OF THE
JASMONATE SIGNALING PATHWAY IN ARABIDOPSIS**

Leah Y.D. Johnson, Ian T. Major, Qiang Guo, Gregg A. Howe

Author Contributions: QG performed the ethyl methanesulfonate mutagenesis of *jazD* seeds and the screening for the *suppressor of jazD* (*sjd*) mutants. ITM generated figure 3.1 and jointly with LYDJ performed the insect bioassays. LYDJ performed the remaining experiments. LYDJ and GAH wrote the manuscript.

ABSTRACT

Plants perceive and respond to many environmental cues to achieve optimal fitness. In response to biotic stressors, defense responses are rapidly activated concomitant with growth inhibition. Due to the negative agronomic consequences of this tradeoff, there is interest in understanding how growth and defense processes are antagonistically linked at a mechanistic level. Plant hormones are major targets of study because they control many facets of growth and defense. For example, jasmonate (JA) regulates defense responses to insects and necrotrophic pathogens. Upon activation of JA signaling, metabolism shifts towards the production of defense compounds, which is associated with reduced biomass and reproductive yield. To identify regulatory factors that control the balance between growth and defense, we took advantage of a constitutive JA signaling mutant (*jazD*) that lacks 10 of the 13 JAZ repressors of JA signaling in *Arabidopsis*. *jazD* plants accumulate elevated levels of defense compounds and have severe growth and fertility defects. The mutant is also hypersensitive to exogenous JA; when treated with a JA agonist, coronatine, *jazD* plants undergo a rapid autoimmune response involving leaf senescence and death. Using *jazD* as a parental line, we conducted two genetic suppressor screens to identify molecular components that regulate JA-mediated growth and defense responses. In total, we identified six mutant alleles of *COI1* and five mutant alleles of *MYC2* that block JA signaling. These findings support a key role for JAZ proteins in attenuating JA signaling and, more generally, control of the growth-defense balance.

INTRODUCTION

Plants use environmental cues to optimize fitness. Integration of these signaling networks leads to large-scale changes in gene expression underlying phenotypic plasticity. For example, the activation of defense programs is accompanied by inhibition of growth, a phenomenon known as the “growth-defense tradeoff”. There are many plausible explanations for how growth and defense are coordinately regulated (Monson et al. 2022). Early models suggested that growth-defense tradeoffs result from resource limitation, such that allocation of nutrients to defense responses restricts nutrient availability for growth or reproduction (Bazzaz et al. 1987). This model is supported by the frequent occurrence of hyper-immune mutants that display reproductive and vegetative growth defects (Guo et al. 2018; Ellis and Turner 2001). Due to the difficulty in quantifying defense “costs”, direct evidence for the resource allocation hypothesis is scant (Havko et al. 2016). The precise relationship between nutrient availability and the production of defense compounds is also unclear. For example, nutrient stress can increase the production of defensive glucosinolates in *Brassica* species and glucosinolates can be broken down to provide nutrients such as sulfur, suggesting a role for specialized metabolites in nutrient sequestration (Del Carmen Martínez-Ballesta et al. 2013; Sugiyama et al. 2021). These observations indicate a much more complex relationship between growth and defense.

It has also been proposed that growth and defense are coordinated to optimize fitness but that, under certain conditions, resources may be abundant enough for both processes to occur simultaneously because different processes utilize a variety of nutrients rather than all processes drawing on the same pools (Kliebenstein 2016). Growth signaling through the red-light receptor PHYTOCHROME B is integrated with defense responses through the defense hormone jasmonate (JA). These pathways can be genetically uncoupled to restore the growth defects of a

constitutive JA mutant (*jazQ*) without a reduction in defense, suggesting that growth and defense can be activated simultaneously without detriment to either process (Campos et al. 2016).

However, as the amplitude of JA signaling is further increased through removal of additional JAZ repressors in a *jaz* decuple mutant (*jazD*), the loss of phy B signaling is not sufficient to overcome the strong growth defects. This finding suggests that the mechanisms of growth-defense tradeoffs depend on the level of defense and that extremely high levels of defense may impose resource-based costs (Major et al. 2020). Ecological considerations further complicate efforts to explain why growth and defense are antagonistically linked. For example, plants with lower defense generally have greater ability to compete with neighboring plants for limiting light (Lankau and Kliebenstein 2009).

It is also possible that growth inhibition *per se* is a defense mechanism because it makes the plant less apparent to herbivores and other plant-consuming organisms. Conversely, active suppression of defense may favor rapid growth in shaded environments where competition for light among neighboring plants is intense (Ballaré and Austin 2019; Cerrudo et al. 2012; de Wit et al. 2013). Accordingly, the abiotic environment (e.g., light) plays a key role in achieving a delicate balance between growth and protection (Ballaré and Austin 2019). The genetic uncoupling of antagonism between JA and phyB signaling to achieve growth and defense at the same time further indicates that transcriptional regulation, rather than resource availability, is a major driver of growth-defense balance (Campos et al. 2016). A better understanding of how growth and defense are coordinated may inform biotechnological strategies to prevent yield loss from stressors while limiting the reproductive costs associated with elevated defense.

The hormone jasmonate (JA) provides an interesting signaling system to answer questions regarding metabolic reprogramming and the growth-defense tradeoff, as JA controls a

large sector of defense-related specialized metabolites as well as initiates a well-characterized inhibition of growth upon activation of the pathway (Schweizer et al. 2013; Guo et al. 2018; Zhang and Turner 2008; Savchenko et al. 2019). When JA levels are low, the JAZ repressors bind and inhibit transcription factors such as MYC2. Rapid synthesis of JA-Ile in response to tissue damage allows for the F-box protein COI1 to form a co-receptor complex with JAZ, resulting in JAZ ubiquitination and degradation via the 26S proteasome. This frees the inhibition on MYC2 to allow expression of genes involved in the synthesis of specialized defense compounds.

In the context of resource allocation, it is possible that JA-induced diversion of metabolism towards defense reduces nutrient allocation towards growth. For example, in the Brassicaceae family, the glucosinolates are defense compounds generally associated with anti-herbivory properties (Beekwilder et al. 2008; Schweizer et al. 2013; Pangesti et al. 2016). Flux studies analyzing the metabolic costs of these compounds suggest that glucosinolate production boosts photosynthetic requirements by at least 15%, indicating that overproduction of these compounds could have negative consequences on available carbon for growth (Bekaert et al. 2012). Additionally, many specialized metabolites are derived from aromatic amino acids, which have been modeled as some of the most costly building blocks to synthesize in terms of ATP usage (Sajitz-Hermstein and Nikoloski 2010; Arnold and Nikoloski 2014). Recent studies suggest that the MYC transcription factors coordinate tryptophan biosynthesis with the production of tryptophan-derived defense compounds, and that the upregulation of tryptophan is correlated with the inhibition of growth (Major et al. 2020; Guo et al. 2022).

Antagonism between JA-induced changes in growth and defense is driven primarily by the MYC TFs (Major et al. 2017; Guo et al. 2022). However, it is possible that other regulatory

factors are involved as well. Here, we used genetic suppressor screens to attempt to identify additional components that are involved in regulating the growth-defense interplay. These screens were based on the use of a *jazD* parental line that exhibits constitutive JA signaling as a result of mutations in ten of thirteen *JAZ* genes in Arabidopsis (Guo et al. 2018). Among a total of 12 suppressors mutants characterized, six were shown to harbor mutant alleles of *COI1* and six were mutant alleles of *MYC2*. These findings support a key role for COI1-JAZ-MYC2 signaling module in the control of growth-defense balance.

MATERIALS AND METHODS

Plant material and growth conditions

Arabidopsis thaliana accession Columbia-0 (Col-0) was used as the wild-type (WT) control for all experiments. The construction of the *jaz* decuple mutant, *jazD*, and the tredecuple mutant *jazD mycT* lacking ten *jaz* genes and *myc2*, *myc3*, and *myc4*, was previously described (Guo et al. 2018; Guo et al. 2022). The *jazD myc2* mutant was identified during the construction of the *jazD mycT* mutant. The *jazD coi1* mutant was constructed with the previously described alleles and the *coi1-1* allele, which is a G>A nonsense mutation at position 1401. *jazD* seeds were mutagenized in a solution containing 1% EMS (ethyl methanesulfonate). The resulting M₁ plants were grown for production of M₂ seed, which was used for screening. M₂ seeds were pooled into 30 families and independent families were screened. Allele information is provided in Table 3.1. For growth and anthocyanin assays, plants were grown in soil at 21°C under a long-day light regime of 16 h light (100 $\mu\text{mol m}^{-2}\text{s}^{-1}$) and 8 h dark. Plants were grown under short-day conditions of 8 h light (100 $\mu\text{mol m}^{-2}\text{s}^{-1}$) and 16 h dark for use in insect bioassays.

Growth measurements

Plants of the indicated genotypes were grown side-by-side for four weeks under long-day conditions. The entire rosette was excised above the soil and weighed immediately to obtain total fresh weight.

Anthocyanin measurements

Anthocyanins were extracted in 480 μL methanol and hydrochloric acid (99:1 v/v) per 50 mg fresh weight tissue overnight in the dark at 4°C. The following day, 320 μL water and 320 μL chloroform:isoamyl alcohol (24:1 v/v) were added to the mixture, followed by brief vortexing. Samples were centrifuged at 4°C for 10 minutes. The upper aqueous layer (190 μL) was transferred to a 96-well plate and absorbance was measured at A530 and A657. Anthocyanin concentrations were calculated with the formula $A530 - (A657 \times 0.25)$, with the resulting value normalized to tissue weight.

Root growth assays

Seeds were surface sterilized by treatment for five minutes in 70% (v/v) ethanol, five minutes in 30% (v/v) bleach, and rinsed in sterile deionized water six to eight times. Seeds were then stratified at 4°C for three to four days. Seeds were plated onto media containing half-strength Linsmaier and Skoog (LS; Caisson Labs), 0.8% (w/v) sucrose, 0.8% (w/v) phytoblend agar (Caisson Labs), and the indicated concentrations of methyl-jasmonate (MeJA; Sigma Aldrich). Stock solutions of MeJA were prepared in 70% ethanol. Plates were incubated under 16 h light ($80 \mu\text{mol m}^{-2}\text{s}^{-1}$) / 8 h dark conditions at 21°C. Roots were scanned after 10 days of growth and measured using ImageJ software (<https://imagej.nih.gov/ij/>).

Screen for coronatine resistance

EMS-mutagenized seeds (M2 generation) were sterilized as described above and plated onto media containing half-strength Linsmaier and Skoog (LS; Caisson Labs), 0.8% (w/v) sucrose, and 0.8% (w/v) phytoblend agar (Caisson Labs). Plates were incubated under 16 h light (80 $\mu\text{mol m}^{-2}\text{s}^{-1}$) / 8 h dark conditions at 21°C. After eight days of growth, seedlings were sprayed with a solution containing 1 μM coronatine (COR, Sigma Aldrich). Four days after COR treatment, seedlings were visually screened for reduced degreening compared to the *jazD* control. To test coronatine resistance in mature plants, leaves of 26-day-old plants were spotted with 5 μl of a solution containing 50 μM coronatine. Leaves were excised and photographed four days after treatment. Coronatine stocks were dissolved in 100% ethanol and diluted in water.

Complementation testing

Reciprocal crosses were performed between *sjd10* and *sjd78* using M₃ plants. The resulting F₁ plants grown in soil at 21°C under a long-day light regime of 16 h light (100 $\mu\text{mol m}^{-2}\text{s}^{-1}$) and 8 h dark. Complementation testing of *suppressor of coronatine hypersensitivity* (*sch*) mutants were performed by using *sch* lines as the pollen donor for crosses to *jazD coi1* and *jazD myc2* F₁ seed was plated onto media containing half-strength Linsmaier and Skoog (LS; Caisson Labs), 0.8% (w/v) sucrose, and 0.8% (w/v) phytoblend agar (Caisson Labs). Plates were incubated under 16 h light (80 $\mu\text{mol m}^{-2}\text{s}^{-1}$) / 8 h dark conditions at 21°C. After eight days of growth, seedlings were sprayed with 5 μM coronatine (COR, Sigma Aldrich).

Whole-genome resequencing for identification of candidate genes

DNA was extracted from 26-day-old using the Wizard Genomic DNA Purification Kit (Promega). DNA concentrations were measured using the Qubit fluorometer (Invitrogen) in the MSU RTSF Genomics Core facility. Equal concentrations of DNA were pooled from 76 plants

that expressed the suppressor phenotype. Library preparation and sequencing was performed by BGI Americas. Sequence data was cleaned and trimmed by BGI. Sequencing reads were aligned and allele frequency was calculated using the SIMPLE pipeline (Wachsman et al. 2017).

Sanger sequencing for identification of mutations

PCR amplification of genomic DNA containing *COII* and *MYC2* from mutants of interest was performed with primer sets spanning the 5' and 3' UTRs. Primer sequences are provided in Table A3.1. PCR reaction conditions were as follows: 95°C for 5 min, 35 cycles of denaturation (95°C, 30 s), annealing (59.6°C, 30 s for *MYC2*; 48.6°C, 30 s for *COII*), elongation (72°C, 1.5 min), and one final elongation step at 72°C for 5 min. Reactions were held at 12°C until removed from the PCR instrument and analyzed on a 1% agarose gel with DNA standards (1 kb plus DNA ladder, Invitrogen). PCR products were purified from agarose gel slices using the Qiaquick Gel Extraction Kit (Qiagen). Purified product was combined with each primer (i.e. individual Fwd and Rev reactions) and sequenced at the MSU RTSF Genomics Core Facility. Sequencing reads were aligned to the genomic sequence using Benchling online alignment software to identify polymorphisms.

Insect bioassay

Insect feeding assays were performed as previously described (Herde et al. 2013) with minor modifications. *Trichoplusia ni* (cabbage looper) eggs (Benzon Research) were incubated at room temperature for 3 day on moist filter paper. Once hatched, 3-4 larvae were placed on 7- to 8-week-old, short-day-grown plants. Larval weights were determined 8-10 day after the start of feeding.

Accession numbers

Genes described here have the following Arabidopsis Genome Initiative (AGI) gene accession numbers: *JAZ1* (AT1G19180), *JAZ2* (AT1G74950), *JAZ3* (AT3G17860), *JAZ4* (AT1G48500),

JAZ5 (AT1G17380), *JAZ6* (AT1G72450), *JAZ7* (AT2G34600), *JAZ9* (AT1G70700), *JAZ10* (AT5G13220), *JAZ13* (AT3G22275), *MYC2* (AT1G32640), and *COII* (AT2G39940).

RESULTS

Screen design for suppressors of growth and senescence in *jazD*

Two suppressor screens were conducted using an ethyl methanesulfonate-mutagenized population of *jazD*. In one screen, two mutants showing a recovery of the small rosette size of *jazD* were identified. These mutants were designated as *suppressor of jazD* (*sjd*). The second screen identified mutants having reduced sensitivity to exogenous coronatine, which causes severe chlorosis and death in *jazD*. These mutants were designated as *suppressor of coronatine hypersensitivity* (*sch*) (Fig. 3.1).

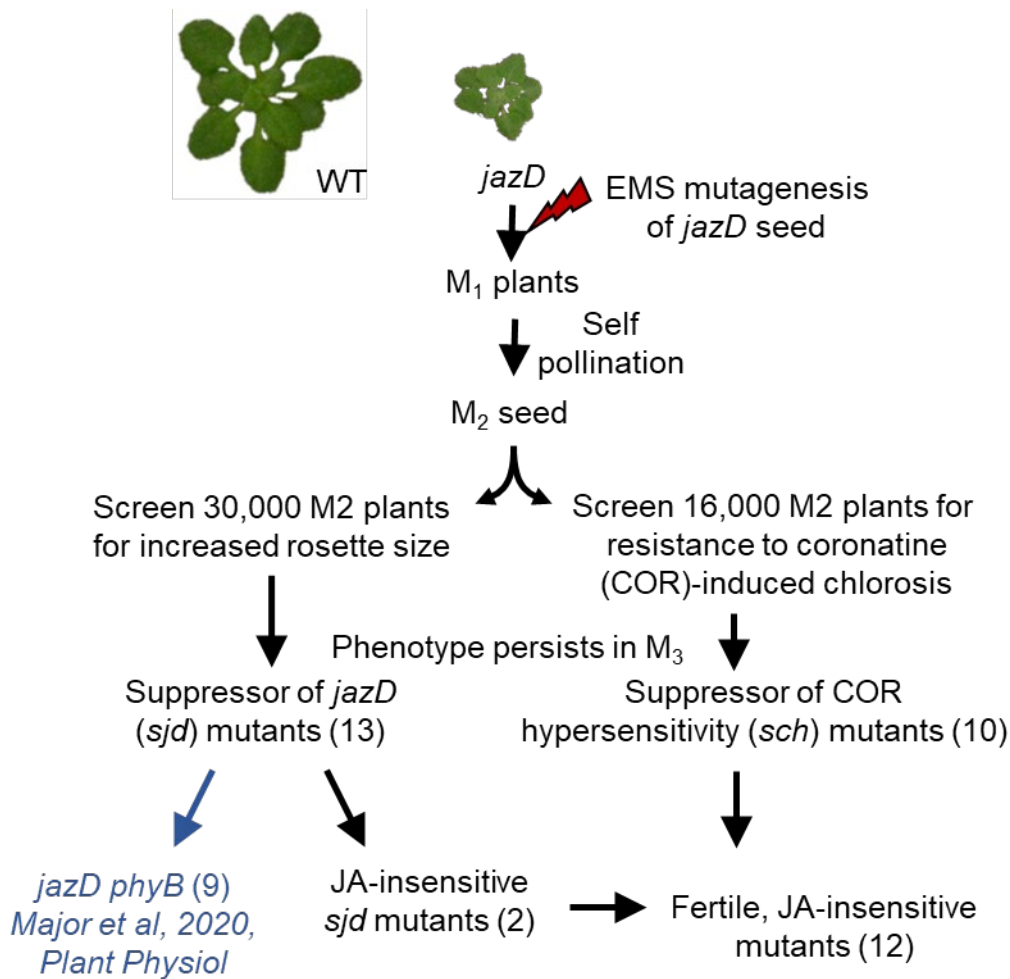


Figure 3.1 Workflow for identification of two classes of *jazD* suppressor mutants.

A photograph of a wild-type (WT) plant is shown for size comparison. Together, the two screens identified 12 fertile mutants with improved growth and reduced sensitivity to exogenous jasmonate.

Restored growth of *sjd10* and *sjd78* negatively correlates with defense

Previous studies identified 13 *suppressor of jazD* (*sjd*) mutants on the basis of restoration of the small rosette size of *jazD* (Major et al. 2020). Nine of these mutants harbored null mutations in *PHYB* (Fig. 3.1). Here, I characterized two of the remaining non-*phyB* mutants, *sjd10* and *sjd78*. Measurements of rosette fresh weight of M₃ plants showed that *sjd10* and *sjd78* have a growth rate that is intermediate between wild type (WT) and *jazD* (Fig. 3.2a-b).

Anthocyanin measurements and insect feeding assays were used to determine whether defense responses are maintained in *sjd10* and *sjd78*. Leaf anthocyanin levels in *sjd10* and *sjd78* were more similar to *jazD* than to WT (Fig. 3.2c). The *sjd10* and *sjd78* mutants were also more resistant than WT to challenge by *Trichoplusia ni* larvae, although this increased level of resistance was less than that of the *jazD* parental line (Fig. 3.2d). These data indicate that growth restoration in *sjd10* and *sjd78* negatively correlates with the expression of defense-related traits.

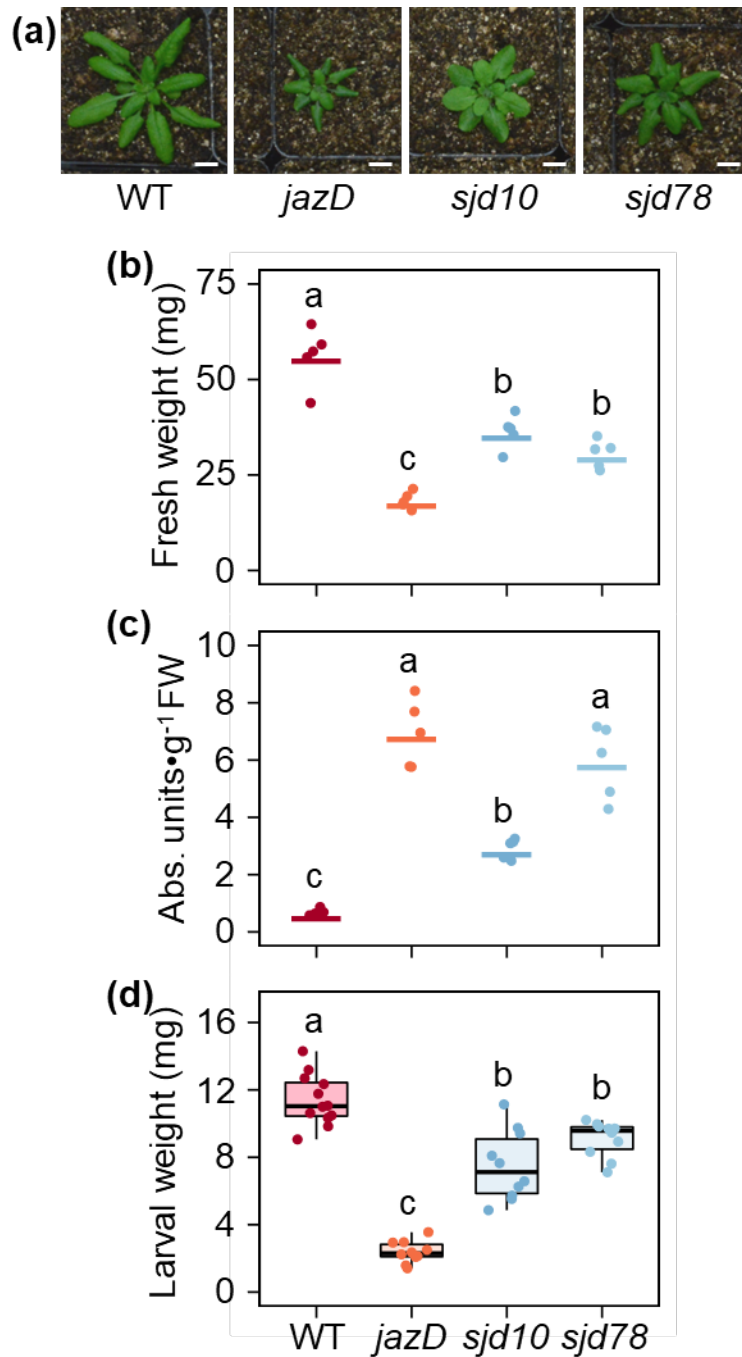


Figure 3.2 Suppressor mutants *sjd10* and *sjd78* have an intermediate level of growth and defense relative to WT and *jazD*.

(a) Photographs of representative 30-d-old WT, *jazD*, *sjd10*, and *sjd78* plants. Scale bars are 1 cm. (b-c) Fresh weight (b) and anthocyanin levels (c) in leaves of 23-d-old WT, *jazD*, *sjd10*, and *sjd78* plants (n=5 plants per genotype). (d) Weights of *T. ni* larvae measured after nine days of feeding on WT, *jazD*, *sjd10*, and *sjd78* plants (n=10-12 larvae per genotype). Different letters (b-

Figure 3.2 (cont'd)

d) represent significant differences at $P < 0.05$ with Tukey's honest significant difference (HSD) test.

sjd10* and *sjd78* contain mutations in *COII

Complementation testing is useful to determine whether phenotypically similar mutants harbor recessive mutations in the same gene (Yook 2005). Accordingly, *sjd10* and *sjd78* (M4 generation) were crossed to generate F_1 progeny containing mutations from both parents. When grown in soil, all of the resulting F_1 plants displayed a rosette size similar to the parents (i.e., intermediate between WT and *jazD* (Fig. 3.3a). This finding indicates that the *sjd78* and *sjd10* mutations fail to complement and are therefore allelic.

Having established that *sjd10* and *sjd78* define the same gene, whole-genome resequencing by bulk-segregant analysis (BSA) of *sjd78* was employed to identify the position of this mutation (Magwene et al. 2011). Within a population of 464 F_2 plants derived from a cross between *sjd78* and *jazD*, 76 plants having large rosettes were selected (Fig. 3.3b). Equal amounts of DNA from each plant was pooled and sequenced. Using the SIMPLE pipeline (Wachsman et al. 2017) to align the sequence data and identify allele frequencies, a putative mutation in *COII* (At2g39940) was identified. Sanger sequencing of the entire *COII* gene confirmed that the *sjd78* line has a single G-to-A missense mutation predicted to cause a E361K substitution in the 12th Leucine-Rich Repeat (LRR) of the protein (Fig. 3.3c, Table 3.1). Identification of this mutation suggested that *sjd78* might be affected in its sensitivity to coronatine, which is perceived in plant cells by COII-JAZ co-receptor complexes. Indeed, I found that the coronatine-induced senescence phenotype in *jazD* is completely blocked by the *sjd78* mutation (Fig 3.4).

Sanger sequencing of the *COII* gene in *sjd10* also identified G-to-A missense mutation. This mutation causes a E172K substitution in LRR 5 of the protein (Fig 3.3c, Table 3.1). Unlike

coil null alleles (e.g., *coil-1*) but similar to the reported phenotypes of *coil-41*, both *sjd10* and *sjd78* are fertile.

Table 3.1 Summary of suppressor mutants described in this study

Line¹	Family²	Gene affected	Causal mutation³	Major phenotypes in comparison to WT⁴
<i>sjd10</i>	Unknown	<i>COI1</i>	E172K	Fertile; increased anthocyanin levels and insect resistance; reduced fresh weight; increased sensitivity to MeJA
<i>sjd78</i>	Unknown	<i>COI1</i>	E361K also known as <i>coil-41</i>	Fertile; increased anthocyanin levels and insect resistance; reduced leaf fresh weight; increased sensitivity to MeJA
<i>sch4</i>	24	<i>COI1</i>	E203K	Fertile; increased sensitivity to MeJA; COR resistant, WT-like MeJA sensitivity
<i>sch7</i>	22	<i>COI1</i>	G98D	Fertile; more resistant to COR but not MeJA
<i>sch17</i>	6	<i>COI1</i>	G82D	Fertile; more resistant to COR and MeJA
<i>sch18</i>	8	<i>MYC2</i>	R347*	Weakly resistant to COR but not MeJA
<i>sch19</i>	23	<i>COI1</i>	E350K	Severely reduced fertility; more resistant to COR but normal sensitivity to MeJA
<i>sch20</i>	23	<i>MYC2</i>	Q174*	Weakly resistant to COR but not MeJA
<i>sch21</i>	22	<i>MYC2</i>	W166*	Weakly resistant to COR but not MeJA
<i>sch22</i>	22	<i>MYC2</i>	W266*	Weakly resistant to COR but not MeJA
<i>sch23</i>	22	<i>MYC2</i>	Q174*	Weakly resistant to COR but not MeJA
<i>sch24</i>	24	<i>MYC2</i>	W266*	Weakly resistant to COR but not MeJA

¹Mutant nomenclature reflects the two suppressor screens. *sjd* (*suppressor of jazD*) lines were identified as having larger rosettes than *jazD*. *sch* (*suppressor of coronatine hypersensitivity*)

Table 3.1 (cont'd)

lines were identified as being less sensitive to coronatine-induced leaf senescence relative to *jazD*.

²Family denotes independent bulks of M₂ EMS seed.

³Asterisk denotes a mutation that generates a pre-mature stop codon.

⁴COR, coronatine; MeJA, methyl-jasmonate; WT, Wild-type.

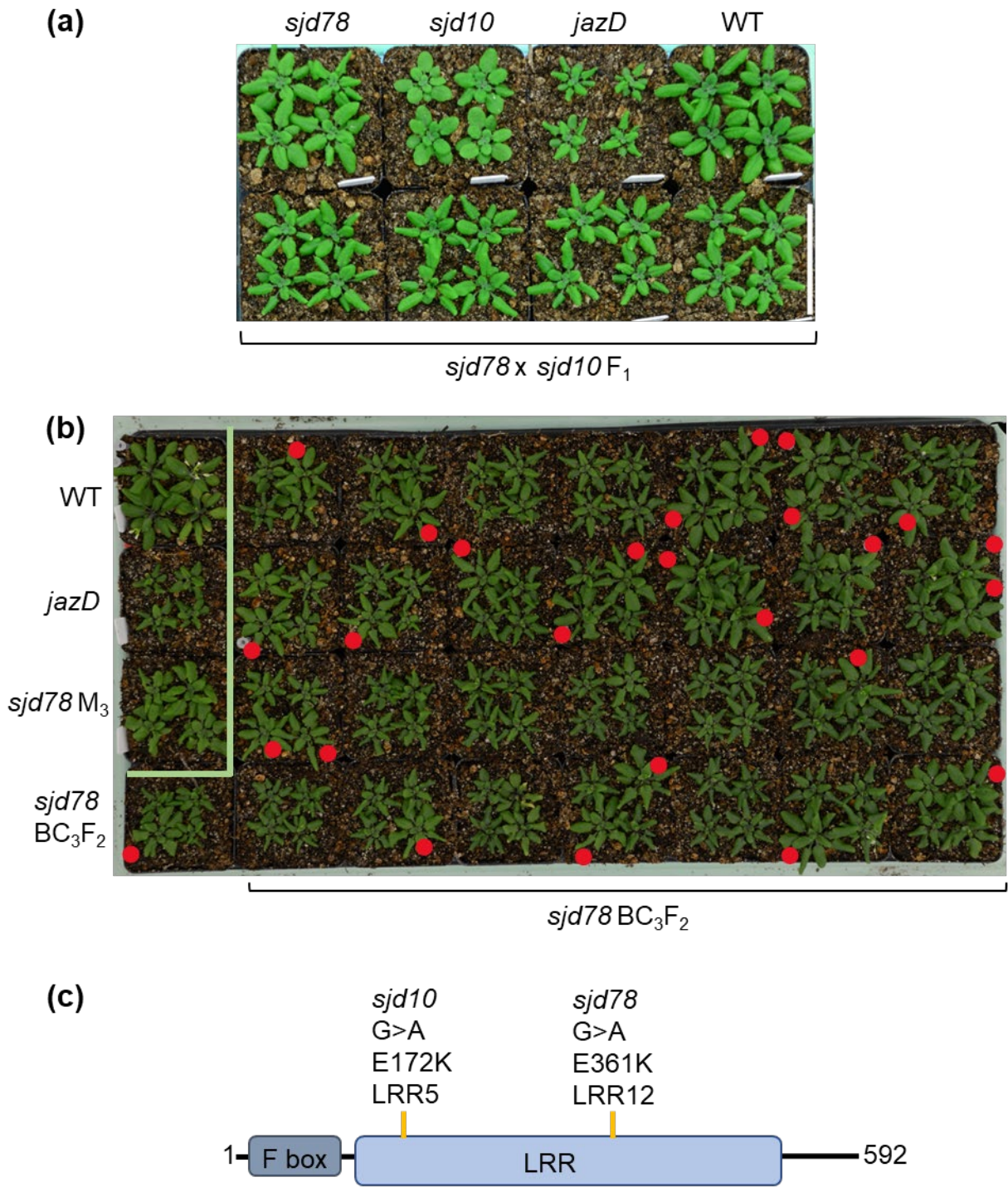


Figure 3.3 Molecular genetic analysis of *sjd10* and *sjd78*.

(a) Genetic complementation test of *sjd10* and *sjd78*. Upper row, photograph of WT, *jazD*, *sjd10*, and *sjd78* (M₃ generation) plants as controls. Lower row, photograph of F₁ plants derived from a cross between *sjd78* and *sjd10*. Retention of the large-rosette phenotype in all F₁ plants

Figure 3.3 (cont'd)

indicates lack of complementation (b) Photograph of segregating F₂ population (BC₃F₂) derived from a cross between *sjd78* and *jazD*. The *sjd78* parent was previously backcrossed to *jazD* three times. Red circles indicate large-rosette progeny selected for bulk segregant sequencing. Green inset: WT, *jazD*, and *sjd78* M₃ plants are shown as controls. (c) Protein model of COI1 and the location of the single-nucleotide polymorphisms in *sjd10* and *sjd78*. LRR, Leucine rich repeat domain.

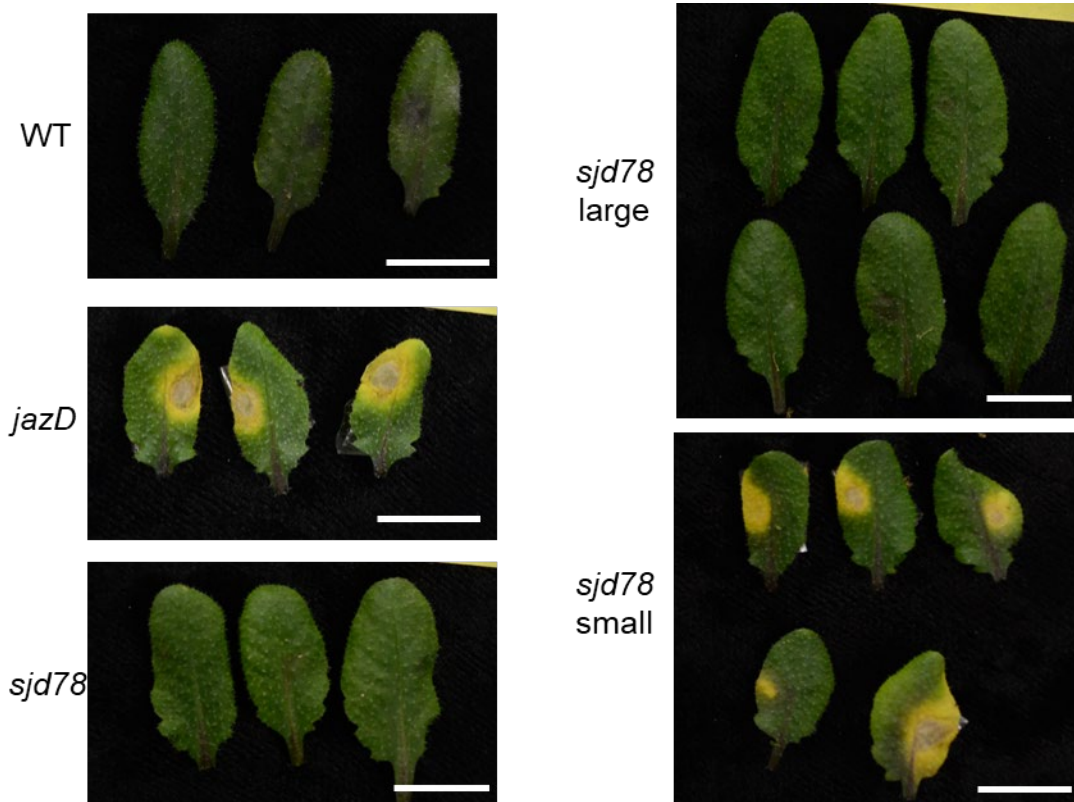


Figure 3.4 Coronatine (COR) resistance correlates with the growth phenotype of suppressor mutant *sjd78*.

The F₂ population derived from a cross between *sjd78* and *jazD* consisted of two distinct phenotypes: plants with large leaves that were insensitive to COR and plants with smaller leaves that turned chlorotic in response to COR treatment. WT, *jazD*, and *sjd78* M₅ generation plants are shown as controls. Scale bars = 1 cm.

Identification of mutations that impair coronatine-induced senescence of *jazD*

Exogenous jasmonate has long been known to promote chlorophyll loss (Zhu et al. 2015; Major et al. 2017). However, because JA signaling and biosynthesis mutants are not affected in age-dependent senescence, the physiological significance of JA-induced leaf de-greening

remains unknown. JAZ depletion in the *jazD* mutant is associated with extreme hypersensitivity to exogenous JA (Guo et al. 2018). Moreover, treatment of *jazD* with coronatine leads to rapid development of senescence-like symptoms, including loss of chlorophyll, tissue necrosis, and cell death (Guo et al. 2018). We sought to identify molecular components required for COR-induced senescence. An EMS-mutagenized M₂ population of *jazD* was screened for mutants that are impaired in leaf de-greening following foliar application of coronatine. Of approximately 16,000 seedlings screened, ten *suppressor of coronatine hypersensitivity* (*sch*) mutants were selected for further characterization (Fig. 3.5). Qualitative differences in the level of COR-induced leaf de-greening were observed among these mutants. In particular, *sch4*, *sch7*, *sch17*, *sch18*, *sch19*, *sch20* and *sch22* appeared to be largely insensitive to COR treatment, whereas *sch21*, *sch23*, and *sch24* showed mild chlorotic symptoms (Fig. 3.5).

The extreme hypersensitivity of *jazD* root growth to exogenous JA (Guo et al. 2018) provided a simple assay to test whether JA signaling is impaired by *sjd* and *sch* suppressor mutations. Consistent with previous studies, JA-induced root growth inhibition in *jazD* was much stronger than that in the WT control (Fig. 3.6a). *sjd10* and *sjd78* roots were less sensitive to growth inhibition by JA, indicating that these mutants are impaired in JA signaling. Similar results were obtained with *sch* mutants. Lines *sch4*, *sch18*, *sch19*, *sch20*, *sch21*, *sch22*, *sch23*, and *sch24* displayed decreased sensitivity to MeJA compared to *jazD* and were not significantly different from WT. *sch7* and *sch17* appeared to be the least sensitive of all mutants to root growth inhibition by MeJA (Fig. 3.6b). These findings suggest that *sjd* and *sch* mutations define components of the JA signaling pathway.

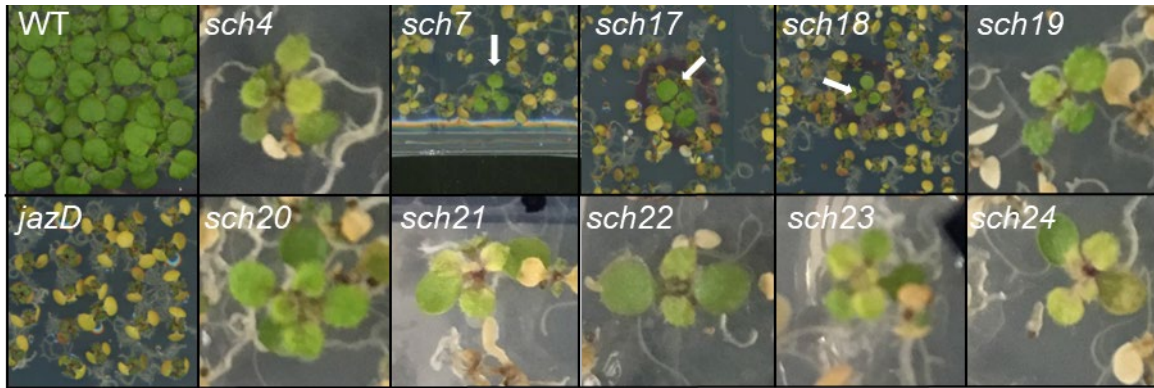


Figure 3.5 Identification of coronatine-resistant *sch* suppressor mutants.

EMS-mutagenized seedlings (M2 generation) were selected for resistance to foliar application with a solution containing 1 μ M coronatine. Seedlings were treated eight days after germination and screened for resistance four days post-treatment. WT and *jazD* plants are shown as controls. White arrows indicate the resistant seedlings.

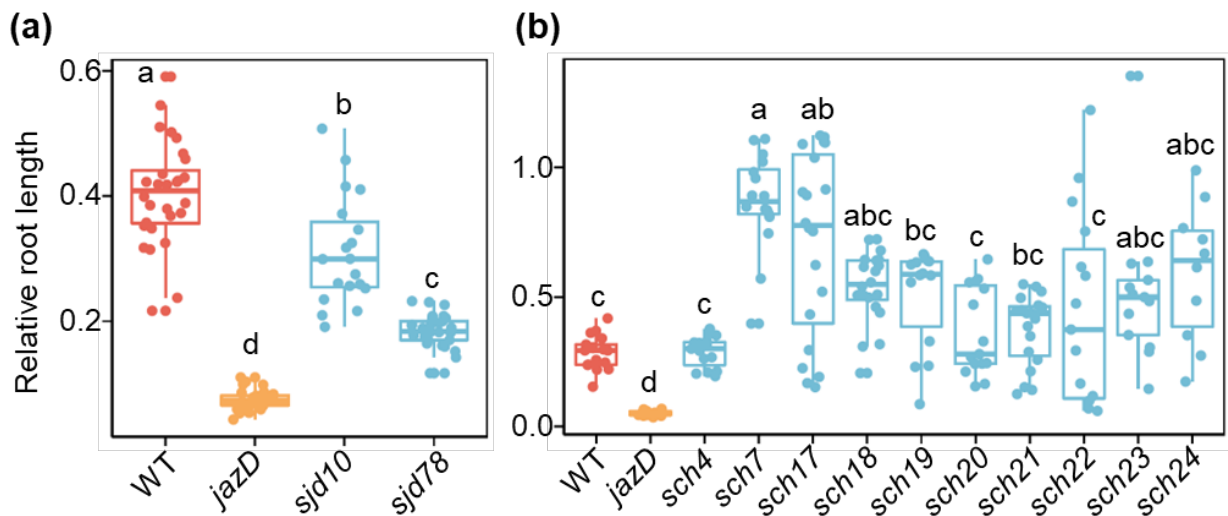


Figure 3.6 *sjd* and *sch* suppressor lines have reduced sensitivity to methyl jasmonate (MeJA)-induced root growth inhibition.

Seedlings of the indicated genotype were grown for 10 days on agar medium supplemented or not (mock) supplemented with 10 μ M MeJA. Relative root length was determined by normalizing the root length on MeJA-containing medium to that of mock-treated roots. (a) Relative root length of *suppressor of jazD* (*sjd*) mutants (n = 19-30). (b) Relative root length of *suppressor of coronatine hypersensitivity* (*sch*) mutants (n = 10-20). Wild-type (WT) and *jazD* plants were included as controls. Letters indicate significant differences at $P < 0.05$ according to Tukey's honestly significant difference (HSD) test.

***sch* mutants define two genetic complementation groups**

Genetic complementation tests were performed to determine whether *sch* mutants are defective in either *COI1* or *MYC2*, which are major positive regulators of the JA signaling pathway. The *sch* mutants were crossed to two tester lines, *jazD coi1* and *jazD myc2*, and the resulting F₁ seedlings were assessed for sensitivity to COR-induced leaf chlorosis. Crosses between *jazD coi1* and *sch4*, *sch7*, *sch17*, and *sch19* yielded F₁ progeny that retained resistance to coronatine, suggesting that these suppressor lines carry mutations in *COI1* (Fig. 3.7). The remaining *sch* lines were then crossed to *jazD myc2*. Testing of the resulting F₁ progeny for sensitivity to COR indicated that *sch18*, *sch20*, *sch21*, *sch23*, and *sch24* failed to complement *jazD myc2*, which is indicative of mutations in *MYC2* (Fig. 3.7). Unexpectedly, *sch22* failed to complement *jazD coi1* in approximately 50% of the F₁ progeny and also failed to complement *jazD myc2*.

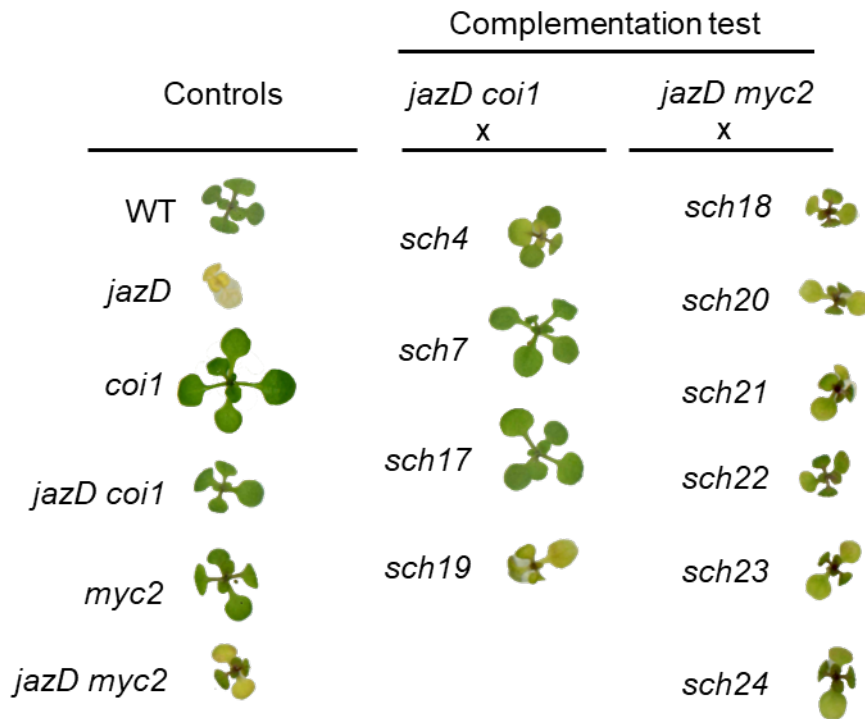


Figure 3.7 Complementation testing of *sch* mutants.

Figure 3.7 (cont'd)

sch4, *sch7*, *sch17*, and *sch19* failed to complement *jazD coi1*, which lacks ten JAZ repressors and COI1. *sch18*, *sch20*, *sch21*, *sch22*, *sch23*, and *sch24* failed to complement a *jazD myc2* tester line. Representative images of 12-day-old seedlings four days after treatment with 5 μ M coronatine.

sch* mutants contain mutations in *COI1* and *MYC2

DNA sequencing was used to further test the hypothesis that *sch* suppressor lines harbor mutations in *COI1* or *MYC2*, as suggested by the genetic complementation tests. Point mutations were identified in the *COI1* gene of *sch4*, *sch7*, *sch17*, and *sch19* (Fig. 3.8) but not in *sch22*. In all cases, the identified mutation created an amino acid substitution within the leucine-rich repeat (LRR) domain of the COI1 protein. Nonsense mutations in *MYC2* were identified in *sch18*, *sch20*, *sch21*, *sch22*, *sch23*, and *sch24*. Each of these base changes is predicted to create a stop codon that truncates the C-terminal end of the protein containing the DNA binding basic-helix-loop-helix (bHLH) domain (Fig. 3.8). It is noteworthy that the mutations identified in *sch20* and *sch23* are identical and the mutations identified in *sch22* and *sch24* are identical (Table 3.1). It is most likely that these mutants arose from distinct mutagenic events because they were obtained from different pools of M₂ bulk seed.

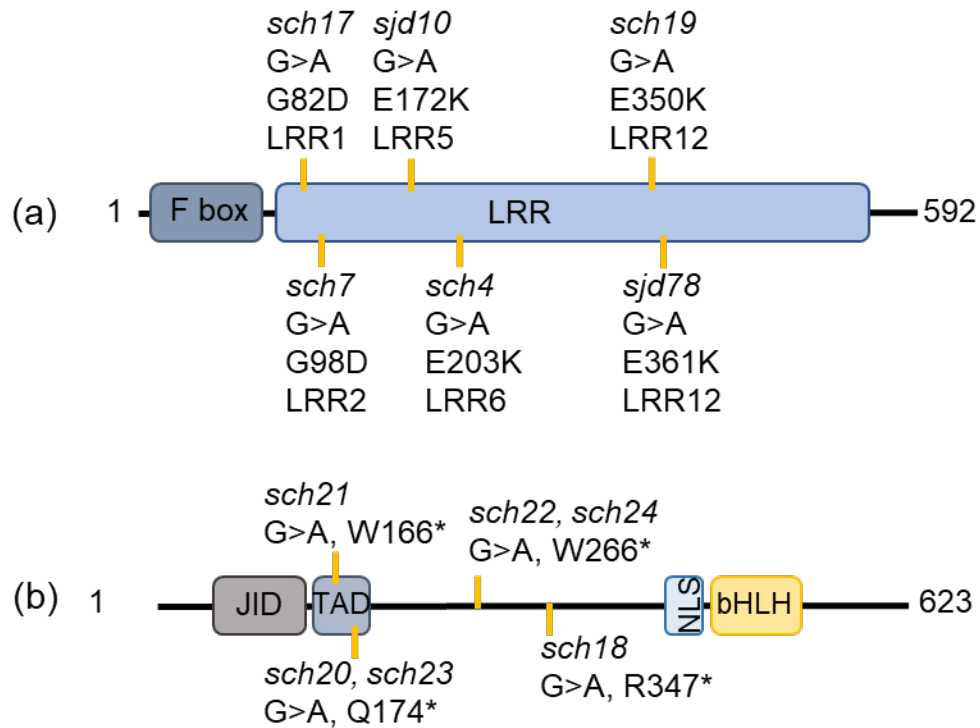


Figure 3.8 *sjd* and *sch* suppressor mutants contain mutations in either the *COI1* or *MYC2* gene.

Sanger sequencing was used to identify mutations in *COI1* or *MYC2*. Vertical yellow lines denote position of single nucleotide changes identified in the indicated mutant. (a) Schematic diagram of Arabidopsis *COI1* protein. LRR; Leucine rich repeat domain. (b) Schematic diagram of Arabidopsis *MYC2* protein. Asterisk denotes a mutation that generates a pre-mature stop codon. JID; JAZ-interacting domain; TAD, Transactivation domain; bHLH, basic Helix-Loop-Helix domain.

DISCUSSION

Characterization of *COI1* and *MYC2* mutations

The *COI1* protein contains two major domains. The N-terminal F-box domain binds to the ASK1 (called SKP in non-plant systems) component of the SCF^{*COI1*} complex (SKP-CULLIN-F box complex). The C-terminal Leucine-Rich Repeat (LRR) domain consists of 18 tandem LRR repeats that interact with JAZ substrates, the bioactive form of JA (JA-Ile), and an inositol phosphate cofactor (Yan et al. 2009; Sheard et al. 2010). The *coil* mutations identified in this study are all amino acid substitutions in the LRR region. Three of the *coil* mutations (*sch7*,

sch19, and *sjd78*) are located in LRR 2 and LRR 12, which are important components of the JA-Ile binding pocket (Sheard et al. 2010). It is well established that LRR mutations can block COI1-JAZ interactions by altering the protein conformation at the JAZ binding pocket of COI1 (Sheard et al. 2010). The remaining *coil* mutations identified in this study reside in different LRRs and may disrupt COI1-JAZ interactions by altering the JAZ binding pocket, the cofactor interaction residues, or the JA-Ile binding pocket. It is also possible that the LRR mutations disrupt the stability or overall structure of COI1 and therefore disrupt the SCF complex formation. Overall, these findings highlight the importance of the COI1 LRRs in JA signaling.

The MYC2 protein is comprised of an N-terminal JAZ-interacting domain (JID), a transactivation domain (TAD) that interacts with MED25, a C-terminal nuclear localization signal (NLS), and a basic-helix-loop-helix (bHLH) domain that binds DNA (Lian et al. 2017; Kazan and Manners 2013). The *myc2* mutations identified in this study all generate stop codons that truncate NLS and bHLH domains. Thus, these mutations likely abolish the activity of MYC2 and prevent the expression of MYC2-dependent target genes. However, because *MYC2* is a member of a small gene family that includes the partially redundant *MYC3*, *MYC4*, and *MYC5*, null mutations in *MYC2* do not eliminate the expression of JA-responsive genes (Fernández-Calvo et al. 2011; Song et al. 2017). Genome-wide analysis of MYC2 and MYC3 binding sites showed that MYC2 regulates the expression of nearly three thousand genes independently of MYC3 (Zander et al. 2020). Therefore, a large suite of processes may be controlled by MYC2 that are not compensated for by the other MYC TFs in the absence of MYC2.

Growth negatively correlates with defense in *coil* alleles, *sjd10* and *sjd78*

Two independent alleles of *COI1* (*sjd10* and *sjd78*) were identified that partially restore the reduced growth of *jazD*. The *sjd78* mutation was previously identified as *coil-41* in a

suppressor screen for enhanced resistance to the coronatine producing plant pathogen *Pseudomonas syringae* (Cui et al. 2018). Unlike *coi1* null alleles such as *coi1-1* (Xie et al. 1998), these suppressor mutants are fertile and retain sensitivity to root growth inhibition by JA. These results indicate that JA signaling is partially active in these mutants. The *jazD* parental line lacks all JAZ family members except JAZ8, JAZ11, and JAZ12. Reduced COI1 activity in the *jazD* background is expected to stabilize these remaining JAZ proteins to reduce the amplitude of JA responses, including growth inhibition and promotion of defense. Consistent with this interpretation, *sjd10* and *sjd78* exhibited increased growth and reduced defense against insect herbivory relative to *jazD*. The precise mechanism by which growth is restored in these suppressor lines remains to be determined. These data highlight the need to better understand the negative association between growth and defense.

COI1 and MYC2 are major signaling components of JA-induced senescence

The genetic screen for suppressors of COR-induced senescence led to the identification of mutations in two well characterized JA signaling genes, *COI1* and *MYC2*. The recovery of multiple *coi1* and *myc2* alleles suggests that the screen was saturated. While the original screening was performed with 1 μ M coronatine treatment, the complementation testing was performed with 5 μ M coronatine, which may account for the weaker phenotypes of *sch4* and *sch19* in the complementation test compared to the M₂ screen. Additionally, complementation crosses may display weaker or stronger phenotypes than either parent (Yook 2005). The design of the screen, and in particular the selection of mutants that are strongly resistant to COR, likely precluded the identification of genes that have a minor but nevertheless direct contribution to JA-induced degreening. For example, previous studies have shown that synergistic crosstalk between the JA and ethylene signaling pathways is required for JA-induced senescence (Li et al.

2013). Our failure to identify ethylene signaling components in this screen may reflect genetic redundancy within the ethylene response pathway, such that loss of one family member is compensated by other family members. Alternatively, JA-induced senescence in *jazD* may be mediated by a genetic program that is distinct from dark-induced or age-dependent senescence pathways that depend on ethylene action. In addition to ethylene signaling, we also anticipated the recovery of mutations in the chlorophyll catabolism pathway, such as the *STAY GREEN* (*SGR*) genes (Ono et al. 2019). Again, however, the presence of three *SGR* paralogs in Arabidopsis may have hindered the identification of mutations affecting a single *SGR* gene (Ono et al. 2019). Further characterization of JA-induced leaf degreening in *jazD* is needed to determine the precise mechanism of chlorophyll loss and its relationship to other types of leaf senescence (e.g., age-dependent senescence).

Modulation of JA signaling may provide balance between growth and defense tradeoffs

The identification of multiple *coi1* and *myc2* alleles suggests that COI1-mediated modulation of MYC2 activity underlies JA-dependent leaf growth and senescence responses. The primary function of COI1 is to promote JAZ degradation through the ubiquitin-26S proteasome pathway (Thines et al. 2007). Consistent with this view, all JAZ directly interact with MYC TFs to negatively regulate JA-dependent transcriptional responses. Interestingly, several suppressor mutants (e.g., *sjd10*, *sjd78*, *sch4*, *sch7*, *sch17*, and *sch19*) identified in our screens were sensitive to MeJA but resistant to coronatine treatment. Given that the virulence of the pathogen *Pseudomonas syringae* depends on coronatine, it will be interesting to test these mutants for resistance to *P. syringae* challenge (Zheng et al. 2012). It is also worth noting previous work in which site-directed mutagenesis identified point mutations that reduce COI1 responses to coronatine without affecting responses to the endogenous hormone, JA-Ile (Zhang

et al. 2015). The *jazD* mutant is hypersusceptible to *P. syringae* due to increased sensitivity to coronatine. The mutant *coil* alleles in *sjd78* and *sjd10* may thus provide a starting point for rational engineering of plants with robust resistance to both *P. syringae* and insect herbivores. Because *jazD* has elevated levels of anti-microbial defense compounds, it would also be interesting to test whether resistance against *P. syringae* is elevated in the coronatine-resistant *jazD coil-1* line (Guo et al. 2018, Chapter 2). In addition to testing different *coil* mutations for altered binding affinity to coronatine and JA-Ile, another group screened multiple coronatine agonists and identified a coronatine stereoisomer that selectively enhances COI1 interaction with JAZ9, resulting in activation of the JA-ethylene branch of immunity without a reduction in growth (Saito et al. 2018). The combination of modified COI1 receptors and JA-Ile agonists could provide a strategy to induce specific defense responses with synthetic small molecules. While it may not be practical to generate high-order *jaz* mutants in crop plants, a better understanding of small molecule-dependent COI1-JAZ interactions across tissue types may inform biotechnological approaches to enhance stress resilience with minimal impacts on growth and yield.

REFERENCES

- Arnold A, Nikoloski Z. 2014.** Bottom-up metabolic reconstruction of *Arabidopsis* and its application to determining the metabolic costs of enzyme production. *Plant Physiology* **165**: 1380–1391.
- Ballaré CL, Austin AT. 2019.** Recalculating growth and defense strategies under competition: Key roles of photoreceptors and jasmonates. *Journal of Experimental Botany* **70**: 3425–3436.
- Bazzaz FA, Chiariello NR, Coley PD, Pitelka LF. 1987.** Allocating resources to reproduction and defense. *Bioscience* **37**: 58–67.
- Beekwilder J, van Leeuwen W, van Dam NM, Bertossi M, Grandi V, Mizzi L, Soloviev M, Szabados L, Molthoff JW, Schipper B, et al. 2008.** The impact of the absence of aliphatic glucosinolates on insect herbivory in *Arabidopsis*. *PLoS One* **3**: e2068.
- Bekaert M, Edger PP, Hudson CM, Pires JC, Conant GC. 2012.** Metabolic and evolutionary costs of herbivory defense: systems biology of glucosinolate synthesis. *New Phytologist* **196**: 596–605.
- Campos ML, Yoshida Y, Major IT, De Oliveira Ferreira D, Weraduwege SM, Froehlich JE, Johnson BF, Kramer DM, Jander G, Sharkey TD, et al. 2016.** Rewiring of jasmonate and phytochrome B signalling uncouples plant growth-defense tradeoffs. *Nature Communications* **7**: 1–10.
- Cerrudo I, Keller MM, Cargnel MD, Demkura PV, de Wit M, Patitucci MS, Pierik R, Pieterse CMJ, Ballaré CL. 2012.** Low red/far-red ratios reduce *Arabidopsis* resistance to *Botrytis cinerea* and jasmonate responses via a COI1-JAZ10-dependent, salicylic acid-independent mechanism. *Plant Physiology* **158**: 2042–2052.
- Cui H, Qiu J, Zhou Y, Bhandari DD, Zhao C, Bautor J, Parker JE. 2018.** Antagonism of transcription factor MYC2 by EDS1/PAD4 complexes bolsters salicylic acid defense in *Arabidopsis* effector-triggered immunity. *Molecular Plant* **11**: 1053–1066.
- Del Carmen Martínez-Ballesta M, Moreno DA, Carvajal M. 2013.** The physiological importance of glucosinolates on plant response to abiotic stress in *Brassica*. *International Journal of Molecular Sciences* **14**: 11607–11625.
- Ellis C, Turner JG. 2001.** The *Arabidopsis* mutant *cev1* has constitutively active jasmonate and ethylene signal pathways and enhanced resistance to pathogens. *The Plant Cell* **13**: 1025–1033.
- Fernández-Calvo P, Chini A, Fernández-Barbero G, Chico J-M, Gimenez-Ibanez S, Geerinck J, Eeckhout D, Schweizer F, Godoy M, Franco-Zorrilla JM, et al. 2011.** The *Arabidopsis* bHLH transcription factors MYC3 and MYC4 are targets of JAZ repressors and act additively with MYC2 in the activation of jasmonate responses. *The Plant Cell* **23**: 701–715.

- Guo Q, Major IT, Kapali G, Howe GA. 2022.** MYC transcription factors coordinate tryptophan-dependent defense responses and compromise seed yield in *Arabidopsis*. *New Phytologist* **236**: 132-145.
- Guo Q, Yoshida Y, Major IT, Wang K, Sugimoto K, Kapali G, Havko NE, Benning C, Howe GA. 2018.** JAZ repressors of metabolic defense promote growth and reproductive fitness in *Arabidopsis*. *Proceedings of the National Academy of Sciences* **115**: E10768-10777.
- Havko NE, Major IT, Jewell JB, Attaran E, Browse J, Howe GA. 2016.** Control of carbon assimilation and partitioning by jasmonate: an accounting of growth-defense tradeoffs. *Plants* **5**: 7.
- Kazan K, Manners JM. 2013.** MYC2: the master in action. *Molecular Plant* **6**: 686–703.
- Kliebenstein DJ. 2016.** False idolatry of the mythical growth versus immunity tradeoff in molecular systems plant pathology. *Physiological and Molecular Plant Pathology* **95**: 55–59.
- Lankau RA, Kliebenstein DJ. 2009.** Competition, herbivory and genetics interact to determine the accumulation and fitness consequences of a defence metabolite. *Journal of Ecology* **97**: 78–88.
- Li Z, Peng J, Wen X, Guo H. 2013.** Ethylene-insensitive3 is a senescence-associated gene that accelerates age-dependent leaf senescence by directly repressing miR164 transcription in *Arabidopsis*. *The Plant Cell* **25**: 3311–3328.
- Lian T-F, Xu Y-P, Li L-F, Su X-D. 2017.** Crystal structure of tetrameric *Arabidopsis* MYC2 reveals the mechanism of enhanced interaction with DNA. *Cell Reports* **19**: 1334–1342.
- Magwene PM, Willis JH, Kelly JK. 2011.** The statistics of bulk segregant analysis using next generation sequencing. *PLoS Computational Biology* **7**: e1002255.
- Major IT, Guo Q, Zhai J, Kapali G, Kramer DM, Howe GA. 2020.** A phytochrome B-independent pathway restricts growth at high levels of jasmonate defense. *Plant Physiology* **183**: 733–749.
- Major IT, Yoshida Y, Campos ML, Kapali G, Xin X-F, Sugimoto K, Ferreira DDO, He SY, Howe GA. 2017.** Regulation of growth – defense balance by the JASMONATE ZIM-DOMAIN (JAZ) -MYC transcriptional module. *New Phytologist* **215**: 1533–1547.
- Monson RK, Trowbridge AM, Lindroth RL, Lerdau MT. 2022.** Coordinated resource allocation to plant growth-defense tradeoffs. *New Phytologist* **233**: 1051–1066.
- Ono K, Kimura M, Matsuura H, Tanaka A, Ito H. 2019.** Jasmonate production through chlorophyll a degradation by Stay-Green in *Arabidopsis thaliana*. *Journal of Plant Physiology* **238**: 53–62.

- Pangesti N, Reichelt M, Mortel JEVD, Kapsomenou E, Gershenzon J, Van Loon JJA, Dicke M, Pineda A. 2016.** Jasmonic acid and ethylene signaling pathways regulate glucosinolate levels in plants during rhizobacteria-induced systemic resistance against a leaf-chewing herbivore. *Journal of Chemical Ecology* **42**: 1212–1225.
- Saito H, Chini A, Iwahashi M, Seki M, Kato N, Bashir K, Takaoka Y, Solano R, Ueda M, Tanaka M, et al. 2018.** A rationally designed JAZ subtype-selective agonist of jasmonate perception. *Nature Communications* **9**: 3654.
- Sajitz-Hermstein M, Nikoloski Z. 2010.** A novel approach for determining environment-specific protein costs: the case of *Arabidopsis thaliana*. *Bioinformatics* **26**: i582-i588.
- Savchenko TV, Rolletschek H, Dehesh K. 2019.** Jasmonates-mediated rewiring of central metabolism regulates adaptive responses. *Plant and Cell Physiology* **60**: 2613–2620.
- Schweizer F, Fernandez-Calvo P, Zander M, Diez-Diaz M, Fonseca S, Glauser G, Lewsey MG, Ecker JR, Solano R, Reymond P. 2013.** *Arabidopsis* basic Helix-Loop-Helix transcription factors MYC2, MYC3, and MYC4 regulate glucosinolate biosynthesis, insect performance, and feeding behavior. *The Plant Cell* **25**: 3117–3132.
- Sheard LB, Tan X, Mao H, Withers J, Ben-Nissan G, Hinds TR, Kobayashi Y, Hsu F-F, Sharon M, Browse J, et al. 2010.** Jasmonate perception by inositol-phosphate-potentiated COI1-JAZ co-receptor. *Nature* **468**: 400–405.
- Song S, Huang H, Wang J, Liu B, Qi T, Xie D. 2017.** MYC5 is involved in jasmonate-regulated plant growth, leaf senescence and defense responses. *Plant and Cell Physiology* **58**: 1752–1763.
- Srivastava AK, Orosa B, Singh P, Cummins I, Walsh C, Zhang C, Grant M, Roberts MR, Anand GS, Fitches E, et al. 2018.** Sumo suppresses the activity of the jasmonic acid receptor CORONATINE INSENSITIVE1. *The Plant Cell* **30**: 2099–2115.
- Sugiyama R, Li R, Kuwahara A, Nakabayashi R, Sotta N, Mori T, Ito T, Ohkama-Ohtsu N, Fujiwara T, Saito K, et al. 2021.** Retrograde sulfur flow from glucosinolates to cysteine in *Arabidopsis thaliana*. *Proceedings of the National Academy of Sciences* **118**: e2017890118.
- Thines B, Katsir L, Melotto M, Niu Y, Mandaokar A, Liu G, Nomura K, He SY, Howe GA, Browse J. 2007.** JAZ repressor proteins are targets of the SCF^{COI1} complex during jasmonate signalling. *Nature* **448**: 661–665.
- Wachsman G, Modliszewski JL, Valdes M, Benfey PN. 2017.** A SIMPLE pipeline for mapping point mutations. *Plant Physiology* **174**: 1307–1313.
- de Wit M, Spoel SH, Sanchez-Perez GF, Gommers CMM, Pieterse CMJ, Voesenek LACJ, Pierik R. 2013.** Perception of low red:far-red ratio compromises both salicylic acid- and jasmonic acid-dependent pathogen defences in *Arabidopsis*. *Plant Journal* **75**: 90–103.

- Xie DX, Feys BF, James S, Nieto-Rostro M, Turner JG. 1998.** COI1: an *Arabidopsis* gene required for jasmonate-regulated defense and fertility. *Science* **280**: 1091–1094.
- Yan J, Zhang C, Gu M, Bai Z, Zhang W, Qi T, Cheng Z, Peng W, Luo H, Nan F, et al. 2009.** The *Arabidopsis* CORONATINE INSENSITIVE1 protein is a jasmonate receptor. *The Plant Cell* **21**: 2220–2236.
- Yook K. 2005.** Complementation. In: The *C. elegans* research community ed. *WormBook: the online review of C. elegans biology*. Pasadena, CA: WormBook.
- Zander M, Lewsey MG, Clark NM, Yin L, Bartlett A, Saldierna Guzmán JP, Hann E, Langford AE, Jow B, Wise A, et al. 2020.** Integrated multi-omics framework of the plant response to jasmonic acid. *Nature Plants* **6**: 290–302.
- Zhang Y, Turner JG. 2008.** Wound-induced endogenous jasmonates stunt plant growth by inhibiting mitosis. *PLoS One* **3**: e3699.
- Zhang L, Yao J, Withers J, Xin X-F, Banerjee R, Fariduddin Q, Nakamura Y, Nomura K, Howe GA, Boland W, et al. 2015.** Host target modification as a strategy to counter pathogen hijacking of the jasmonate hormone receptor. *Proceedings of the National Academy of Sciences* **112**: 14354–14359.
- Zheng XY, Spivey NW, Zeng W, Liu PP, Fu ZQ, Klessig DF, He SY, Dong X. 2012.** Coronatine promotes *Pseudomonas syringae* virulence in plants by activating a signaling cascade that inhibits salicylic acid accumulation. *Cell Host and Microbe* **11**: 587–596.
- Zhu X, Chen J, Xie Z, Gao J, Ren G, Gao S, Zhou X, Kuai B. 2015.** Jasmonic acid promotes degreening via MYC2/3/4- and ANAC019/055/072-mediated regulation of major chlorophyll catabolic genes. *Plant Journal* **84**: 597–610.

APPENDIX

Table A3.1 Primers used for Sanger sequencing of suppressor mutants.

AGI accession ¹	Gene name ²	Primer 1 ³	Primer 2 ³
AT2G39940	<i>COI1</i>	TAAGAACAAGAAATCAA AGT	CTCATATATTGGCTTACTA C
		CATCGACGACACAACAT GAA	ATTACAGATCTGCCACTG GA
		GCCTTGTCTCAGATAGA ATG	GAGATAAGGGATATGAAT GC
		CAATATTGCATTCATATC CC	AAACTTCTACATGACGGA GT
		ACCTTCACAGATACCAG AGA	TTATGCTTGCTATTAAG CA
		TTGTAGATAAAATCCGGA TC	TACTGATGGACTTTTGAG CA
		AACCTCAAAGCATCGA GCC	ACGGTTGATGATGTCATC GA
		GAACCATCTCCGACACA CCA	GTCGTGTAGCTGAGATC TGA
		GCATTCATATCCCTTATC TC	CGGGAAATCCAAATATCT TG
		AT1G32640	<i>MYC2</i>
TGTGATACACGTGCGAC CAA	ATAAATCTCCAGCTCCGC CG		
AACCACGTCGAAGCAGA GAG	GCGAGGTGATCGAGGAA GAG		

¹ AGI accession indicates the locus identifier provided by The Arabidopsis Information Resource (TAIR) database and the Arabidopsis Genome Initiative (AGI).

² Gene name indicates the common gene symbol.

³ Primer sequences used for qPCR are written in the 5' to 3' direction. Multiple primer sets were designed to span the genomic sequence from the 5'UTR to the 3'UTR.

**CHAPTER 4: JASMONATE PROMOTES TURNOVER OF PHOTOSYNTHETIC
COMPLEXES DURING THE GROWTH-TO-DEFENSE TRANSITION**

Leah Y.D. Johnson, Ian T. Major, Qiang Guo, David M. Kramer, Gregg A. Howe

Author contributions: QG performed the experiments for figure 4.1. ITM and DMK performed the DEPI analysis in figure 4.2. LYDJ performed the remaining experiments. LYDJ and GAH wrote the manuscript.

ABSTRACT

Many biotic stresses generate endogenous signals that decrease photosynthetic efficiency through the programmed disassembly of photosynthetic complexes. As a major regulator of growth-defense balance, the chloroplast lipid-derived stress signal jasmonate (JA) accelerates the turnover of photosynthetic proteins concomitant with growth inhibition and the transcriptional activation of metabolic pathways fueling defense. Previous studies of JA-induced senescence in *Arabidopsis* used excised leaves treated in the dark with non-physiological concentrations of exogenous JA. Here, we employed a JA hypersensitive mutant (*jazD*) to investigate the mechanism by which the JA pathway promotes leaf senescence in intact plants grown under physiological conditions. Genetic epistasis analysis showed that the transcription factor MYC2 plays a major role in triggering rapid, light-dependent leaf senescence in response to treatment with the JA receptor agonist coronatine. Decreased accumulation of photosynthetic proteins and lipids over a time course of coronatine treatment was accompanied by a loss in photosynthetic performance and a massive increase in the level of free amino acids. Concomitant changes in the abundance of TCA cycle intermediates suggested that amino acids derived from the breakdown of photosynthetic proteins are used as alternative respiratory substrates, indicative of shift in energy production from chloroplasts to mitochondria. Consistent with this notion, treatment of *jazD* plants with coronatine promoted the differentiation of chloroplasts to gerontoplasts but had negligible effects on the ultrastructure of mitochondria. Time-dependent analysis of global changes in gene expression provided insight into the molecular basis of these changes. Our results demonstrate how a retrograde response pathway controls chloroplast metabolism and photosynthesis during growth-to-defense transition and further highlight the critical role of JAZ repressors in preventing overactivation of JA responses. A better understanding of JA-mediated

senescence may inform strategies to increase photosynthetic efficiency in the face of a changing global environment.

INTRODUCTION

Leaves use photosynthesis to assimilate inorganic nutrients into complex macromolecules that fuel plant metabolism, growth, and development. A large portion of these assimilated products are located in the chloroplast in the form of highly abundant proteins (e.g., Ribulose-1,5-bisphosphate carboxylase/oxygenase; Rubisco), galactolipids of the thylakoid membrane, and metabolites such as chlorophyll that perform essential roles in photosynthesis. Metabolic investments in leaf construction and maintenance are rewarded by the remarkable ability of this biological solar panel to convert sunlight into energy-dense compounds needed for growth and development (Wright et al. 2004; Weraduwege et al. 2015). As leaves approach the end of their life span, they enter the senescence stage of development in which previously assimilated macromolecules are systematically degraded to simple metabolic intermediates (e.g., free amino acids) that are utilized by sink tissues and other non-senescent cells. The first visible sign of this developmental transition is the loss of chlorophyll from light harvesting complexes within the thylakoid membrane (Kuai et al. 2018). Leaf de-greening coincides with turnover of chloroplast proteins and membranes, as well as changes in thylakoid membrane structure (Himmelblau and Amasino 2001; Domínguez and Cejudo 2021). Following export from the chloroplast, the resulting catabolic products are mobilized to sink tissues and, in some cases, may be repurposed as alternative respiratory substrates (Yang and Ohlrogge 2009; Araújo et al. 2011). This nutrient recycling process depends on a shift from anabolic to catabolic metabolism within the cell and provides a strategy to reallocate assimilated nutrients prior to cell death and leaf abscission.

The onset of leaf senescence is triggered not only by age-dependent signals in healthy, mature leaves but can also be initiated in younger leaves subjected to environmental stress conditions. Among the environmental factors that promote leaf senescence are light deprivation

(i.e., extended dark) and conditions that lead to imbalances between the production and scavenging of reactive oxygen species (ROS) (Liebsch and Keech 2016; Domínguez and Cejudo 2021). Several stress-related hormones, including ethylene, abscisic acid (ABA), and the lipid-derived signal jasmonate (JA), also promote senescence-like symptoms in response to specific environmental cues (Lim et al. 2007). Senescence programs initiated by natural aging, stress cues, and light deprivation involve the complex interplay between hormonal and environmental signals that appear to converge on the expression of genes encoding chlorophyll catabolic enzymes (CCEs) in the pheophorbide a oxygenase (PAO)/phylobilin pathway (Kuai et al. 2018; Woo et al. 2019). For example, ethylene, ABA, and JA are known to govern the activity of transcription factors (TFs) that modulate senescence via direct binding to promoter elements within chlorophyll catabolic genes (CCGs) and other senescence-associated genes (SAGs) (Lim et al. 2007; Kuai et al. 2018).

Initial insight into the phenomenon of JA-induced senescence came from the bioassay-based identification of methyl-JA (MeJA) as a potent elicitor of chlorophyll loss in detached oat leaves (Ueda and Kato 1980). Subsequent work with barley leaf segments demonstrated that induction of chlorophyll loss by exogenous JA is tightly associated with degradation of rubisco, large-scale changes in nuclear gene expression, and *de novo* synthesis of several stress-related proteins (Parthier 1990; Creelman and Mullet 1997). Genetic studies performed with *Arabidopsis* have been instrumental for understanding the mechanism of JA-induced senescence. The ability of exogenous JA to promote senescence in *Arabidopsis* depends on the action of several positive regulators of transcription, including the JA co-receptor protein CORONATINE INSENSITIVE1 (COI1), members of the MYC family of JA-responsive transcription factors (TFs), and MYC2-associated TFs (He et al. 2002; Shan et al. 2011; Zhu et al. 2015; Song et al. 2017; Zhuo et al.

2020). In agreement with their function repressing MYC TFs, JAZ proteins play a crucial role negatively regulating JA-triggered senescence (Yu et al. 2016; Guo et al. 2018).

The physiological significance of leaf senescence promoted by JA remains unclear. JA levels increase in naturally senescing Arabidopsis leaves, possibly as a consequence of the release of fatty acid precursors of JA during chloroplast membrane degradation. This increased pool of endogenous JA, however, does not appear to be required for the initiation or progression of age-dependent senescence (He et al. 2002; Seltnann et al. 2010a; Seltnann et al. 2010b). Consistent with this view, mutants defective in JA biosynthesis or signaling do not exhibit an obvious delay in age-dependent leaf senescence (He et al. 2002; Schommer et al. 2008; Shan et al. 2011). It is also noteworthy that exogenous JA does not readily promote chlorophyll loss in Arabidopsis plants grown under physiological conditions; most studies employ senescence-permissive conditions in which excised leaves are treated with JA in the dark. The recent finding that a *jaz* decuple mutant (*jazD*) of Arabidopsis grown under physiological conditions undergoes rapid leaf degreening and necrosis in response to treatment with the JA receptor agonist coronatine highlights the role of JAZs in preventing senescence in JA-treated wild-type plants (Guo et al. 2018).

Here, we use *jazD* as an experimental model system to study the progression of coronatine-induced leaf senescence over a 72-hour time course. Using intact plants grown under physiological conditions, we found that this senescence program depends both on light and the master JA-responsive TF MYC2. RNA sequencing of time points within the first 24 hours showed that broad transcriptional changes precede leaf degreening. Gene ontology analysis revealed coronatine-induced downregulation of genes related to photosynthesis, growth, and chloroplast metabolism, whereas upregulated processes were related to defense responses and

general catabolism. Biochemical analyses showed that plastid lipids and proteins were preferentially degraded during the time course. Decreased accumulation of photosynthetic proteins and lipids was accompanied by a loss of photosynthesis and an increase in the level of free amino acids. Simultaneous changes in TCA cycle intermediates suggested a shift in energy production from chloroplasts to mitochondria. Coronatine application also promoted the unstacking of chloroplast thylakoid membranes but had negligible effects on the ultrastructure of mitochondria. These findings provide insight into how the JA signaling pathway controls chloroplast metabolism and photosynthesis during growth-to-defense transition.

MATERIALS AND METHODS

Plant materials and growth conditions

Arabidopsis thaliana accession Columbia-0 (Col-0) was used as the wild-type (WT) control for all experiments. The construction of the *jazD* decuple mutant, *jazD*, and the tredecuple mutant *jazD mycT* lacking ten *JAZ* genes and *MYC2*, *MYC3*, and *MYC4*, was previously described (Guo et al. 2018; Guo et al. 2022). The *jazD myc2*, *jazD myc3*, *jazD myc4*, *jazD myc2/3*, *jazD myc2/4*, and *jazD myc3/4* mutants were identified during the construction of the *jazD mycT* mutant.

Plants were grown in soil at 21°C under a long-day light regime of 16 h light (100 $\mu\text{mol m}^{-2}\text{s}^{-1}$) and 8 h dark. To acquire photosynthesis fluorescence measurements, plants were acclimated for 24 h in the dynamic environmental photosynthesis imager (DEPI) chamber and grown under the non-fluctuating/flat light conditions (100 $\mu\text{mol m}^{-2}\text{s}^{-1}$) described in (Cruz et al. 2016)

Chlorophyll measurements

Chlorophyll was extracted from 26-day-old whole rosettes in 1 mL acetone/2.5 mM sodium phosphate buffer (pH 7.8) (4:1 v/v) per 100-200 mg fresh weight (FW) tissue and centrifuged for 10 min at 4°C. 800 μL of the supernatant were transferred to a 1 cm cuvette and absorbances

were measured at A₆₄₆, A₆₆₃, and A₇₅₀. Chlorophyll concentrations were calculated with the following formulas and the resulting values were normalized to volume and tissue FW.

$$\text{Chl a} = (12.25 \times (\text{A}_{663} - \text{A}_{750})) - (2.55 \times (\text{A}_{646} - \text{A}_{750}))$$

$$\text{Chl b} = (20.31 \times (\text{A}_{646} - \text{A}_{750})) - (4.91 \times (\text{A}_{663} - \text{A}_{750}))$$

$$\text{Chl a} + \text{b} = (17.76 \times (\text{A}_{646} - \text{A}_{750})) + (7.34 \times (\text{A}_{663} - \text{A}_{750}))$$

Microscopy

Coronatine-treated (5 μM) and mock-treated 26-day-old *jazD* leaf sections were fixed in 2.5% glutaraldehyde and 2.0% paraformaldehyde in 0.1 M cacodylate buffer. Samples were stained with 1% osmium tetroxide then fixed in Spurr resin (10.0 g 3,4-Epoxy-cyclohexanemethyl 3,4-epoxy-cyclohexanecarboxylate; 6.0 g DER 736 Epoxy Resin; 26.0 g Nonenyl Succinic Anhydride; 0.2 g 2-Dimethylaminoethanol). Reagents described above were obtained from Electron Microscopy Sciences (EMS). TEM sections (Ultramicrotome Powertome XL RMC Products by Boeckeler) were placed on grids and stained with 4% uranyl acetate and lead citrate as described (Reynolds 1963). Light microscope sections (Ultramicrotome Powertome XL RMC Products by Boeckeler) were placed on glass slides and stained with epoxy tissue stain (EMS). TEM images were acquired using the JEOL 1400 Flash Transmission Electron Microscope and light microscope images were acquired using the Leica DM750.

Amino acid measurements

Amino acids were extracted with Milli-Q water containing ¹³C, ¹⁵N-labeled amino acid standards (Sigma-Aldrich). Extracts were incubated at 90°C for 5 min and cooled on ice. The extracts were clarified by centrifugation and filtered through low-binding hydrophilic polytetrafluoroethylene (PTFE) filters (0.2 μM ; Millipore). Filtered extracts were diluted with 20 mM perfluoroheptanoic acid (PFHA; Sigma-Aldrich) and analyzed using a Quattro Micro API LC-MS/MS (Waters)

equipped with an Acquity 623 UPLC HSS T3 1.8 μm column (2.1 \times 100 mm; 1.8 μm particle size; Waters) as described previously (Major et al. 2020). Amino acid concentrations were determined from an external standard curve and normalized to tissue fresh weight.

Hormone measurements

WT and *jazD* plants were grown for 26 days and then treated with a solution containing 5 μM coronatine. Samples were extracted at 4°C overnight (~16 h) using 0.45 ml ice-cold methanol:water (80:20 v/v) containing 0.1% formic acid, 0.01% butylated hydroxytoluene (BHT) and spiked with abscisic acid (ABA)-d6 (100 nM) as an internal standard. Filtered plant extracts were injected onto an Acquity UPLC BEH C18 column (2.1 x 100 mm; 1.7 μM particle size) and analyzed as described previously (Liu et al. 2016). Selected ion monitoring (SIM) was conducted in the negative electrospray channel for jasmonic acid (JA; m/z 209.1>59), JA-isoleucine (JA-Ile; m/z 322.2>130.1), 12-hydroxy-JA (12OH-JA; m/z 225.2>59), 12-hydroxy-JA-Ile (12OH-JA-Ile; m/z 338.2>130.1), 12-oxophytodienoic acid (OPDA; m/z 291.2>165.1) and the internal ABA-d6 standard (m/z 269.1>159.1). Hormone concentrations were determined from external standard curves and normalized to tissue fresh weight.

mRNA sequencing and analysis

Global gene expression profiling was performed on the BGISEQ platform at BGI Genomics. Rosette leaves of 26-day-old soil-grown *jazD* plants were treated with a solution containing 5 μM coronatine or mock control. The entire rosette was harvested at 0, 1, 3, 12, and 24 hours after treatment and immediately frozen in liquid N₂. At 0 hours, the rosette was harvested immediately after treatment with mock or coronatine solutions to minimize rapid JA responses. Four rosettes were pooled for each sample and homogenized using the TissueLyser II (Qiagen). Tissue was stored at -80C until further use. RNA was extracted using the NucleoSpin RNA Plant kit

(Machery Nagel). RNA quality was assessed using the Agilent 4200 TapeStation and RNA concentrations were measured using the Qubit fluorometer (Invitrogen) in the MSU RTSF Genomics Core facility. Three independent RNA samples (biological replicates) were used for each time point and treatment, with each replicate derived from pooling rosette leaves from four plants. Data preprocessing was performed by BGI Genomics to provide adaptor-trimmed, high-quality reads. Raw sequencing reads were mapped to TAIR10 gene models by RSEM (version 1.3.3) (Li and Dewey 2011). mRNA abundances for all Arabidopsis genes were expressed as transcripts per million (TPM). DESeq2 (version 3.12) was used to normalize expected counts from RSEM and to determine differential gene expression by comparing normalized counts in mock-treated samples to the coronatine-treated samples at each time point (Love et al. 2014). DAVID (version 2021) was used to perform gene ontology (GO) analysis of enriched functional categories (Sherman et al. 2022). Over- and underrepresented GO categories among differentially expressed genes were assessed by hypergeometric test with Benjamini & Hochberg's false discovery rate (FDR) correction at $P < 0.05$.

Lipid measurements

Polar lipids were extracted and monogalactosyldiacylglycerol (MGDG), phosphatidylglycerol (PG), and phosphatidylethanolamine (PE) were purified by thin layer chromatography as previously described (Wang and Benning 2011). MGDG, PG, PE, and total lipid extract for each sample were analyzed by gas chromatography with flame-ionization detection following as previously described (Wang and Benning 2011) to obtain peak areas for individual fatty acyl methylesters (16:0, 16:1 cis and trans, 16:2, 16:3, 18:0, 18:1, 18:2, and 18:3) of each lipid. Percent of total lipid was calculated by summing the total abundance of each of the fatty acyl

methylesters for each lipid. This value was then divided by the total fatty acyl methylester abundance of the total lipid extract for each sample.

Protein analysis

Following the time course of coronatine treatment, proteins were extracted from leaves of 26-day-old soil-grown plants in a buffer containing 80 mM Tris-HCl pH 6.8, 10% glycerol, 2% sodium dodecyl sulphate (SDS), and one tablet of Complete Mini ethylene diamine tetraacetic acid (EDTA)-free proteinase inhibitors (Roche) and 500 μ L 2-mercaptoethanol per 10 mL of buffer. Extracted proteins were separated by SDS–polyacrylamide gel electrophoresis (SDS-PAGE) (4-20% Mini-PROTEAN TGX Precast Protein Gel; BioRad) and stained with Coomassie Brilliant Blue R-250. Protein molecular weight standards were obtained from the All Blue Prestained Protein Standard (BioRad).

Measurement of TCA cycle intermediates

Rosette leaves of 26-d old WT and *jazD* were treated with a solution containing 5 μ M coronatine. Whole rosettes were harvested in the chamber to maintain the light conditions and frozen immediately in liquid N₂. Samples were extracted in 500 μ l of ice-cold CHCl₃/CH₃OH (3:7, v/v) and 2.5 μ g adonitol (Millipore Sigma) as the internal standard per 50 mg FW tissue. Samples were dried and then derivatized with a solution containing 20 mg/mL methoxyamine hydrochloride in dry pyridine and *N*-methyl-*N*-trimethylsilyltrifluoroacetamide (MSTFA) containing 1% trimethylsilyl chloride (TMSCl) (Millipore Sigma). 100 μ L of the derivatized samples were analyzed in splitless mode using an Agilent 5975 GC/single quadrupole mass spectrometer. Separation was achieved on an Agilent J&W VF-5ms (30 m x 0.25 mm x 0.25 mm) (Agilent, Santa Clara, CA) using the following temperature profile: 70°C for 2 min; 20°C min⁻¹ to 230°C. The mass spectrometer was operated using 70 eV electron ionization in full scan

mode with a m/z range from 50 to 600. Peak areas of extracted ion chromatograms for the indicated derivative of each compound were normalized to the adonitol standard and tissue fresh weight.

Accession numbers

Genes described here have the following Arabidopsis Genome Initiative (AGI) gene accession numbers: *JAZ1* (AT1G19180), *JAZ2* (AT1G74950), *JAZ3* (AT3G17860), *JAZ4* (AT1G48500), *JAZ5* (AT1G17380), *JAZ6* (AT1G72450), *JAZ7* (AT2G34600), *JAZ9* (AT1G70700), *JAZ10* (AT5G13220), *JAZ13* (AT3G22275), *MYC2* (AT1G32640), *MYC3* (AT5G46760), and *MYC4* (AT4G17880).

RESULTS

MYC2 is the predominant regulator of coronatine-induced senescence in *jazD*

Members of the MYC family of transcription factors (MYC2-5) have overlapping and redundant roles in a wide range of JA responses (Fernández-Calvo et al. 2011; Gao et al. 2016). To investigate the contribution of these TFs in coronatine-induced senescence in *jazD*, we genetically combined *jazD* with various combinations of *myc* mutations and then assessed the resulting mutant lines for their response to coronatine (Fig. 4.1). WT plants accumulated anthocyanin pigments at the site of coronatine application but showed no signs of chlorosis or necrosis. *jazD* leaves, by contrast, lost nearly all chlorophyll and exhibited necrosis within four days of treatment. The triple *myc2/3/4* mutation completely rescued the severe coronatine-induced senescence phenotype of *jazD* (Fig 4.1). The *myc2* single and *myc2/3* and *myc2/4* double mutations partially inhibited the senescence response of *jazD*. The single *myc3* and *myc4* mutations, as well as the *myc3/4* double mutation, had no effect on the coronatine-induced

senescence in *jazD* (Fig 4.1). These data indicate that MYC2 is the major positive regulator of senescence and that MYC3 acts additively with MYC2.

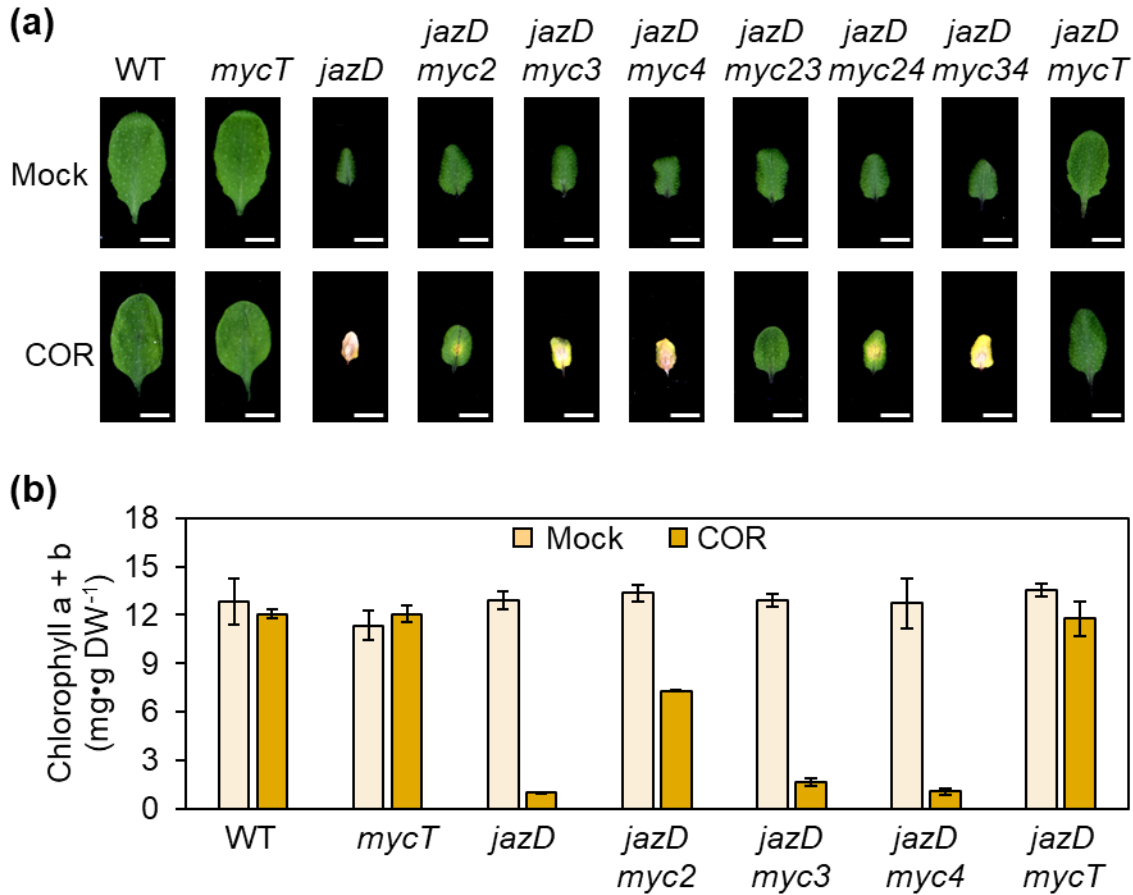


Figure 4.1 MYC2 is a major regulator of coronatine-induced de-greening in *jazD*.

(a) Chlorophyll loss in response to coronatine (COR) treatment. The 5th rosette leaf of 24-day-old plants grown under 16-h-light/8-h-dark photoperiod were spotted with 5 μ L of water (mock) or a solution containing 50 μ M COR. Leaves were excised and photographed four days after treatment. Scale bars, 0.5 cm. (b) Chlorophyll content (chlorophyll a + b) in COR-treated leaves. Soil-grown plants (25-day-old) were sprayed with either water (mock) or a solution containing 5 μ M COR. Leaves were harvested three days after treatment for chlorophyll extraction. Data show the mean \pm SD of three samples per genotype.

Coronatine treatment initiates rapid chlorophyll loss in *jazD* leaves.

Measurements of chlorophyll and photosystem II efficiency (Φ_{II}) were used to establish the timing of coronatine-induced senescence in *jazD* over a 96-h time course, which terminated

with complete leaf necrosis (Fig. 4.2a, c). Chlorophyll levels began to decline within 24 h of treatment and reached undetectable levels at the 96-h time point. The loss of chlorophyll in treated *jazD* leaves was accompanied by a steady decline in Φ_{II} , which was first observed 48 h after treatment (Fig. 4.2b, d). Importantly, coronatine treatment had little or no effect on chlorophyll levels or Φ_{II} in WT plants. These data are consistent with the hypothesis that coronatine treatment of *jazD* results in proteolytic removal of the remaining JAZ repressors (JAZ8/11/12), thereby initiating an unrestrained JA response leading to leaf chlorosis, necrosis, and death.

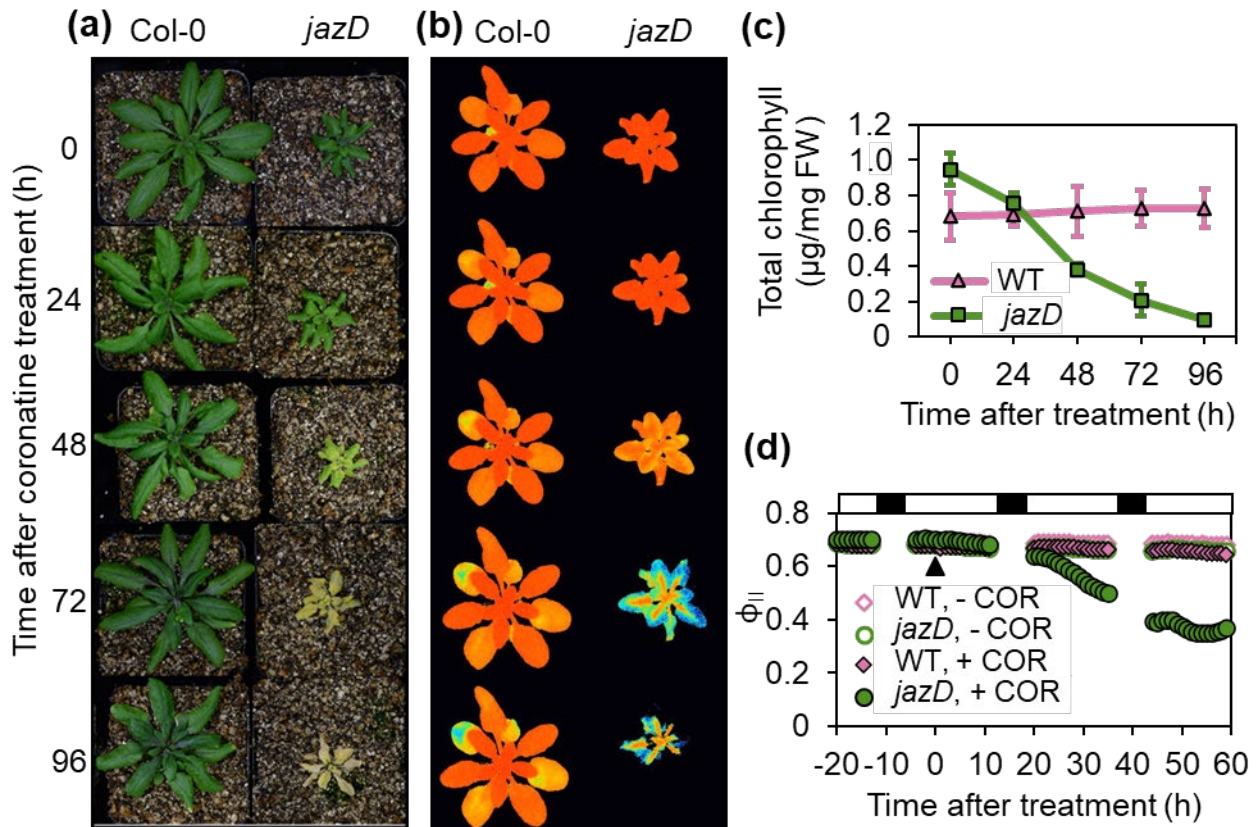


Figure 4.2 Time course of leaf de-greening in response to coronatine treatment.

(a) WT and *jazD* plants were sprayed with a solution containing 5 μ M coronatine. Plants were photographed at the indicated time points after treatment. (b) Representative false-colored images depicting the quantum efficiency of photosystem II (Φ_{II}) as measured by Dynamic Environmental Photosynthetic Imaging (DEPI). The time course of coronatine treatment was the

Figure 4.2 (cont'd)

same as shown in panel a. (c) Quantification of total chlorophyll content (Chl a + b) in whole rosettes of WT and *jazD* plants after treatment with coronatine (n = 3). (d) Measurements of ϕ_{II} in WT and *jazD* plants treated with coronatine (COR) or mock control. ϕ_{II} values were determined from DEPI images similar to those shown in panel b. Plants were acclimated to the DEPI growth chamber for one day (negative time points) prior to treatment with coronatine at the 0 h time point (black triangle). Dark and white bars indicate light and dark cycles.

Coronatine treatment reprograms gene expression in *jazD*

We used RNA sequencing (RNA-seq) to identify time-dependent changes in global patterns of gene expression in coronatine- versus mock-treated *jazD* plants. Samples were collected for RNA-seq analysis at 0, 1, 3, 12, and 24 hours after treatment. Each time point included a mock-treated control, with three biological replicates per time point and treatment group (Fig 4.3a). Differentially expressed genes (DEGs) were identified using the following filtering criteria. For each time point after treatment (1, 3, 12, 24 hr), transcripts whose abundance was ≥ 2 -fold (\log_2) higher in the coronatine-treated sample (relative to the time-matched mock control) were flagged as potential upregulated genes. Similarly, transcripts whose abundance was ≤ 2 -fold (\log_2) lower in the coronatine-treated sample (relative to the matched mock control) were identified as putative downregulated genes. Further filtering of these DEGs for significant change in expression (p-value < 0.05) in coronatine- versus mock-treated samples generated a final list of 7,676 genes that are differentially expressed at one or more time points.

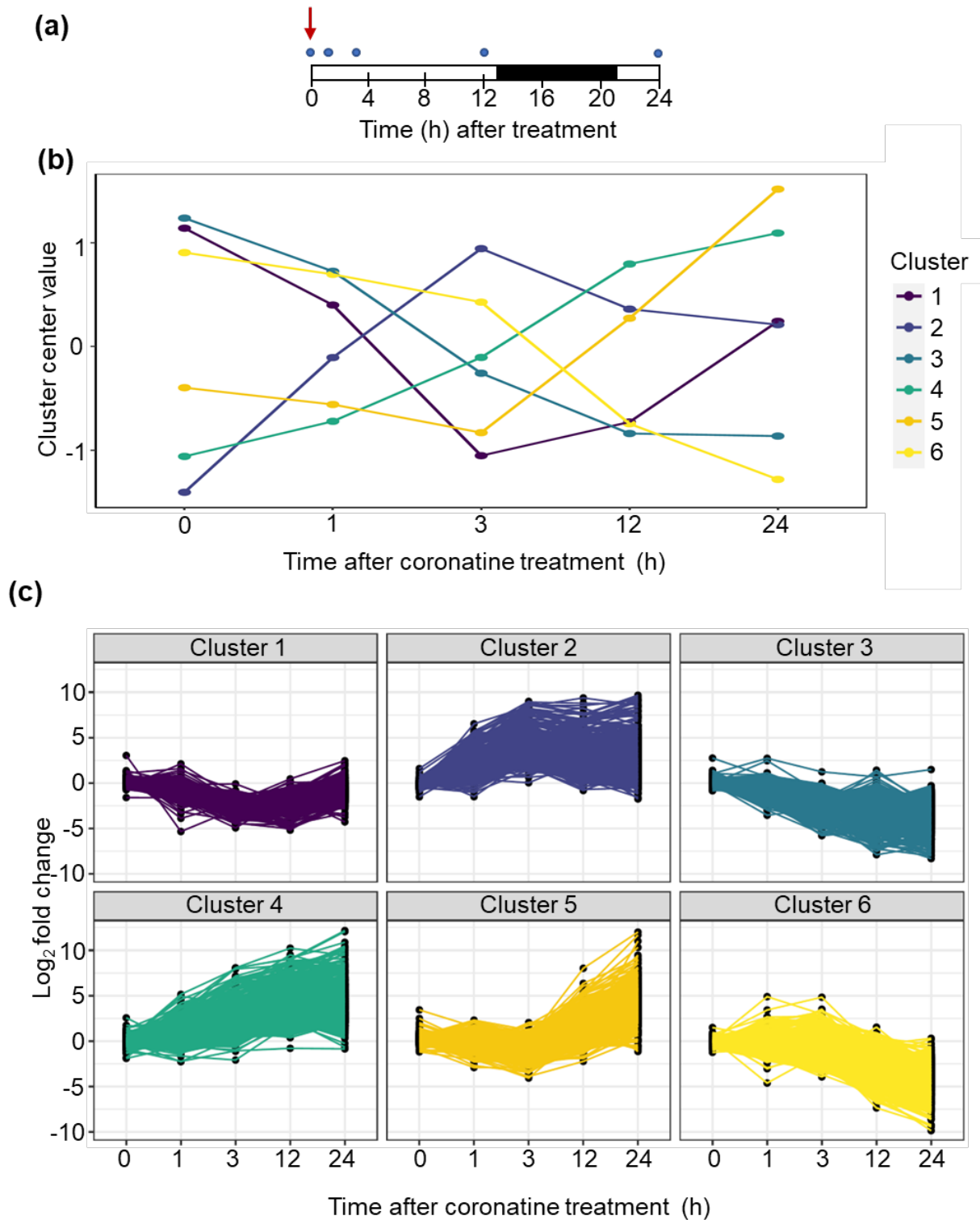


Figure 4.3 Time course of coronatine-induced changes in gene expression in *jazD*.







(a) Schematic of RNA sequencing timeline. Whole rosettes were harvested at 0, 1, 3, 12, and 24 hours after coronatine treatment, indicated by the blue circles. The red arrow indicates when the

Figure 4.3 (cont'd)

mock or coronatine solutions were applied. The white and black bars denote the light and dark cycle, respectively. (b) 26-day-old *jazD* plants were sprayed with a solution containing 5 μ M COR or a mock control (water). Whole rosettes were harvested at the indicated time points for RNA extraction using triplicate samples per time point for each treatment. (b-c) RNA sequencing data was analyzed by *k*-means clustering to identify differentially expressed genes (DEGs) at each time point. (c) *k*-means centroids plotted over time. (c) Expression profiles of DEGs within each cluster.

K-means clustering of the 7,676 DEGs identified six groups of transcripts having distinct temporal expression patterns in response to coronatine treatment (Fig 4.3b-c). Functional annotation of each cluster using DAVID identified several non-redundant gene ontology (GO) terms that are significantly enriched within each cluster (Table 4.1, Suppl File 1, Suppl File 2). Genes in cluster 1 were sharply downregulated within 3 h of coronatine treatment followed by a strong increase in expression at later time points (Fig. 4.3). Significant GO terms in this cluster included response to “salicylic acid” and “regulation of defense response” (Table 4.1). This finding is consistent with previous studies describing antagonism between the JA and salicylic acid (SA) pathways during responses to infection with biotrophic pathogens (Kloek et al. 2001). The expression profile of cluster 1 is exemplified by the *WRKY53* gene, which was strongly repressed at 1, 3, and 12 h time points. The proposed role of *WRKY53* as a positive regulator of SA-mediated senescence may provide clues as to how specific stress signals such as SA and JA control senescence pathways through changes in transcription (Miao et al. 2004; Miao and Zentgraf 2007).

Table 4.1 Gene ontologies of differentially expressed genes in *jazD* after coronatine treatment.

Cluster ¹	Pattern ²	Significant Gene Ontology (GO) terms ³	Number of genes ⁴
1		Response to salicylic acid; defense response to fungus; regulation of defense responses; integral component of plasma membrane	603
2		Ethylene-activated signaling pathway; regulation of jasmonic acid-mediated signaling pathway; ER body; jasmonic acid biosynthetic process	562
3		Chloroplast RNA modification; cell membrane; auxin-activated signaling pathway; cell division	2,169
4		Glucosinolate catabolic process; response to jasmonic acid; response to water deprivation; response to abscisic acid; response to oxidative stress; aging; leaf senescence	831
5		Integral component of membrane; UDP-glucosyltransferase activity; peroxisome; proteasome complex	980
6		Chloroplast; ribosome; thylakoid; cell division; cell cycle; photosystem II; photosystem I; photosynthesis; light harvesting; plastoglobuli; chlorophyll biosynthetic process; reductive pentose-phosphate cycle	2,531

¹Cluster indicates the cluster identifier for each gene after *k*-means clustering

²General time-dependent profile of each cluster derived from figure 4.3

³Significant GO terms were filtered by a Benjamini-Hochberg adjusted p-value of <0.05

⁴Number of genes in each cluster derived from the filtered list of 7,676 differentially expressed genes. Genes are unique to each cluster.

Genes in cluster 2 were characterized by a rapid increase in transcript abundance between 0 and 3 h post treatment followed by a downward taper at the later time points (Fig 4.3b-c). The most significantly enriched GO terms within this cluster were associated with the JA and ethylene signaling pathways (Table 4.1). This finding is consistent with the fact that the JA and ethylene signaling pathways are generally synergistic and are both de-repressed in response to JAZ degradation (Guo et al. 2018; Zhu et al. 2011). It is also well established that JA and ethylene are positive regulators of senescence (He et al. 2002; Qiu et al. 2015). Most canonical “early” JA-responsive genes were included in cluster 2, including those encoding JA biosynthetic enzymes such as LIPOXYGENASE 2 (LOX2), ALLENE OXIDE SYNTHASE (AOS), ALLENE OXIDE CYCLASE (AOC1), 12-OXO-PHYTODIENOIC ACID REDUCTASE 3 (OPR3), and OPCL1, which are rapidly and coordinately upregulated by wounding and insect herbivory (Chung et al. 2008). The inclusion in cluster 2 of *JA OXIDASE (JOX)*, *JA METHYL TRANSFERASE (JMT)*, and *CYP94B1* genes, which encode enzymes involved in the catabolism of JA and JA-Ile, further suggest that turnover of bioactive JAs is a key part of the *jazD* response to coronatine.

Genes in cluster 3 showed a steadily decreasing level of expression throughout the time course. Among the most significant GO categories in this group was “chloroplast RNA modification”, “cell division”, and “auxin signaling” (Fig 4.3b-c, Table 4.1). The central role of auxin in promoting cell division is consistent with the negative effect of JA signaling on growth and cell division (Noir et al. 2013). The prolonged downregulation of many *PENTATRICOPEPTIDE REPEAT (PPR)* and *TETRATRICOPEPTIDE REPEAT (TPR)* genes further suggests a sustained decrease in the stability of chloroplast mRNAs over time. The PPR proteins have been implicated in chloroplast biogenesis and development, and mutants lacking

these proteins display reduced levels of chloroplast mRNAs (Chi et al. 2008; Wang et al. 2021). The temporal expression profile of genes in cluster 6 was similar to genes in cluster 3, with the exception that the maximum rate of downregulation was delayed in the former group (Fig 4.3b-c). Like cluster 3, enriched GO terms in cluster 6 were also related to growth and cell division. The most striking functional feature of cluster 6 was the preponderance of GO terms related to the chloroplast and photosynthesis, including chlorophyll biosynthesis and carbon assimilation. The combination of genes comprising clusters 3 and 6 indicate that growth-related processes are strongly downregulated throughout the time course (Fig 4.3b-c, Table 4.1).

Transcripts in cluster 4 steadily accumulated during the entire time course (Fig 4.3). Functional annotation of these genes revealed GO terms related to leaf aging and senescence, catabolic processes, and response to various stress signals. The enrichment of ABA and “late” JA-responsive genes such as *VEGETATIVE STORAGE PROTEIN 1* and *2* may reflect similarities between the JA- and ABA-induced senescence pathways. The expression pattern of genes in cluster 5 genes was relatively stable (or slightly decreasing) in the early time points, followed by a sharp increase in transcript accumulation at the later time points (Fig 4.3b-c). Functional analysis of this cluster indicated an enrichment of genes involved in detoxification, catabolism, and proteolysis (Table 4.1).

In summary, DEGs exhibiting rapid induction or repression in response to coronatine were related to defense and growth, respectively. Conversely, genes whose induction or repression occurred at later time points were generally related to catabolic processes in the chloroplast and photosynthesis, respectively. These findings are consistent with the observed timing of coronatine-induced loss of chlorophyll and photosynthetic performance.

Coronatine-induced senescence is dependent on the MYC transcription factor signaling network

Our data indicate that MYC2 is a primary positive regulator of coronatine-induced senescence in *jazD*, and that MYC3 acts additively with MYC2 during this response (Fig. 4.1). A recent multi-omics study in *Arabidopsis* provided evidence that MYCs control a much larger TF network in which MYC2 and MYC3 directly bind the promoters of 122 TFs with annotated functions in hormone pathways, while over 500 TFs are differentially regulated after JA treatment (Zander et al. 2020). Consistent with this finding, genes encoding many members of the bHLH and MYB TF families were differentially regulated in coronatine-treated *jazD* plants. Members of senescence-associated transcription factor families such as ERF, NAC, and WRKY were also strongly upregulated during this response (Table 4.2, Suppl File 1). Additionally, examination of the 122 MYC-bound transcription factor promoters of TFs with annotated roles in hormone signaling showed that TFs associated with growth hormones such as brassinosteroids, gibberellic acid, and auxin, are generally downregulated, while many of the stress-responsive hormones such as ethylene, ABA, and JA are upregulated (Table 4.2, Suppl File 1). These data suggest that the MYC transcription factors are activating stress-related downstream regulators to promote the senescence response while also downregulating growth responses.

Table 4.2 Numbers of differentially expressed transcription factors in *jazD* after coronatine treatment.

Time point ¹	Upregulated TFs ²	Downregulated TFs ³
1	236	349
3	385	521
12	552	443
24	557	505

¹Time in hours (h) after coronatine treatment

²Significantly upregulated transcription factors determined using a Benjamini-Hochberg adjusted p-value less than 0.05 and a log₂ fold change greater than 0. A total of 1,717 TFs were examined from the Plant TF database.

³Significantly downregulated transcription factors determined using a Benjamini-Hochberg adjusted p-value less than 0.05 and a log₂ fold change less than 0. A total of 1,717 TFs were examined from the Plant TF database.

Chloroplast lipids in *jazD* are preferentially degraded in response to coronatine treatment

Lipid degradation is a hallmark of leaf senescence and typically follows the initiation of chlorophyll catabolism (Tamary et al. 2019). To determine whether coronatine-induced chlorophyll loss in *jazD* leaves is also associated with lipid turnover, various lipid species in WT and *jazD* plants were purified and quantified over a three-day time course of coronatine treatment. Among the lipid species quantified in this experiment were the plastid-localized lipids monogalactosyldiacylglycerol (MGDG) and phosphatidylglycerol (PG), as well as the extra-plastidic lipid phosphatidylethanolamine (PE). WT plants showed no change in the relative abundance of these three lipids following treatment with coronatine (Fig 4.4). The relative abundances of the lipids at 0 h were not significantly different between WT and *jazD* plants. In *jazD*, coronatine application promoted a time-dependent decrease in the level of MGDG relative to the total lipid pool. At 72 h post treatment, the amount of MGDG in *jazD* leaves was 40% of

that at the 0-h time point (Fig 4.4a). Coronatine treatment of *jazD* also led to decreased abundance of PG at the 72-h time point (Fig 4.4b). By contrast to PG and MGDG, coronatine did not have a significant effect on the level of PE in *jazD* leaves (Fig 4.4c). These data suggest that lipid remodeling resulting from overactivation of JA signaling is specific to the degradation of chloroplast lipids.

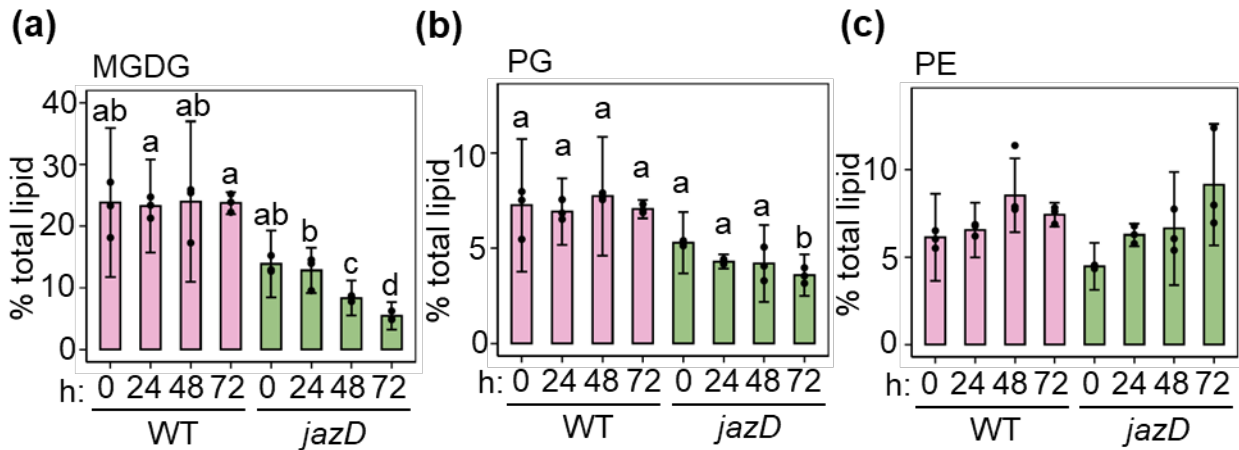


Figure 4.4 Coronatine treatment decreases the accumulation of plastid-localized lipids in *jazD*.

Time course of polar lipid accumulation in response to coronatine treatment of wild-type (WT) and *jazD* plants. Plants were treated with a solution containing 5 μ M coronatine and leaves were harvested for analysis of MGDG (a, monogalactosyldiacylglycerol), PG (b, phosphatidylglycerol), and PE (c, phosphatidylethanolamine) at the indicated time points (hours, h) after treatment. Letters represent different statistical groupings from two-way ANOVA with Tukey's HSD post-hoc test for each lipid while no letters indicate no statistical difference ($n = 3$).

Coronatine-induced senescence in *jazD* is associated with accumulation of 12-hydroxy-jasmonates

Fatty acid constituents of chloroplastic galactolipids serve as precursors for the biosynthesis of jasmonic acid (JA) and the bioactive form of the hormone, jasmonoyl-L-isoleucine (JA-Ile). Disruption of chloroplast lipid integrity by environmental stress cues (e.g., wounding) or developmental programs (e.g., age-dependent senescence) can release fatty acid precursors for subsequent conversion to JA (Wang et al. 2018; Ono et al. 2019). To determine

whether coronatine-induced senescence and lipid degradation in *jazD* are associated with changes in JA content, the levels of several jasmonate species in WT and *jazD* leaves were quantified by liquid chromatography-mass spectrometry at various times after coronatine treatment. The use of internal standards allowed quantification of the absolute abundance 12-oxophytodienoic acid (OPDA), jasmonic acid (JA), jasmonoyl-L-isoleucine (JA-Ile), 12-hydroxy-JA (12OH-JA), and 12-hydroxy-JA-Ile (12OH-JA-Ile). The abundance of all five jasmonate species in WT plants remained unchanged throughout the 72 h time course (Fig 4.5). Prior to coronatine treatment, the level of jasmonates in *jazD* plants was consistently higher than that in the WT, with the exception of OPDA. Treatment of *jazD* with coronatine resulted in a large increase in the amount of 12OH-JA and 12OH-JA-Ile at the 72-hr time point (Fig 4.5). These data suggest that the breakdown of chloroplast lipids generates precursors for the synthesis of JA and JA-Ile, which are subsequently converted to their corresponding 12-hydroxylated forms. Consistent with this notion, genes encoding JA biosynthetic enzymes and the relevant 12-hydroxylases (e.g., *JOX* and *CYP94B1*) were strongly upregulated in response to treatment of *jazD* with coronatine (Table A4.1).

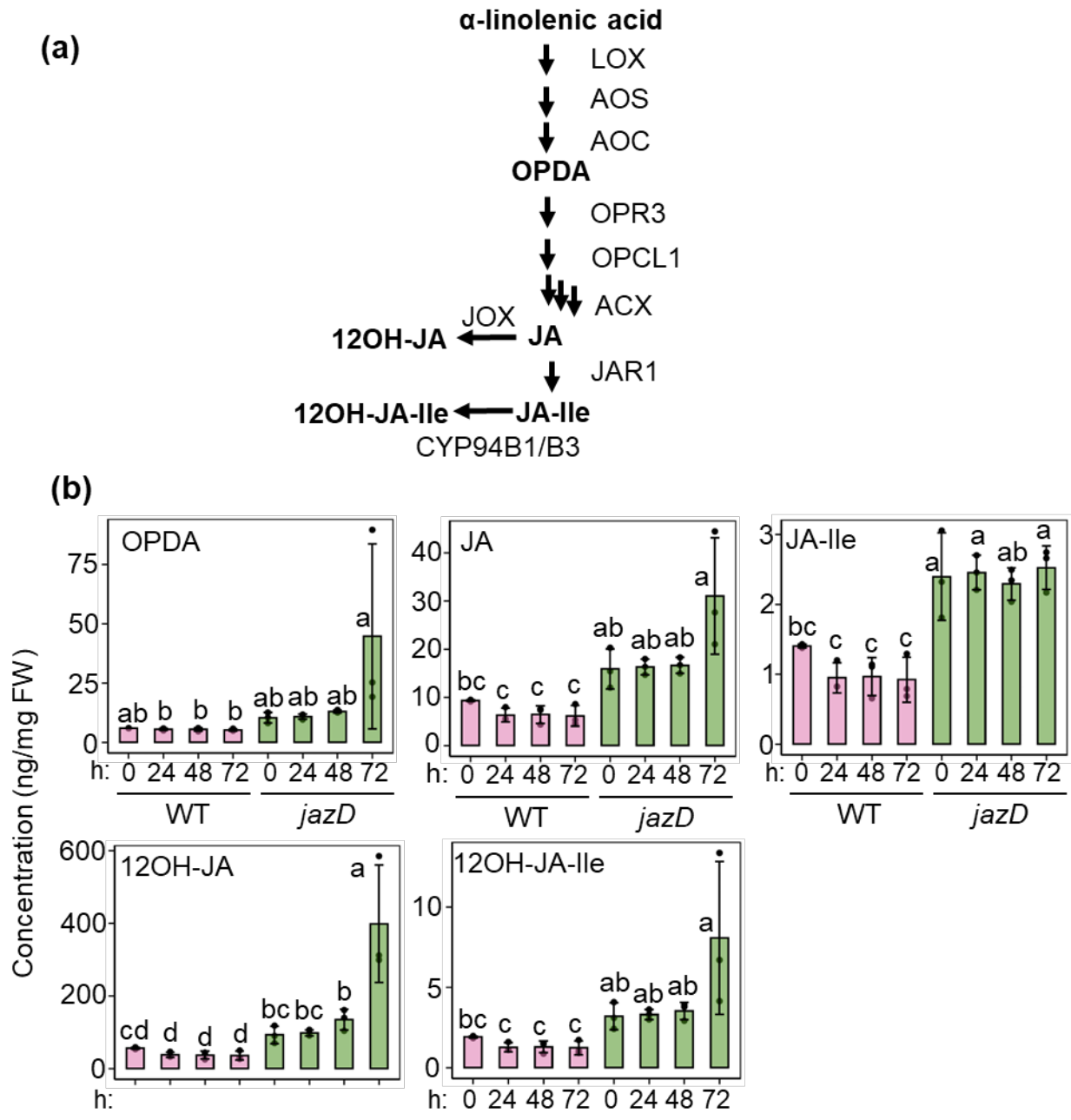


Figure 4.5 Coronatine promotes jasmonate inactivation in *jazD*.

(a) Schematic of JA biosynthesis. α -linolenic acid is converted to OPDA by LIPOXYGENASE (LOX), ALLENE OXIDE SYNTHASE (AOS), and ALLENE OXIDE CYCLASE (AOC). OPDA is converted to JA by OXOPHYTODIENOATE-REDUCTASE 3 (OPR3), OPC-8:0 COA LIGASE 1 (OPCL1), and ACYL-COA OXIDASES (ACXs), which can then be conjugated to isoleucine (Ile) to form JA-Ile by JA RESISTANT 1 (JAR1) or oxidized by JA OXIDASEs (JOXs) to form 12OH-JA. JA-Ile can be oxidized by the CYP94 cytochrome P450s (CYP94B1/B3) to form 12OH-JA-Ile. (b) Time course of coronatine-induced changes in the level of various jasmonate derivatives in wild-type (WT) and *jazD* plants. Plants were treated

Figure 4.5 (cont'd)

with a solution containing 5 μ M coronatine and leaves were harvested for quantification of jasmonates by LC-MS (n = 3). Different letters represent significant difference at $P < 0.05$ with Tukey's honest significant difference (HSD) test. OPDA, 12-oxophytodienoic acid; JA, jasmonic acid; JA-Ile, JA-isoleucine; 12OH-JA, 12-hydroxy-JA; 12OH-JA-Ile, 12-hydroxy-JA-Ile.

Degradation of chloroplast proteins during coronatine-induced senescence

The proteolytic turnover of chloroplast proteins is a conserved feature of plant senescence programs (Lim et al. 2007). To determine whether chloroplast-associated proteins are degraded in response to coronatine treatment, protein extracts from coronatine-treated WT and *jazD* plants were analyzed by SDS-PAGE. WT leaves showed no obvious changes in bulk protein profile over a 72-h time course (Fig 4.6). In contrast, samples isolated from *jazD* leaves showed a marked loss of several highly abundant proteins at the 48 and 72-h time points. This was most evident for protein bands corresponding to the large (55 kDa) and small (14 kDa) subunits of Rubisco, as well as the light-harvesting complex II subunits (LHCII; 24-26 kDa) (Fig 4.6). As reported previously (Guo et al. 2022), this experiment showed that *jazD* leaves over-accumulate a 65 kDa isoform of β -glucosidase (BGLU18), which is a major component of endoplasmic reticulum (ER) bodies. The abundance of BGLU18 in *jazD* appeared to be unchanged throughout the time course of coronatine treatment (Fig. 4.6). This finding suggests that coronatine-induced proteolysis in *jazD* is selective for chloroplast proteins.

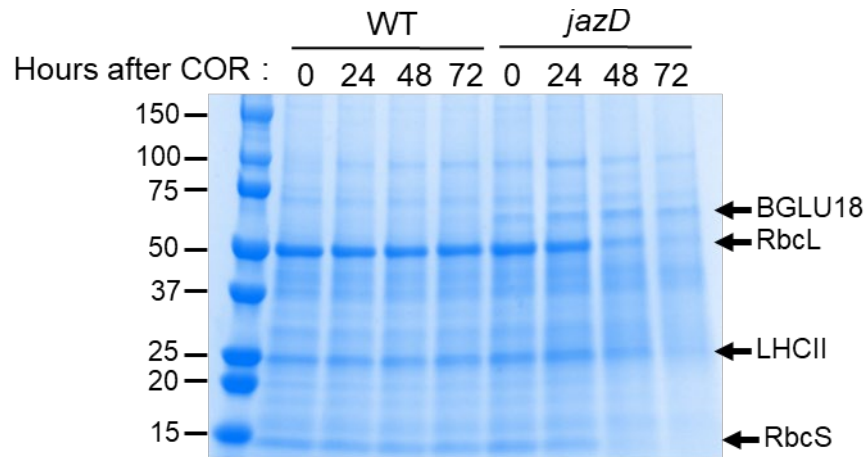


Figure 4.6 Coronatine treatment decreases the accumulation of photosynthetic proteins in *jazD*.

Time course of protein accumulation in response to coronatine treatment of wild-type (WT) and *jazD* plants. Plants were treated with a solution containing 5 μ M coronatine and leaves were harvested for protein extraction. Photograph shows a Coomassie blue-stained sodium dodecyl sulphate–polyacrylamide gel electrophoresis (SDS-PAGE) gel of bulk leaf protein. Arrows denote protein bands corresponding to β -GLUCOSIDASE 18 (BGLU18), the large subunit of Rubisco (RbcL), LIGHT HARVESTING COMPLEX II (LHCII), and the small subunit of Rubisco (RbcS). Protein standards and their corresponding mass (kDa) are shown on the left. COR, coronatine

Coronatine treatment promotes high level accumulation of most amino acids in *jazD* leaves

To determine whether the reduction in bulk chloroplast protein levels are associated with changes in the accumulation of amino acids, we used liquid chromatography-mass spectrometry to quantify the level of proteinaceous amino acids in response coronatine treatment. Consistent with the lack of senescence symptoms, the level of free amino acids in WT plants was not affected by coronatine treatment (Fig A4.1). The level of most amino acids, including Ala, Arg, Asn, Cys, Gln, His, Ile, Leu, Lys, Met, Phe, Thr, Trp, Tyr, and Val, in *jazD* leaves increased steadily during the course (Fig 4.7, Fig A4.1). The increased accumulation of these amino acids was most evident at the 48- and 72-h time points, which correlated with the time of maximum loss of abundant chloroplast proteins (Fig. 4.6). Glu and Asp levels in *jazD* decreased over time, whereas the level of Gly, Pro, and Ser remained relatively constant (Fig 4.7, Fig A4.1). These

data indicate that the increased level of most amino acids in coronatine-treated *jazD* likely results from proteolytic degradation of bulk chloroplast proteins. The depletion of Glu and Asp, however, suggests the occurrence of metabolic pathways or transport processes that recycle these compounds during senescence. Glu, for example, can enter the TCA cycle through the action of glutamate dehydrogenase (GDH) or the GABA shunt leading to the formation of succinate (Michaeli and Fromm 2015; Miyashita and Good 2008).

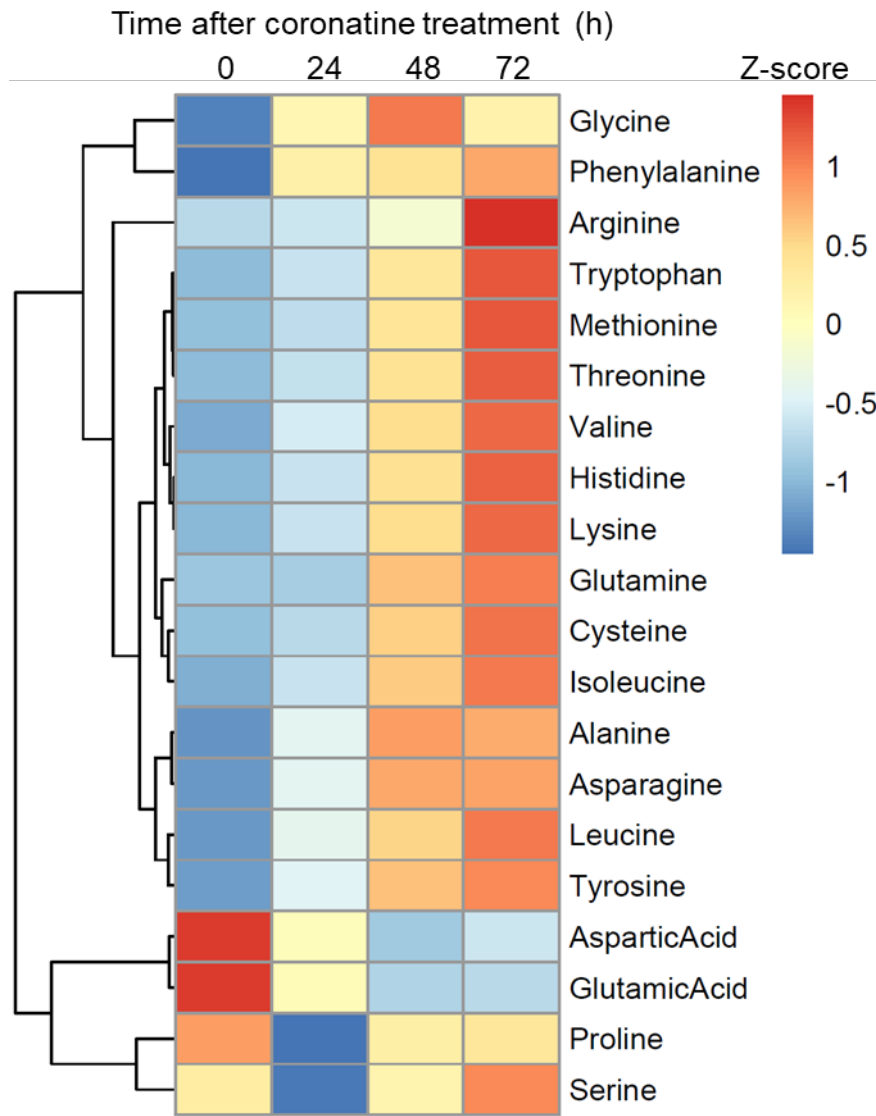


Figure 4.7 Coronatine treatment alters the free amino acid levels in *jazD*.

Figure 4.7 (cont'd)

Time course of coronatine-induced amino acid changes in *jazD* plants. 26-day-old *jazD* plants were sprayed with a solution containing 5 μM COR. Whole rosettes were harvested at the indicated time points for quantification of amino acids ($n = 3$). Data are displayed as a heatmap of z-score-scaled free amino acid concentrations normalized to leaf fresh weight.

TCA cycle intermediates fumarate and succinate increase during leaf senescence of *jazD*

Analysis of RNA-seq data indicated that genes encoding enzymes in the tricarboxylic acid cycle (TCA) are generally upregulated by 24h (Table A4.2). To test whether these changes in transcript abundance are associated with differences in the pool size of TCA cycle intermediates, gas chromatography-mass spectrometry was used to measure the relative abundance of pyruvate, citrate, α -ketoglutarate, succinate, fumarate, and malate in WT and *jazD* plants. No significant differences in metabolite levels were detected in coronatine-treated WT leaves (Fig. 4.8). Coronatine treatment of *jazD*, however, led to an increase in the level of fumarate and succinate, with no significant changes in the pool size of pyruvate, citrate, α -ketoglutarate, and malate (Fig 4.8). These results suggest that amino acids generated from the breakdown of chloroplast proteins may be used as alternative respiratory substrates during senescence, indicative of shift in energy production from chloroplasts to mitochondria.

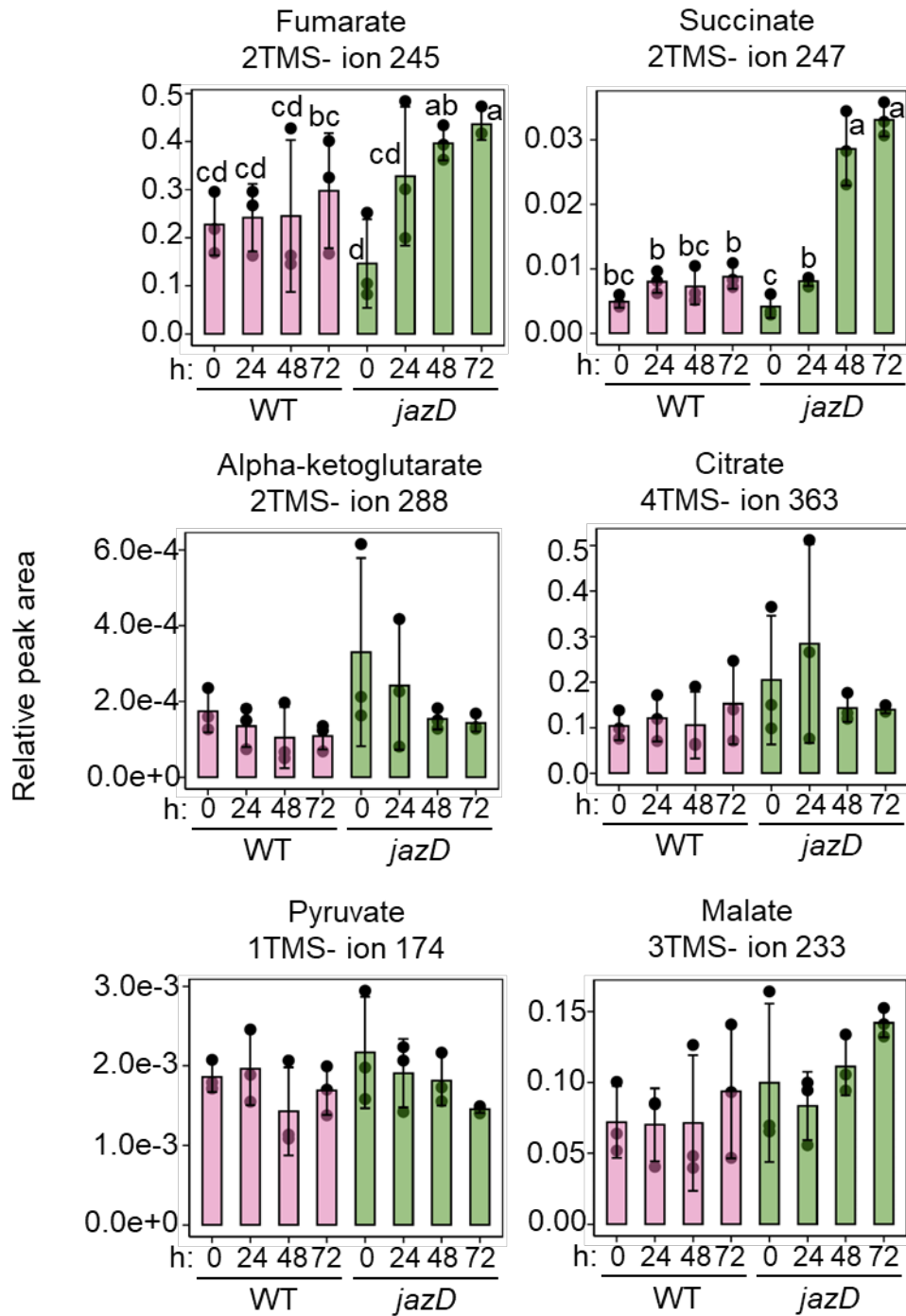


Figure 4.8 Fumarate and succinate levels increase in the Arabidopsis *jaz* decuple mutant, *jazD*.

26-day old WT and *jazD* plants were treated with a solution of 5 μ M coronatine and leaves were harvested for quantification of TCA cycle intermediates by GC-MS. Peak area is normalized to the adonitol internal standard and the fresh weight of the sample. Different letters represent significant difference at $P < 0.05$ with Tukey's honest significant difference (HSD) test and no

Figure 4.8 (cont'd)

letters indicate no significant differences. #TMS, number of trimethylsilyl derivatized groups; ion #, mass-to-charge ratio used for extracted ion chromatogram; h, time point in hours.

Senescence in *jazD* is associated with changes in the ultrastructure of chloroplasts but not mitochondria

In addition to protein and lipid degradation, major changes in chloroplast development during age-dependent senescence include the loss (i.e., unstacking) of thylakoid membranes and increased accumulation of plastoglobuli (Thomas and Stoddart 1980; Domínguez and Cejudo 2021). The term gerontoplast is often used to define the unique morphological features of this type of differentiated chloroplast in senescing plant tissues (Domínguez and Cejudo 2021). We used light and transmission electron microscopy to visualize structural changes in chloroplast morphology in *jazD* leaves treated with coronatine. Light microscopy showed that cell morphology was mildly altered at 48 hours in coronatine-treated *jazD* compared to mock-treated *jazD*. By 72 h, the cell morphology of coronatine-treated *jazD* was severely altered compared to mock-treated *jazD* (Fig 4.9a). Transmission electron microscopy showed unstacking of thylakoid membranes in *jazD* chloroplasts between the 48- and 72-h time points. In parallel with these changes in thylakoid membrane structure, the size of plastoglobuli also increased (Fig 4.9b). The findings show that overactivation of JA signaling in coronatine-treatment *jazD* plants promotes a developmental transition from chloroplasts to gerontoplasts. Consistent with the hypothesis that JA-mediated leaf senescence selectively promotes the breakdown of chloroplasts, transmission electron microscopy suggested that coronatine treatment has little or no effect on the ultrastructure of mitochondria in *jazD* (Fig 4.9b).

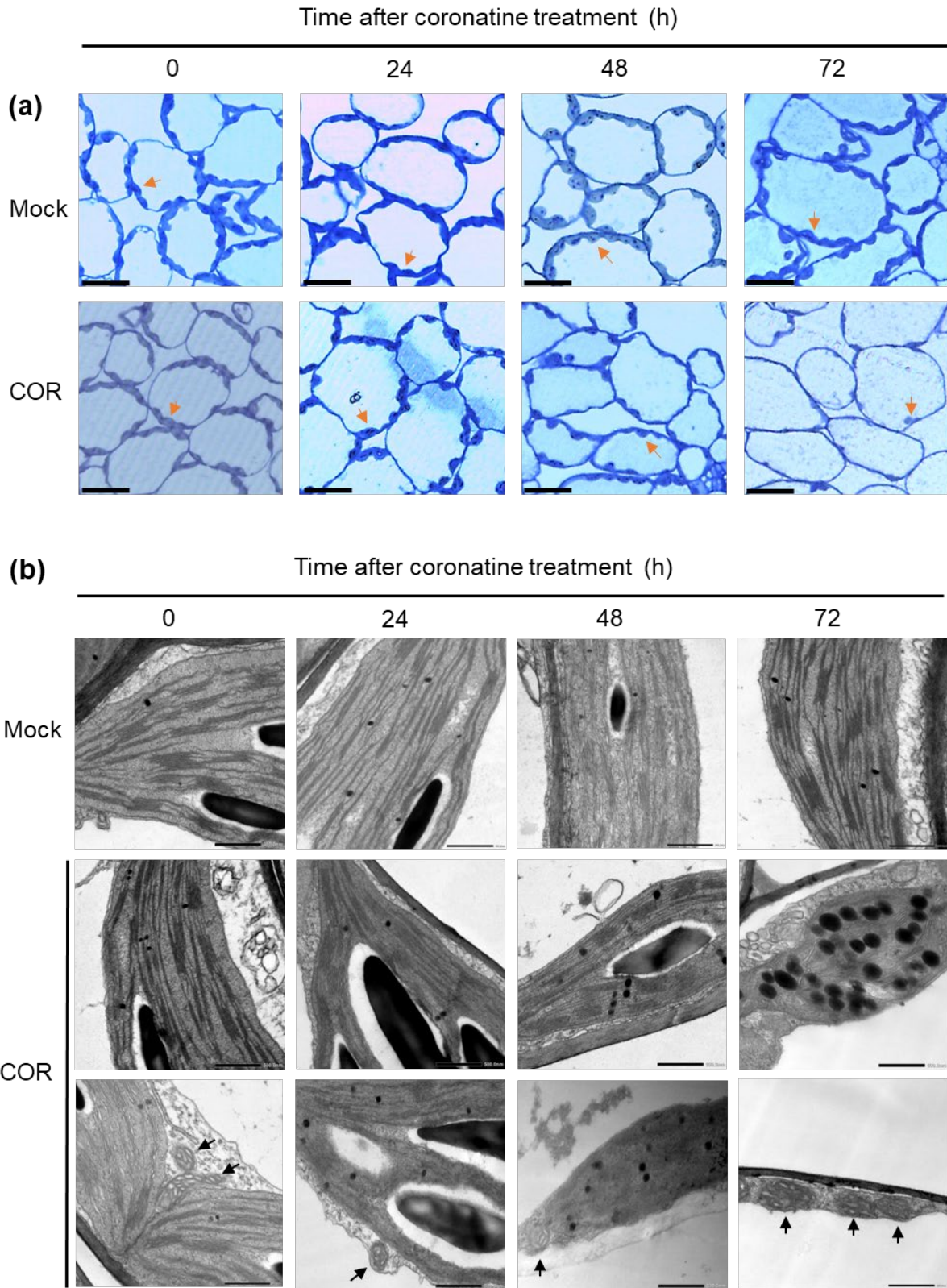


Figure 4.9 Coronatine treatment alters chloroplast but not mitochondrion morphology in *jazD*.

Figure 4.9 (cont'd)

Time course of chloroplast and mitochondrion changes after coronatine treatment. 26-day-old *jazD* plants were treated with a solution containing 5 μ M coronatine and leaves were harvested for imaging. (a) Representative leaf cross-sections of *jazD*. Orange arrowheads indicate chloroplasts. Magnification, 400x; scale bar, 0.02 mm. (b) Transmission electron microscopy sections of representative chloroplasts and mitochondria from *jazD* plants treated with coronatine. Black arrowheads indicate mitochondria. Magnification, 15,000x; scale bar, 500 nm.

DISCUSSION**MYC transcription factor network suggests a stress-responsive cascade leading to senescence**

Coronatine treatment of *jazD* plants resulted in a rapid upregulation of stress-related transcription factors, while many growth regulators were downregulated. There were several notable patterns within MYC-bound transcription factor genes (Zander et al. 2020), such as the strong downregulation of *ORA59*, a transcription factor characterized within the JA/ET branch of necrotrophic pathogen responses, as well as a strong upregulation of senescence-related transcription factors such as *NAC6* and *ORE1*. The downregulation of *ORA59* suggests that the MYC branch of JA signaling is predominantly activated over the JA/ET branch during coronatine-induced senescence, and that the MYC branch of signaling exerts major control over the senescence pathway. The rapid and strong expression of these transcription factors further suggests that a threshold is overcome in *jazD* which may not be activated in WT. The absence of senescence symptoms in coronatine-treated WT plants highlights the importance of JAZ proteins in attenuating JA signaling.

Processes related to chloroplast transcription were strongly downregulated throughout the RNA-sequencing time course. The early downregulation of these genes suggests that jasmonate rapidly modulates the metabolic status of the chloroplast, including the RNA-modifying and stabilizing pentatricopeptide family genes, photosynthesis related genes, and chlorophyll biosynthesis genes. Treatment of WT plants with coronatine reduces the expression of

photosynthetic genes but does not significantly affect photosynthetic performance (Attaran et al. 2014). The increased levels of JA signaling in *jazD* may create a primed state for the activation and execution of these senescence-related transcriptional programs.

Selective turnover of chloroplast components during senescence may reflect a JA-inducible nitrogen or carbon scavenging mechanism

Plastids degrade rapidly during senescence compared to organelles like mitochondria, which remain intact through the late stages of senescence (Thomas and Stoddart 1980). The present study provides evidence for selective degradation of chloroplast proteins and lipids relative to other subcellular compartments. Thus, a major conclusion of this study is the leaf senescence resulting from overactivation of the JA shares many hallmarks of other types of senescence, including natural senescence and dark-induced senescence. Chloroplast autophagy has been implicated as a mechanism for balancing carbon and nitrogen levels in nutrient-limited conditions (Izumi et al. 2010; Kikuchi et al. 2020). A study with labeled nitrogen showed that recently assimilated nitrogen was a major contributor towards the biosynthesis of specialized metabolites after herbivory (Ullmann-Zeunert et al. 2013). However, leaf carbon status appears to be more important for chloroplast degradation and Rubisco turnover (Izumi et al. 2010). Soil-grown *jazD* not treated with exogenous JA or coronatine exhibit elevated expression of markers of sugar starvation. Moreover, the slow growth of *jazD* can be partially restored by treatment with exogenous sucrose (Guo et al. 2018). Data presented here is consistent with the hypothesis that carbon-nitrogen imbalances in *jazD* are further exacerbated by coronatine-induced depletion of the remaining pool of JAZs. In this scenario, turnover of highly abundant macromolecular complexes in the chloroplast may provide a mechanism to mobilize nitrogen or carbon via degradation of chloroplast proteins. These same processes may occur transiently at low levels in

WT plants subject to wounding and other stresses that activate the JA pathway. A full complement of JAZ proteins in WT plants, however, would effectively restrain the response, thereby explaining the lack of detectable chlorophyll loss. Chloroplasts account for the vast majority (70%) of nitrogen in the cell, most of which is found in highly abundant photosynthetic proteins such as Rubisco and LHCII (Evans and Clarke 2019). JA-induced turnover of a very small proportion of photosynthetic proteins is likely to generate sufficient resources to support stress responses without compromising photosynthetic performance.

Coronatine-induced senescence in *jazD* displays unique metabolic changes

Coronatine treatment of *jazD* samples resulted in several notable changes in metabolism. While lipid degradation and changes in free amino acid levels were similar to the shifts seen in both developmental and dark-induced senescence studies, the levels of jasmonates did not increase significantly with the exception of 12-OH-JA (Watanabe et al. 2013; Selmann et al. 2010). The lack of increase in JA species may indicate that the JA oxidases are not typically as active during dark-induced senescence compared to the high expression of these genes in coronatine-treated *jazD*.

Analysis of total proteins suggests that the proteolysis of plastid-localized proteins correlates with the increases in free amino acid levels. However, the decreases in glutamate and aspartate in contrast to the other amino acids suggest these two amino acids may be metabolized for nitrogen metabolism and respiration during coronatine-induced senescence (Galili 2011; The et al. 2020). For example, glutamate and glycine have well-characterized roles in nitrogen assimilation and mobilization, while aspartate conversion to asparagine may support long-distance nitrogen transport (Launay et al. 2019; The et al. 2020). Serine levels have been implicated in promoting senescence in oat, although it is not clear whether serine levels are

regulated in *jazD* to delay senescence (Martin and Thimann 1972). Although the TCA cycle intermediates did not display significant changes except for increases in fumarate and succinate, the abundance of free amino acids released from proteolysis may provide alternative respiratory substrates as photosynthesis decreases in the senescing leaves (Araújo et al. 2011; Galili 2011; Launay et al. 2019).

Fumarate and succinate have been shown to decrease in abundance throughout senescence, in contrast to the increase of these TCA cycle metabolites during coronatine-induced senescence (Watanabe et al. 2013). Fumarate has been implicated as a carbon sink and the shift in coronatine-treated *jazD* may correlate with the decrease in photosynthesis leading to a reduction in photoassimilate (Chia et al. 2000; Zell et al. 2010). A systemic study to determine whether metabolites are transported from treated leaves would provide interesting insight into how the senescence phenotype in *jazD* may be connected to carbon and nitrogen allocation during stress or biotic challenge.

REFERENCES

- Araújo WL, Tohge T, Ishizaki K, Leaver CJ, Fernie AR. 2011.** Protein degradation - an alternative respiratory substrate for stressed plants. *Trends in Plant Science* **16**: 489–498.
- Attaran E, Major IT, Cruz JA, Rosa BA, Koo AJK, Chen J, Kramer DM, He SY, Howe GA. 2014.** Temporal dynamics of growth and photosynthesis suppression in response to jasmonate signaling. *Plant Physiology* **165**: 1302–1314.
- Camm EL, Green BR. 2004.** How the chlorophyll-proteins got their names. *Photosynthesis Research* **80**: 189–196.
- Chi W, Ma J, Zhang D, Guo J, Chen F, Lu C, Zhang L. 2008.** The pentatricopeptide repeat protein DELAYED GREENING1 is involved in the regulation of early chloroplast development and chloroplast gene expression in *Arabidopsis*. *Plant Physiology* **147**: 573–584.
- Chia DW, Yoder TJ, Reiter W-D, Gibson SI. 2000.** Fumaric acid: an overlooked form of fixed carbon in *Arabidopsis* and other plant species. *Planta* **211**: 743–751.
- Chung HS, Koo AJK, Gao X, Jayanty S, Thines B, Jones AD, Howe GA. 2008.** Regulation and function of *Arabidopsis* JASMONATE ZIM-domain genes in response to wounding and herbivory. *Plant Physiology* **146**: 952–964.
- Cruz JA, Savage LJ, Zegarac R, Hall CC, Satoh-Cruz M, Davis GA, Kovac WK, Chen J, Kramer DM. 2016.** Dynamic environmental photosynthetic imaging reveals emergent phenotypes. *Cell Systems* **2**: 365–377.
- Domínguez F, Cejudo FJ. 2021.** Chloroplast dismantling in leaf senescence. *Journal of Experimental Botany* **72**: 5905–5918.
- Evans JR, Clarke VC. 2019.** The nitrogen cost of photosynthesis. *Journal of Experimental Botany* **70**: 7–15.
- Fernández-Calvo P, Chini A, Fernández-Barbero G, Chico J-M, Gimenez-Ibanez S, Geerinck J, Eeckhout D, Schweizer F, Godoy M, Franco-Zorrilla JM, et al. 2011.** The *Arabidopsis* bHLH transcription factors MYC3 and MYC4 are targets of JAZ repressors and act additively with MYC2 in the activation of jasmonate responses. *The Plant Cell* **23**: 701–715.
- Galili G. 2011.** The aspartate-family pathway of plants: linking production of essential amino acids with energy and stress regulation. *Plant Signaling and Behavior* **6**: 192–195.
- Gao C, Qi S, Liu K, Li D, Jin C, Li Z, Huang G, Hai J, Zhang M, Chen M. 2016.** MYC2, MYC3, and MYC4 function redundantly in seed storage protein accumulation in *Arabidopsis*. *Plant Physiology and Biochemistry* **108**: 63–70.

- Guo Q, Major IT, Kapali G, Howe GA. 2022.** MYC transcription factors coordinate tryptophan-dependent defense responses and compromise seed yield in *Arabidopsis*. *New Phytologist*
- Guo Q, Yoshida Y, Major IT, Wang K, Sugimoto K, Kapali G, Havko NE, Benning C, Howe GA. 2018.** JAZ repressors of metabolic defense promote growth and reproductive fitness in *Arabidopsis*. *Proceedings of the National Academy of Sciences* **115**: E10768-10777.
- He Y, Fukushige H, Hildebrand DF, Gan S. 2002.** Evidence supporting a role of jasmonic acid in *Arabidopsis* leaf senescence. *Plant Physiology* **128**: 876–884.
- Himelblau E, Amasino R. 2001.** Nutrients mobilized from leaves of *Arabidopsis thaliana* during leaf senescence. *Journal of Plant Physiology* **158**: 1317-1323.
- Howe GA, Major IT, Koo AJ. 2018.** Modularity in jasmonate signaling for multistress resilience. *Annual Review of Plant Biology* **69**: 387–415.
- Izumi M, Hidema J, Wada S, Kondo E, Kurusu T, Kuchitsu K, Makino A, Ishida H. 2015.** Establishment of monitoring methods for autophagy in rice reveals autophagic recycling of chloroplasts and root plastids during energy limitation. *Plant Physiology* **167**: 1307–1320.
- Izumi M, Wada S, Makino A, Ishida H. 2010.** The autophagic degradation of chloroplasts via rubisco-containing bodies is specifically linked to leaf carbon status but not nitrogen status in *Arabidopsis*. *Plant Physiology* **154**: 1196–1209.
- Kikuchi Y, Nakamura S, Woodson JD, Ishida H, Ling Q, Hidema J, Jarvis RP, Hagihara S, Izumi M. 2020.** Chloroplast autophagy and ubiquitination combine to manage oxidative damage and starvation responses. *Plant Physiology* **183**: 1531–1544.
- Kloek AP, Verbsky ML, Sharma SB, Schoelz JE, Vogel J, Klessig DF, Kunkel BN. 2001.** Resistance to *Pseudomonas syringae* conferred by an *Arabidopsis thaliana* coronatine-insensitive (*coi1*) mutation occurs through two distinct mechanisms. *Plant Journal* **26**: 509–522.
- Koo AJK, Howe GA. 2012.** Catabolism and deactivation of the lipid-derived hormone jasmonoyl-isoleucine. *Frontiers in Plant Science* **3**: 19.
- Launay A, Cabassa-Hourton C, Eubel H, Maldiney R, Guivarc’h A, Crilat E, Planchais S, Lacoste J, Bordenave-Jacquemin M, Clément G, et al. 2019.** Proline oxidation fuels mitochondrial respiration during dark-induced leaf senescence in *Arabidopsis thaliana*. *Journal of Experimental Botany* **70**: 6203–6214.
- Li B, Dewey CN. 2011.** RSEM: accurate transcript quantification from RNA-Seq data with or without a reference genome. *BMC Bioinformatics* **12**: 323.

- Lim PO, Kim HJ, Nam HG. 2007.** Leaf senescence. *Annual Review of Plant Biology* **58**: 115–136.
- Liu L, Sonbol F-M, Huot B, Gu Y, Withers J, Mwimba M, Yao J, He SY, Dong X. 2016.** Salicylic acid receptors activate jasmonic acid signalling through a non-canonical pathway to promote effector-triggered immunity. *Nature Communications* **7**: 1–10.
- Love MI, Huber W, Anders S. 2014.** Moderated estimation of fold change and dispersion for RNA-seq data with DESeq2. *Genome Biology* **15**: 550.
- Major IT, Guo Q, Zhai J, Kapali G, Kramer DM, Howe GA. 2020.** A phytochrome B-independent pathway restricts growth at high levels of jasmonate defense. *Plant Physiology* **183**: 733–749.
- Martin C, Thimann KV. 1972.** The role of protein synthesis in the senescence of leaves: I. The formation of protease. *Plant Physiology* **49**: 64–71.
- Miao Y, Laun T, Zimmermann P, Zentgraf U. 2004.** Targets of the WRKY53 transcription factor and its role during leaf senescence in *Arabidopsis*. *Plant Molecular Biology* **55**: 853–867.
- Miao Y, Zentgraf U. 2007.** The antagonist function of *Arabidopsis* WRKY53 and ESR/ESP in leaf senescence is modulated by the jasmonic and salicylic acid equilibrium. *The Plant Cell* **19**: 819–830.
- Michaeli S, Fromm H. 2015.** Closing the loop on the GABA shunt in plants: are GABA metabolism and signaling entwined? *Frontiers in Plant Science* **6**: 419.
- Miyashita Y, Good AG. 2008.** NAD(H)-dependent glutamate dehydrogenase is essential for the survival of *Arabidopsis thaliana* during dark-induced carbon starvation. *Journal of Experimental Botany* **59**: 667–680.
- Noir S, Bömer M, Takahashi N, Ishida T, Tsui T-L, Balbi V, Shanahan H, Sugimoto K, Devoto A. 2013.** Jasmonate controls leaf growth by repressing cell proliferation and the onset of endoreduplication while maintaining a potential stand-by mode. *Plant Physiology* **161**: 1930–1951.
- Ono K, Kimura M, Matsuura H, Tanaka A, Ito H. 2019.** Jasmonate production through chlorophyll a degradation by Stay-Green in *Arabidopsis thaliana*. *Journal of Plant Physiology* **238**: 53–62.
- Qiu K, Li Z, Yang Z, Chen J, Wu S, Zhu X, Gao S, Gao J, Ren G, Kuai B, et al. 2015.** EIN3 and ORE1 accelerate degreening during ethylene-mediated leaf senescence by directly activating chlorophyll catabolic genes in *Arabidopsis*. *PLoS Genetics* **11**: e1005399.
- Reynolds ES. 1963.** The use of lead citrate at high pH as an electron-opaque stain in electron microscopy. *Journal of Cell Biology* **17**: 208–212.

- Seltmann MA, Hussels W, Berger S. 2010a.** Jasmonates during senescence. *Plant Signaling and Behavior* **5**: 1493–1496.
- Seltmann MA, Stingl NE, Lautenschlaeger JK, Krischke M, Mueller MJ, Berger S. 2010b.** Differential impact of lipoxygenase 2 and jasmonates on natural and stress-induced senescence in *Arabidopsis*. *Plant Physiology* **152**: 1940–1950.
- Shan X, Wang J, Chua L, Jiang D, Peng W, Xie D. 2011.** The role of *Arabidopsis* Rubisco activase in jasmonate-induced leaf senescence. *Plant Physiology* **155**: 751–764.
- Sherman BT, Hao M, Qiu J, Jiao X, Baseler MW, Lane HC, Imamichi T, Chang W. 2022.** DAVID: a web server for functional enrichment analysis and functional annotation of gene lists (2021 update). *Nucleic Acids Research* **50**: W216-W221.
- Song S, Huang H, Wang J, Liu B, Qi T, Xie D. 2017.** MYC5 is involved in jasmonate-regulated plant growth, leaf senescence and defense responses. *Plant and Cell Physiology* **58**: 1752–1763.
- Tamary E, Nevo R, Naveh L, Levin-Zaidman S, Kiss V, Savidor A, Levin Y, Eyal Y, Reich Z, Adam Z. 2019.** Chlorophyll catabolism precedes changes in chloroplast structure and proteome during leaf senescence. *Plant Direct* **3**: e00127.
- The SV, Snyder R, Tegeder M. 2020.** Targeting nitrogen metabolism and transport processes to improve plant nitrogen use efficiency. *Frontiers in Plant Science* **11**: 628366.
- Thomas H, Stoddart JL. 1980.** Leaf senescence. *Annual Review of Plant Physiology* **31**: 83–111.
- Ullmann-Zeunert L, Stanton MA, Wielsch N, Bartram S, Hummert C, Svatos A, Baldwin IT, Groten K. 2013.** Quantification of growth-defense trade-offs in a common currency: nitrogen required for phenolamide biosynthesis is not derived from ribulose-1,5-bisphosphate carboxylase/oxygenase turnover. *Plant Journal* **75**: 417–429.
- Wang X, An Y, Xu P, Xiao J. 2021.** Functioning of PPR proteins in organelle RNA metabolism and chloroplast biogenesis. *Frontiers in Plant Science* **12**: 627501.
- Wang Z, Benning C. 2011.** *Arabidopsis thaliana* polar glycerolipid profiling by thin layer chromatography (TLC) coupled with gas-liquid chromatography (GLC). *Journal of Visualized Experiments* **49**: 2518.
- Wang K, Guo Q, Froehlich JE, Hersh HL, Zienkiewicz A, Howe GA, Benning C. 2018.** Two abscisic acid-responsive plastid lipase genes involved in jasmonic acid biosynthesis in *Arabidopsis thaliana*. *The Plant Cell* **30**: 1006–1022.
- Watanabe M, Balazadeh S, Tohge T, Erban A, Giavalisco P, Kopka J, Mueller-Roeber B, Fernie AR, Hoefgen R. 2013.** Comprehensive dissection of spatiotemporal metabolic shifts in primary, secondary, and lipid metabolism during developmental senescence in *Arabidopsis*. *Plant Physiology* **162**: 1290–1310.

- Weraduwage SM, Chen J, Anozie FC, Morales A, Weise SE, Sharkey TD. 2015.** The relationship between leaf area growth and biomass accumulation in *Arabidopsis thaliana*. *Frontiers in Plant Science* **6**: 167.
- Wostrikoff K, Stern D. 2007.** Rubisco large-subunit translation is autoregulated in response to its assembly state in tobacco chloroplasts. *Proceedings of the National Academy of Sciences* **104**: 6466–6471.
- Wright IJ, Reich PB, Westoby M, Ackerly DD, Baruch Z, Bongers F, Cavender-Bares J, Chapin T, Cornelissen JHC, Diemer M, et al. 2004.** The worldwide leaf economics spectrum. *Nature* **428**: 821–827.
- Yu J, Zhang Y, Di C, Zhang Q, Zhang K, Wang C, You Q, Yan H, Dai SY, Yuan JS, et al. 2016.** JAZ7 negatively regulates dark-induced leaf senescence in *Arabidopsis*. *Journal of Experimental Botany* **67**: 751–762.
- Zander M, Lewsey MG, Clark NM, Yin L, Bartlett A, Saldierna Guzmán JP, Hann E, Langford AE, Jow B, Wise A, et al. 2020.** Integrated multi-omics framework of the plant response to jasmonic acid. *Nature Plants* **6**: 290–302.
- Zell MB, Fahnenstich H, Maier A, Saigo M, Voznesenskaya EV, Edwards GE, Andreo C, Schleifenbaum F, Zell C, Drincovich MF, et al. 2010.** Analysis of *Arabidopsis* with highly reduced levels of malate and fumarate sheds light on the role of these organic acids as storage carbon molecules. *Plant Physiology* **152**: 1251–1262.
- Zhu Z, An F, Feng Y, Li P, Xue L, A M, Jiang Z, Kim J-M, To TK, Li W, et al. 2011.** Derepression of ethylene-stabilized transcription factors (EIN3/EIL1) mediates jasmonate and ethylene signaling synergy in *Arabidopsis*. *Proceedings of the National Academy of Sciences* **108**: 12539–12544.
- Zhu X, Chen J, Xie Z, Gao J, Ren G, Gao S, Zhou X, Kuai B. 2015.** Jasmonic acid promotes degreening via MYC2/3/4- and ANAC019/055/072-mediated regulation of major chlorophyll catabolic genes. *Plant Journal* **84**: 597–610.
- Zhuo M, Sakuraba Y, Yanagisawa S. 2020.** A jasmonate-activated MYC2–Dof2.1–MYC2 transcriptional loop promotes leaf senescence in *Arabidopsis*. *The Plant Cell* **32**: 242–262.

APPENDIX

Table A4.1 Differential expression of jasmonic acid biosynthesis genes after coronatine treatment.

AGI ¹	Gene ²	1h log ₂ fc ³	3h log ₂ fc ³	12h log ₂ fc ³	24h log ₂ fc ³	Log ₂ fold change
AT3G45140	LOX2	0.65306	2.468158	1.796123	2.298901	2
AT1G17420	LOX3	3.497332	3.745399	3.163823	4.055272	1
AT1G72520	LOX4	3.515148	3.838622	3.494	3.396269	1
AT1G67560	LOX6	0.206959	0.573411	1.211223	2.380794	1
AT5G42650	AOS	1.512503	3.144093	1.735942	1.598966	1
AT3G25760	AOC1	1.438664	3.190819	1.787832	1.097103	1
AT3G25770	AOC2	0.594904	1.91559	0.907372	-2.512	-2
AT3G25780	AOC3	1.805292	1.139145	1.331949	2.844628	1
AT1G13280	AOC4	0.750546	1.997823	1.49572	0.971551	1
AT2G06050	OPR3	2.898575	3.982943	2.418991	2.696549	1
AT1G20510	OPCL1	2.508251	2.166086	0.426179	0.868148	1
AT4G16760	ACX1	0.86468	1.728357	1.843138	2.58178	1
AT2G35690	ACX5	-0.12632	-0.65062	-0.20635	0.217737	-1
AT2G33150	KAT2	-0.0481	-0.74151	0.844224	2.813744	-1
AT4G29010	AIM1	-0.05988	-0.4539	0.042035	1.39373	-1
AT2G46370	JAR1	-0.14012	-0.51321	-0.72143	0.206899	-1
AT5G63450	CYP94B1	3.635993	7.93534	5.938072	5.286559	2
AT3G48520	CYP94B3	1.904225	5.823463	6.052052	6.998674	2
AT3G11180	JOX1	1.739711	5.56389	4.581808	5.319971	2
AT5G05600	JOX2	1.626683	2.75621	2.908042	3.060614	2
AT3G55970	JOX3	1.993011	3.278895	3.251661	3.63405	2
AT2G38240	JOX4	4.423982	7.456141	7.070871	8.392767	2

¹AGI accession indicates the locus identifier provided by The Arabidopsis Information Resource (TAIR) database and the Arabidopsis Genome Initiative (AGI).

²Gene name indicates the common gene symbol.

³Log₂ fold change (fc) of coronatine/mock samples at the designated time point (h).

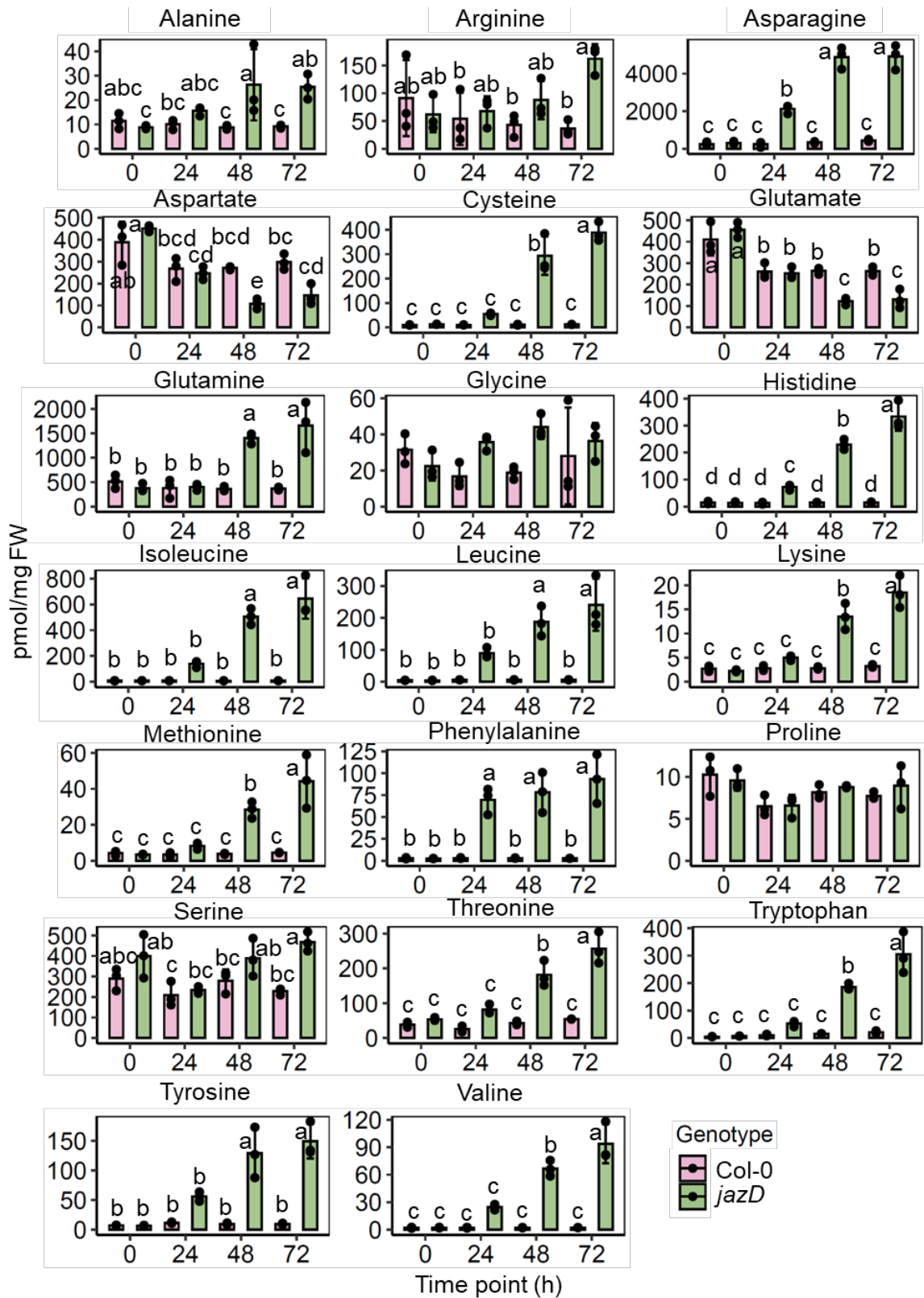


Figure A4.1 Coronatine-induced changes in amino acid levels in WT and *jazD*.

Figure A4.1 (cont'd)

Plants were treated with a solution containing 5 μ M coronatine and whole rosettes were harvested for quantification of amino acids by LC-MS. Different letters represent significant differences at $P < 0.05$ with Tukey's honest significant difference (HSD) test.

Table A4.2 Differential expression of TCA cycle genes in *jazD* after coronatine treatment.

AGI ¹	Gene name ²	1h log ₂ fc ³	3h log ₂ fc ³	12h log ₂ fc ³	24h log ₂ fc ³	Log ₂ fold change
AT1G04410	c-NAD-MDH1	-0.1754	-0.9172	-1.392	-0.316	
AT1G08480	SDH6	-0.0806	-0.4447	-0.1385	0.72177	2
AT1G47420	SDH5	-0.1039	-0.2393	-0.2607	0.36357	1
AT1G48030	mtLPD1	-0.0174	-0.1481	-1.2655	-1.1489	0
AT1G53240	mMDH1	-0.1735	-0.786	-2.0294	-1.7295	-1
AT2G05710	ACO3	0.02597	-0.1614	0.04456	1.38063	-2
AT2G17130	IDH2	0.08538	-0.1337	0.41759	1.99963	
AT2G20420		-0.0905	-0.276	-0.8246	0.03734	
AT2G22780	PMDH1	0.4189	0.87471	0.00577	1.08565	
AT2G42790	CSY3	0.07595	-0.2326	1.10682	2.8562	
AT2G47510	FUM1	0.02073	-0.0937	-0.7723	0.01488	
AT3G16950	LPD1	-0.0904	0.08402	-1.5575	-2.4277	
AT3G17240	mtLPD2	0.16892	0.1115	0.24574	1.48598	
AT3G27380	SDH2-1	0.002	0.29711	1.13534	2.78552	
AT3G47520	MDH	-0.2063	-0.5176	-1.5773	-0.6775	
AT3G47833	SDH7A	-0.1277	-0.2666	-0.5204	0.85106	
AT3G58750	CSY2	-0.1674	-0.4045	-0.0255	1.81745	
AT4G16155		-0.1326	-0.2754	-2.5891	-3.7889	
AT4G26910		0.08031	-0.0534	-0.2894	1.05398	
AT4G32210	SDH3-2	0.03108	0.24693	0.16284	1.14921	
AT4G35260	IDH1	0.00748	0.00557	0.03599	1.17909	
AT4G35830	ACO1	-0.0327	-0.8178	-0.8058	-0.1669	
AT5G03290	IDH-V	-0.0186	0.02121	0.23722	1.4458	
AT5G08300		-0.0207	-0.2008	-0.7326	0.40733	
AT5G09600	SDH3-1	0.09625	-0.0016	-0.0168	1.11259	
AT5G09660	PMDH2	-0.0429	-0.6249	-3.3514	-4.9367	
AT5G40650	SDH2-2	-0.1139	0.16718	0.67278	1.70167	
AT5G43330	c-NAD-MDH2	-0.0736	-0.5448	-1.4835	-0.7157	
AT5G50950	FUM2	0.49204	0.90198	2.71223	2.96133	
AT5G65750		0.03401	-1.15	-2.7416	-2.1364	
AT5G66760	SDH1-1	0.03479	0.08005	1.19924	2.63528	

Table A4.2 (cont'd)

¹AGI accession indicates the locus identifier provided by The Arabidopsis Information Resource (TAIR) database and the Arabidopsis Genome Initiative (AGI).

²Gene name indicates the common gene symbol.

³Log₂ fold change (fc) of coronatine/mock samples at the designated time point (h).

CHAPTER 5: SYNTHESIS

SUMMARY AND FUTURE DIRECTIONS

Jasmonate (JA) signaling is a critical facet of the plant defense repertoire and as such, many studies attempt to elucidate its vast regulatory network (Xie et al. 1998; Zhu et al. 2011; Howe et al. 2018; Zander et al. 2020). In this dissertation, I examined the regulation of metabolism, growth, and senescence by the jasmonate signaling pathway. This work contributes to understanding the regulation of the growth-defense balance and senescence, and how response specificity is mediated in JA signaling.

CHAPTER 2

In chapter 2, we addressed the question of how response specificity can be achieved by a limited suite of core signaling components. The JAZ family is often described as functionally redundant due to a lack of broader defense phenotypes in the single mutants, although examples of specific functions have been described (Moreno et al. 2013; Yu et al. 2016; Gimenez-Ibanez et al. 2017; Guo et al. 2018; Liu et al. 2021). We found that subfunctionalization of the JAZ and MYC families contributes to the regulation of aromatic amino acid biosynthesis to support the production of defense compounds. We conceptualized a novel screening approach that combines forward and reverse genetics that allowed us to screen for *JAZ* candidates in an unbiased manner. Our approach may be more broadly applied to large gene families provided that there is a robust screening phenotype and the ability to generate the screening population from high-order mutants. While this work sheds light on subfunctionalization within the JAZ family, there are still mechanistic gaps in understanding response specificity and magnitude. For instance, the *jazD* mutant always displays significantly stronger phenotypes than the *jazQ* and *jaz1/2/5/6* mutants. This indicates that the other JAZs contribute to these broader defense phenotypes in an unknown manner. Further study into JAZ interactions is needed to understand the full spectrum

of JA signaling regulation by these repressors. For instance, it is unknown how JAZ regulation across specific cell types may coordinate responses, although there is evidence for cell-specific expression of JA signaling components (Gasperini et al. 2015; Gimenez-Ibanez et al. 2017; Lewsey et al. 2022). Single-cell sequencing would provide insights into how JA responses are coordinated systemically and whether response specificity is regulated in a cell-type specific manner. Additionally, further study into JAZ protein interactions would provide insight into how these proteins coordinate responses *in planta*. It has previously been shown that some JAZs form heteromers and homomers but the contribution of this to response specificity is not well established (Chini et al. 2009; Chung and Howe 2009).

This chapter shows that mutations in different subgroups of *JAZ* genes, *jaz1/3/4/9/10* (*jazQ*) and *jaz1/2/5/6*, specifically regulate the production of distinct metabolite classes such as the aliphatic glucosinolates compared to camalexin and the hydroxycinnamic acid amides (HCAA). It is unclear how specific metabolic programs are regulated by JAZ but presumably occurs through differential interactions of downstream TFs. This chapter shows how MYCs differentially regulate pathways such as aromatic amino acid biosynthesis, but other transcription factors coordinate responses with the MYCs as well. MYC and MYB interactions, for example, suggest that co-regulation provides some specificity in the production of specialized metabolites (Millard et al. 2019). MYB28, MYB29, and MYB76 regulate the production of aliphatic glucosinolates, while MYB34, MYB51, and MYB122 regulate the production of indolic glucosinolates (Frerigmann and Gigolashvili 2014; Sønderby et al. 2010). The ORA59 TF regulates HCAA production, and ERF1 and WRKY33 are involved in camalexin biosynthesis (Li et al. 2018; Zhou et al. 2022). In addition to TF interactions, complex co-repression mechanisms are being discovered that likely contribute to response specificity, such as EAR-

motif CONTAINING ADAPTOR PROTEIN (ECAP) regulation of anthocyanin production or conflicting regulation of JA-responsive genes seen in *HISTONE DEACETYLASE 6 (hda6)* mutants (Li et al. 2020; Wu et al. 2008; Zhu et al. 2011). Further study into the interactors of the core JA signaling pathway components will provide insight into how the main JA components identified in chapter 2 may be further modulated to provide specific responses, such as through multi-omics approaches to capture different aspects of regulation at chromatin, protein, and transcript levels (Zander et al. 2020).

CHAPTER 3

Growth and defense regulation is a complex phenomenon that remains to be fully elucidated. Additionally, the physiological role of JA-induced senescence has yet to be identified. Chapter 3 aimed to identify molecular components involved in the regulation of the growth-defense balance and jasmonate-induced senescence. Previous work suggests that phytochrome B is a key regulator of growth-defense responses in JA signaling (Campos et al. 2016; Leone et al. 2014; Major et al. 2020). However, the *phyB* mutant is unable to fully restore growth in *jazD*, suggesting that there are other growth-defense regulators. I identified six *COII* alleles and six *MYC2* alleles from screens for restored growth or inhibition of senescence. The identification of JA signaling components indicates strong regulatory control by the core components, while downstream programs may have redundant roles. It is possible that tuning JA signaling through these mutations in the core pathway serves a similar role to WT attenuation mechanisms and emphasizes the importance of balancing defense signals to optimize fitness. Our lab is characterizing an additional growth-defense suppressor that will provide key insight into additional growth-defense regulators. This mutant restores many of the elevated metabolites in *jazD* to WT levels, suggesting that this mutant is a key component of sensing the changes in

metabolism. Chapter 4 lays the foundation for a deeper understanding of JA-induced senescence.

CHAPTER 4

Many studies depend on dark-induction of senescence in excised leaves and high exogenous concentrations of JA, but studies of JA-induced senescence in physiologically relevant growth conditions are limited (Ueda and Kato 1980; Yu et al. 2016; Wang et al. 2022). In chapter 4, I characterized coronatine-induced senescence in *jazD* to assess JA-induced senescence under physiological conditions. This work presents a novel system to study JA-induced senescence across many developmental stages as well as capturing energy changes throughout the plant. A remaining question in this study is whether there are conditions that would promote JA-induced senescence in WT Arabidopsis. Coronatine induces chlorosis in tomato, and long-term application of JA can induce early senescence in tobacco (Palmer and Bender 1995; Wang et al. 2022). Further characterization of JA signaling mechanics under dark induction of senescence may provide insight into how JA is able to promote senescence in WT plants under dark conditions but not in light. Our lab is currently assessing JAZ stability in dark conditions to determine whether JAZ turnover contributes towards dark-induced senescence. It is also possible that these programs are activated in WT to free plastid-localized resources but repression by the JAZ proteins maintains a non-senescent state. It would be interesting to test whether complete removal of JAZ proteins leads to a non-viable plant. The *jazU* plant, in which eleven *JAZ* genes are mutated, appears to have altered senescence phenotypes in the flowers and senescence after challenge with insect larvae (unpublished data, Ian Major). This suggests that the removal of an additional JAZ depletes the pool of repressors sufficiently to induce senescence by biotic stressors and emphasizes the requirement of JAZ to inhibit senescence

programming. Interestingly, the senescence phenotype in *jazD* displays light-dependency (unpublished data, Qiang Guo), which indicates reactive oxygen species (ROS) may play a key role in promoting senescence. Further studies into understanding the mechanism of ROS in this system may also contribute to understanding whether ROS-producing environmental stressors can trigger JA-induced senescence.

The metabolic shifts in *jazD* suggest that the mitochondria become the primary energy sources as photosynthetic capacity is diminished. Further analysis of a broader metabolomics study would provide insight into how *jazD* is partitioning resources from the TCA cycle pools. The TCA cycle provides precursor material for processes such as amino acid biosynthesis, and fumarate accumulation can act as a carbon source when other carbohydrates such as starch are limited (Araújo et al. 2011). Fumarate is also needed for plant growth on high nitrogen, suggesting a role of fumarate in nitrogen assimilation (Pracharoenwattana et al. 2010). Interestingly, low levels of fumarate and malate accelerate dark-induced senescence, likely due to more rapid starvation (Fahnenstich et al. 2008). Flux analysis may be a useful method to understand how carbon is partitioned in this system and the role of increased fumarate during JA-induced senescence. Additionally, systemic studies may provide insight into how JA-induced senescence programs distribute the catabolized macromolecules, such as whether nutrients are transported to other leaves or to the roots.

REFERENCES

- Araújo WL, Nunes-Nesi A, Fernie AR. 2011.** Fumarate: Multiple functions of a simple metabolite. *Phytochemistry* **72**: 838–843.
- Campos ML, Yoshida Y, Major IT, De Oliveira Ferreira D, Weraduwage SM, Froehlich JE, Johnson BF, Kramer DM, Jander G, Sharkey TD, et al. 2016.** Rewiring of jasmonate and phytochrome B signalling uncouples plant growth-defense tradeoffs. *Nature Communications* **7**: 1–10.
- Chini A, Fonseca S, Chico JM, Fernández-Calvo P, Solano R. 2009.** The ZIM domain mediates homo- and heteromeric interactions between *Arabidopsis* JAZ proteins. *Plant Journal* **59**: 77–87.
- Chung HS, Howe GA. 2009.** A critical role for the TIFY motif in repression of jasmonate signaling by a stabilized splice variant of the JASMONATE ZIM-domain protein JAZ10 in *Arabidopsis*. *The Plant Cell* **21**: 131–145.
- Fahnenstich H, Saigo M, Andreo C, Drincovich MF, Flügge U-I, Maurino VG. 2008.** Malate and fumarate emerge as key players in primary metabolism: *Arabidopsis thaliana* overexpressing C4-NADP-ME offer a way to manipulate the levels of malate and to analyse the physiological consequences. In: *Photosynthesis. Energy from the Sun*. Springer Netherlands, 971–975.
- Frerigmann H, Gigolashvili T. 2014.** MYB34, MYB51, and MYB122 distinctly regulate indolic glucosinolate biosynthesis in *Arabidopsis thaliana*. *Molecular Plant* **7**: 814–828.
- Gasperini D, Chételat A, Acosta IF, Goossens J, Pauwels L, Goossens A, Dreos R, Alfonso E, Farmer EE. 2015.** Multilayered organization of jasmonate signalling in the regulation of root growth. *PLoS Genetics* **11**: e1005300.
- Gimenez-Ibanez S, Boter M, Ortigosa A, Garcia-Casado G, Chini A, Lewsey MG, Ecker JR, Ntoukakis V, Solano R. 2017.** JAZ2 controls stomata dynamics during bacterial invasion. *New Phytologist* **213**: 1378–1392.
- Guo Q, Yoshida Y, Major IT, Wang K, Sugimoto K, Kapali G, Havko NE, Benning C, Howe GA. 2018.** JAZ repressors of metabolic defense promote growth and reproductive fitness in *Arabidopsis*. *Proceedings of the National Academy of Sciences* **115**: E10768–10777.
- Howe GA, Major IT, Koo AJ. 2018.** Modularity in jasmonate signaling for multistress resilience. *Annual Review of Plant Biology* **69**: 387–415.
- Leone M, Keller MM, Cerrudo I, Ballaré CL. 2014.** To grow or defend? Low red : far-red ratios reduce jasmonate sensitivity in *Arabidopsis* seedlings by promoting DELLA degradation and increasing JAZ10 stability. *New Phytologist* **204**: 355–367.

- Lewsey MG, Yi C, Berkowitz O, Ayora F, Bernado M, Whelan J. 2022.** scCloudMine: A cloud-based app for visualization, comparison, and exploration of single-cell transcriptomic data. *Plant Communications* **3**: 100302.
- Li C, Shi L, Wang Y, Li W, Chen B, Zhu L, Fu Y. 2020.** *Arabidopsis* ECAP is a new adaptor protein that connects JAZ repressors with the TPR2 co-repressor to suppress jasmonate-responsive anthocyanin accumulation. *Molecular Plant* **13**: 246–265.
- Li J, Zhang K, Meng Y, Hu J, Ding M, Bian J, Yan M, Han J, Zhou M. 2018.** Jasmonic acid/ethylene signaling coordinates hydroxycinnamic acid amides biosynthesis through ORA59 transcription factor. *Plant Journal* **95**: 444–457.
- Liu B, Seong K, Pang S, Song J, Gao H, Wang C, Zhai J, Zhang Y, Gao S, Li X, et al. 2021.** Functional specificity, diversity, and redundancy of *Arabidopsis* JAZ family repressors in jasmonate and COI1-regulated growth, development, and defense. *New Phytologist* **231**: 1525–1545.
- Major IT, Guo Q, Zhai J, Kapali G, Kramer DM, Howe GA. 2020.** A phytochrome B-independent pathway restricts growth at high levels of jasmonate defense. *Plant Physiology* **183**: 733–749.
- Millard PS, Weber K, Kragelund BB, Burow M. 2019.** Specificity of MYB interactions relies on motifs in ordered and disordered contexts. *Nucleic Acids Research* **47**: 9592–9608.
- Moreno JE, Shyu C, Campos ML, Patel LC, Chung HS, Yao J, He SY, Howe GA. 2013.** Negative feedback control of jasmonate signaling by an alternative splice variant of JAZ10. *Plant Physiology* **162**: 1006–1017.
- Palmer D, Bender CL. 1995.** Ultrastructure of tomato leaf tissue treated with the pseudomonad phytotoxin coronatine and comparison with methyl jasmonate. *Molecular Plant-Microbe Interactions* **8**: 683–692.
- Pracharoenwattana I, Zhou W, Keech O, Francisco PB, Udomchalothorn T, Tschoep H, Stitt M, Gibon Y, Smith SM. 2010.** *Arabidopsis* has a cytosolic fumarase required for the massive allocation of photosynthate into fumaric acid and for rapid plant growth on high nitrogen. *Plant Journal* **62**: 785–795.
- Sønderby IE, Burow M, Rowe HC, Kliebenstein DJ, Halkier BA. 2010.** A complex interplay of three R2R3 MYB transcription factors determines the profile of aliphatic glucosinolates in *Arabidopsis*. *Plant Physiology* **153**: 348–363.
- Ueda J, Kato J. 1980.** Isolation and identification of a senescence-promoting substance from wormwood (*Artemisia absinthium* L.). *Plant Physiology* **66**: 246–249.
- Wang C, Ding Y, Wang W, Zhao X, Liu Y, Timko MP, Zhang Z, Zhang H. 2022.** Insights into gene regulation of jasmonate-induced whole-plant senescence of tobacco under non-starvation conditions. *Plant and Cell Physiology* **63**: 45–56.

- Wu K, Zhang L, Zhou C, Yu C-W, Chaikam V. 2008.** HDA6 is required for jasmonate response, senescence and flowering in *Arabidopsis*. *Journal of Experimental Botany* **59**: 225–234.
- Xie DX, Feys BF, James S, Nieto-Rostro M, Turner JG. 1998.** *COI1*: an *Arabidopsis* gene required for jasmonate-regulated defense and fertility. *Science* **280**: 1091–1094.
- Yu J, Zhang Y, Di C, Zhang Q, Zhang K, Wang C, You Q, Yan H, Dai SY, Yuan JS, et al. 2016.** JAZ7 negatively regulates dark-induced leaf senescence in *Arabidopsis*. *Journal of Experimental Botany* **67**: 751–762.
- Zander M, Lewsey MG, Clark NM, Yin L, Bartlett A, Saldierna Guzmán JP, Hann E, Langford AE, Jow B, Wise A, et al. 2020.** Integrated multi-omics framework of the plant response to jasmonic acid. *Nat Plants* **6**: 290–302.
- Zhou J, Mu Q, Wang X, Zhang J, Yu H, Huang T, He Y, Dai S, Meng X. 2022.** Multilayered synergistic regulation of phytoalexin biosynthesis by ethylene, jasmonate, and MAPK signaling pathways in *Arabidopsis*. *The Plant Cell*.
- Zhu Z, An F, Feng Y, Li P, Xue L, A M, Jiang Z, Kim J-M, To TK, Li W, et al. 2011.** Derepression of ethylene-stabilized transcription factors (EIN3/EIL1) mediates jasmonate and ethylene signaling synergy in *Arabidopsis*. *Proceedings of the National Academy of Sciences* **108**: 12539–12544.
- Zubimendi JP, Martinatto A, Valacco MP, Moreno S, Andreo CS, Drincovich MF, Tronconi MA. 2018.** The complex allosteric and redox regulation of the fumarate hydratase and malate dehydratase reactions of *Arabidopsis thaliana* Fumarase 1 and 2 gives clues for understanding the massive accumulation of fumarate. *FEBS Journal* **285**: 2205–2224.